The role of the AAA^{+}- ATPase p97 in the regulation of cell cycle checkpoint activation in response to DNA damage

Inaugural-Dissertation
zur
Erlangung des Doktorgrades

Dr. rer. nat.

der Fakultät für
Biologie
an der

Universität Duisburg-Essen

vorgelegt von
Anne Riemer

aus Dresden
Juni 2014

Die der vorliegenden Arbeit zugrunde liegenden Experimente wurden am Zentrum für Medizinische Biotechnologie der Universität Duisburg-Essen durchgeführt.

1. Gutachter: * Prof. Dr. H. Meyer

2. Gutachter: * Prof. Dr. G. Iliakis

3. Gutachter: *

Vorsitzender des Prüfungsausschusses: * Prof. Dr. M. Kaiser

Tag der mündlichen Prüfung: *

___05.09.2014_____*

Contents

Summary

The cell cycle is a tightly regulated process that governs faithful replication and segregation of the DNA material into two daughter cells during proliferation. In order to ensure ordered cell cycle progression, and thus maintain genomic integrity, the mammalian cell cycle harbours a number of checkpoints. The activation of cell cycle checkpoints as well as the regulation of the DNA damage response signalling pathway strongly depends not only on multiple phosphorylation events, but also on the timely degradation of cell cycle regulators by the ubiquitin-proteasome system (UPS). A central component of the UPS is the AAA+-type ATPase p97, which recognizes ubiquitylated substrates and targets them for proteasomal degradation. Together with one of its co-factors, Ufd1-Npl4, p97 acts at multiple stages during cell cycle progression, including mitosis and S phase, thus ensuring ordered progression under physiological conditions and, importantly, in response to DNA damage. Depletion of $p97^{Ufd1\text{-}Npl4}$ leads to severe defects in chromosome segregation during mitosis, which might not be fully explained by its mitotic function but may as well be caused by its interphase functions. Therefore, this work aimed at elucidating the relevance of $p97^{Ufd1\text{-}Npl4}$ interphase functions on the manifestation of chromosome segregation defects in mitosis. Furthermore, we investigated the molecular basis of the role of $p97^{Ufd1\text{-}Npl4}$ complex in modulating the G_2/M checkpoint after DNA damage induction in human somatic cells.

Here, we show that p97 is required to ensure robust activation of the G_2/M checkpoint after ionizing irradiation (IR), protecting cells from entering mitosis despite DNA damage and thus suppressing the manifestation of chromosomal instability. Depletion of $p97^{Ufd1\text{-}Npl4}$ in cells exposed to IR, led to an increase in segregation defects, which are caused by pre-mitotic errors not being repaired before entering mitosis, indicating a defective DNA damage response. Indeed, analysing the key regulators and effectors of the DNA damage response pathway, we found a delayed CDC25A degradation in Ufd1-Npl4 depleted cells. Moreover, using a quantitative FACS approach, we showed that depletion of the $p97^{Ufd1\text{-}Npl4}$ complex led to an impaired G_2/M checkpoint after irradiation with a considerable fraction of mitotic cells. Importantly, we showed that $p97^{Ufd1\text{-}Npl4}$ ensures proper degradation of CDC25A and that persistent activity of the stabilized CDC25A causes a negligent G_2/M checkpoint activation, as this phenotype was rescued by additional inhibition of CDC25 phosphatases. Moreover, we showed that $p97^{Ufd1\text{-}Npl4}$ physically interacts with the SCF E3 ligase F-box protein βTrCP, confirming the emerging evidence for the connection of p97 to multiple E3 ligase substrates. These results establish a novel

function of the $p97^{Ufd1\text{-}Npl4}$ complex in facilitating CDC25A degradation downstream of ubiquitination by βTrCP and highlight a crucial aspect of p97 function for maintaining genome stability and integrity.

Zusammenfassung

Der Zellzyklus ist ein streng regulierter Prozess, welcher die exakte Replikation und Segregation des genetisches Materials in zwei Tochterzellen reguliert. Um einen geordneten Verlauf durch den Zellzyklus und damit der Bewahrung der genomischen Integrität zu gewährleisten, enthält der Zellzyklus in Säugetieren sogenannte Kontrollpunkte. Die Aktivierung der Zellzyklus Kontrollpunkte hängt dabei nicht nur von zahlreichen Phosphorylierungsereignissen ab, sondern auch vom koordinierten Abbau der Zellzyklus regulierenden Proteine durch das Ubiquitin-Proteasom-System (UPS). Ein zentraler Regulator im Ubiquitin-Proteasome-System ist die AAA+-ATPase p97, welche ubiquitinierte Substrate erkennt und sie für den proteasomalen Abbau überführt. Zusammen mit dem Ko-Faktor Ufd1-Npl4, reguliert p97 zahlreiche Ereignisse innerhalb des Zellzyklus und beeinflusst dadurch den Fortschritt des Zellzyklus unter physiologischen Bedingungen als auch in Reaktion auf DNA Schaden. Die Depletierung von $p97^{Ufd1\text{-}Npl4}$ führt zu schwerwiegenden Segregationsdefekten in der Mitose, welche nicht vollständig durch die Funktion von p97 in der Mitose erklärt werden können. Vielmehr kann eine Anzahl dieser Segregationsdefekte aus der Funktion von p97 in verschiedenen Interphase Prozessen resultieren. Daher versuchten wir im Rahmen dieser Arbeit die Relevanz der Interphaseprozesse, welche durch p97 reguliert werden, auf die Ausprägung von Segregationsdefekten in der Mitose zu untersuchen.

Darüber hinaus untersuchten wir den molekularen Mechanismus des $p97^{Ufd1\text{-}Npl4}$ Komplexes, welcher die Aktivität des G_2/M Kontrollpunktes nach DNA Schaden in humanen, somatischen Zellen reguliert.

In dieser Arbeit zeigen wir, dass p97 notwendig ist für die vollständige Aktivierung des G_2/M Kontrollpunktes nach ionisierender Bestrahlung und den Eintritt in die Mitose in Anwesenheit von DNA Schaden und die daraus resultierende Ausprägung chromosomaler Instabilität verhindert. Die Depletion von $p97^{Ufd1\text{-}Npl4}$ in bestrahlten Zellen führt zu einer Zunahme an Segregationsdefekten, die durch den Transfer von DNA Schäden in die Mitose entstanden sind. Durch die Analyse der Hauptregulatoren der DNA Schadensantwort, konnten wir einen verzögerten Abbau von CDC25A in $p97^{Ufd1\text{-}Npl4}$ depletierten Zellen nachweisen. Darüber hinaus konnten wir mit quantitativen FACS Experimenten zeigen, dass $p97^{Ufd1\text{-}Npl4}$ depletierte Zellen eine verminderte Aktivierung des DNA Schadenkontrollpunktes aufweisen und ein deutlicher Teil der Zellen sich trotz Bestrahlung in Mitose befindet. Ausschlaggebend für den Defekt in der Aktivierung des Kontrollpunktes ist dabei die Stabilisierung von CDC25A, da eine zusätzliche Inhibierung der CDC25 Phosphatasen den Kontrollpunkt vollständig wiederherstellt. Des Weiteren konnten wir zeigen, dass

$p97^{Ufd1\text{-}Npl4}$ mit dem F-box Protein βTrCP der $SCF^{\beta TrCP}$ E3 Ligase interagiert. Zusammenfassend etablieren unsere Ergebnisse eine neue Funktion des $p97^{Ufd1\text{-}Npl4}$ Komplexes innerhalb der DNA Schadensantwort durch die Interaktion mit der $SCF^{\beta TrCP}$ E3 Ligase und der Vermittlung des Abbaus von ubiquitinierten CDC25A. Die vorliegende Arbeit belegt dadurch eine weitere wichtige Rolle von p97 in der Erhaltung der genomischen Stabilität und Integrität.

1 Introduction

1.1 Mammalian cell cycle regulation

The cell cycle consists of four phases, the G_1, S, G_2 and M phase, during which the genetic material is duplicated and segregated into two daughter cells. To ensure ordered progression through the cell cycle and thus maintain genomic integrity, the mammalian cell cycle harbours a number of checkpoints, which are activated upon DNA damage leading to the transient arrest in the cell cycle. The major drivers of cell cycle progression are the cyclin-dependent kinases (CDKs), which phosphorylate numerous downstream substrates. CDKs belong to the family of Serine/Threonin kinases that form catalytically active heterodimeric complexes with cyclins. Cyclins are small molecules that are expressed and degraded throughout the cell cycle in an oscillating manner. The different cyclins bind to their associated CDKs and activate them, leading to subsequent cell cycle progression by the specific CDK-cyclin complexes. The progression through S phase is coordinated by CDK2-cyclin E-and CDK2-cyclin A-mediated phosphorylation events, whereas initiation and progression through mitosis is regulated by the action of the CDK1-cyclin A complex and the CDK1-cyclin B complex, respectively (Lapenna and Giordano, 2009); (Reinhardt and Yaffe, 2013). The activity of the CDK-cyclin complexes and thus the cell cycle progression is regulated by various mechanisms, leading to the inhibition of CDK-cyclin complexes. CDK activity is directly regulated by CDK-inhibitors (CKI), which can be grouped into two families. The family of inhibitor of CDK4 (INK4)-CKIs inhibit the activity of CDK4 and CDK6 by binding to them and thereby prevent the association with their cyclins. The second family of CKIs are the CDK interacting protein/kinase inhibitory proteins (Cip/Kip) p21, p27 and p57, which can bind to cyclins and thus modulate the activity of cyclin D -, E -, A-and B-CDK complexes (Sherr and Roberts, 1999). In addition to CKIs, CDKs are regulated by inhibitory phosphorylations in their ATP-binding loop by the myelin transcription factor (MYT) and WEE1. Thereby CDK-cyclin complexes are held in a state where they can be activated rapidly by the cell division cycle (CDC) 25 dual-specific phosphatases, which remove the inhibitory phosphorylations and thus promote cell cycle progression (Besson et al., 2008; Donzelli and Draetta, 2003). By regulating the CDK activity through posttranslational modifications of CDK-activating- and inhibiting proteins, the cell can respond immediately to DNA damage induction and arrest cell cycle progression allowing for the repair of DNA lesions. The process of DNA replication and the cellular response to DNA damage are described in more detail below.

1.1.1 DNA replication

During DNA replication the genetic material of the cell is duplicated before it is segregated into two daughter cells in mitosis. The exact and complete replication of the DNA material is essential to maintain the genomic integrity of the cell. In eukaryotic cells, the DNA replication is initiated by the presence of chromosomal elements called origins of replication. These DNA sequences direct the assembly of multiprotein complexes leading to the formation of two replication forks at each origin. The first step of DNA replication initiation is the formation of the pre-replicative complex (pre-RC) (Bell and Dutta, 2002). The origin recognition complex (ORC) binds specifically to the origins of replication and serves as platform for the formation of the pre-RC, consisting of the chromatin licensing and DNA replication factor 1 (Cdt1), the cell division cycle protein 6 (Cdc6) and the mini-chromosome maintaining complex (MCM) 2-7 (Diffley et al., 1994). In the second step, initiation of DNA replication is triggered by the formation of the pre-initiation complex (pre-IC), which requires the phosphorylation of MCM2-7 by CDK2 – cylin E and the Dbf4 – and Drf1 – dependent kinase (DDK) (Tanaka and Araki, 2013). Phosphorylation of MCM2 – 7 leads to the recruitment of Cdc45 and the go-Ichi-Ni-San (GINS)-complex to the origins to form an active helicase complex. Further recruitment of the replication protein A (RPA), the primase- polymerase α, the proliferating-cell nuclear antigen (PCNA) and the DNA polymerases δ and ε to the origins trigger the formation of two bi-directional replication forks and the initiation of DNA replication. The unwinding of the DNA by the DNA helicase complex enables the DNA polymerase α to initiate DNA synthesis and the DNA polymerase δ continues the DNA replication (Bell and Dutta, 2002).

To avoid re-replication of the same origin and thus preventing chromosomal instability, each origin just fires once in each cell cycle. The firing of origins is regulated either by the regulation of the availability of pre-RC components in the nuclei or the regulation of the activity of pre-RC components. The ubiquitination of the replication licensing factor Cdt1 leads to its degradation in late S phase. In contrast, binding of Cdt1 to geminin prevents the ubiquitination of Cdt1, but inhibits the DNA-binding activity of Cdt1 thereby preventing the formation of the pre-RC complex and subsequent initiation of DNA replication (Saxena et al., 2004).

1.1.2 DNA damage response

The integrity and stability of the genetic material is essential for the viability of the living organism. However, the DNA is not inert and is affected by a variety of DNA damage-inducing stimuli, including ultraviolet light (UV), ionizing radiation (IR) or reactive oxygen species that are a by-product of the cellular metabolism. If not repaired, DNA lesions can lead to mutations, which can finally result in a disease outcome including cancer. Therefore the sensing and repair of DNA damage during

the DNA damage response is essential to maintain genomic integrity and thus viability of the cell. To maintain genomic integrity, cells have evolved a number of mechanisms to detect and repair DNA damage, no matter whether this damage is caused by the environment or by errors during DNA replication. The DNA damage response is thereby tightly connected to the regulation of cell cycle progression by cell cycle checkpoints, which will be described in more detail in the following sections.

Translesion synthesis

In S phase cells are highly sensitive to DNA damage as many types of DNA damage lead to a block of the replication fork progression. The prolonged stalling of the replication fork leads to fork collapse, DNA double strand breaks (DSB) and thus promotes genetic instability. To prevent prolonged stalling of the replication fork, DNA damage tolerance (DDT) mechanisms are activated. The single DDT pathways differ in their potential to cause DNA mutations by either being error-prone or error-free mechanisms. The DDT is mediated by the translesion DNA synthesis (TLS) or DNA template switching (Andersen et al., 2008). The template switching is an error-free process that uses the newly synthesised, undamaged DNA strand of the sister chromatid as template to bypass the DNA lesion. In contrast, during TLS the specialized TLS polymerases η and κ replicate directly past the DNA lesion in an either error-prone or error-free fashion. TLS polymerases are low-fidelity polymerases, which are non-processive, lack the proof-reading ability and contain a larger active site that is capable of accommodating dissorted bases and base pair mismatches (Yang and Woodgate, 2007). The exchange of the one polymerase to another happens in a step-wise manner with at least two polymerase switching events. The first switch is the exchange of the stalled replicative polymerase to a TLS polymerase, which expands the TLS-patch to hide the lesion from the 3´ to 5´ exonuclease proofreading activity of the replicative polymerase. The final switch restores the replicative polymerase to the DNA template and DNA replication resumes. The usage of different TLS polymerases allows the specific correction of different kinds of DNA lesions. The polymerase η preferably repairs thymidine dimers, which are induced by UV light. In contrast, the polymerase κ specifically bypasses benzopyrene-induced guanine adducts (Zhang et al., 2000) (Ogi et al., 2002).

In addition to TLS and template switching, the DDT pathway is regulated by post-translational modifications of PCNA. During the normal DNA replication process PCNA is sumoylated at Lys164, which inhibits homologous recombination (Papouli et al., 2005). In response to DNA damage, PCNA is ubiquitinated by the Rad6-Rad18 E2-E3 ligase complex on Lys164 and thus promotes activation of TLS. Further

ubiquitination of PCNA leads to the promotion of the template switching DDT pathway (Hoege et al., 2002).

DNA double strand break repair and checkpoint activation

As mentioned above, the dissociation of the replication machinery from the stalled replication fork leads to collapse of the replication fork and subsequent generation of one-ended DNA double strand breaks (DSB). Replication-induced DSB also result from replication forks encountering a covalently linked topoisomerase, which is generated by topoisomerase inhibitors like doxorubicin (Li and Baker, 2000). In addition to replication stress, DSBs are induced directly by exposure of the cell to ionizing radiation (IR). DSBs are one of the most harmful forms of DNA damage as they result in chromosomal re-arrangement, depletions and chromosomal loss and subsequent genomic instability. DNA double strand breaks are repaired by nonhomologous endjoining (NHEJ) or homologous recombination repair (HR). During NHEJ, the DNA ligase IV directly joins the break ends using short homologous sequences present on the tail of the single DNA strands. If the overhangs are not compatible, NHEJ can lead to the formation of mutation resulting in translocations or telomere fusion. In contrast, during HR the homologues chromosome or the sister chromatid is used as a template for the repair of the DNA lesion (Moore and Haber, 1996). In concert with the activation of the DNA damage repair, the cell cycle progression is arrested by the activation of cell cycle checkpoints. The activation of checkpoints allows the cell to repair DNA lesions before entering the next cell cycle phase and thus prevents genomic instability.

The repair of DSBs starts with the binding of Mre11, Rad50 and Nbs1 (MRN)-complex to the ends of the DSB and subsequent recruitment and activation of the Ataxia-telangiectasia-mutated (ATM)-kinase (Lee and Paull, 2005). ATM phosphorylates the histone 2AX variant (γ-H2AX) thus initiating a signalling cascade involving multiple phosphorylation and ubiquitination events of DNA repair proteins like the breast cancer 1 (BRCA1) protein and the 53-binding protein 1 (53BP1). In addition to ATM, also ATM- and Rad3- related (ATR) and DNA- dependent protein kinase catalytic subunit (DNA-PKcs) are involved in the DDR pathway (Zou and Elledge, 2003) (Harrison and Haber, 2006). ATM, ATR and DNA-PKcs belong to the family of phosphoinositide-3 kinase- related protein kinases (PIKK) and serve as transducers of the DNA damage signal by phosphorylating and thus activating the checkpoint kinases (CHK) 1 and 2 (Li and Zou, 2005). Activated CHK1 and CHK2 phosphorylate CDC25 phosphatases finally leading to the checkpoint arrest of the cell (Figure 1.1).

CDC25 are dual-specific phosphatises, which dephosphorylate CDKs on Thr14 and Tyr15 leading to the activation of CDKs (Pines, 1999). The mammalian genome

encodes three isoforms of CDC25: CDC25A, CDC25B and CDC25C, which are all phosphorylated by CHK1 in response to DNA damage resulting in the functional inactivation of CDC25. CDC25A seems to be implicated in the control of the G_1 to S and the G_2 to M transition whereas CDC25B and C appear to play a role in the regulation of the G_2 to M transition (Rudolph, 2007). The functional inactivation of CDC25 is achieved by either re-localisation of the protein to the cytoplasm or degradation. CDC25B and CDC25C are functionally inactivated upon phosphorylation on Ser309/323 and Ser216, respectively, leading to 14-3-3 binding and nuclear exclusion (Donzelli and Draetta, 2003). In contrast, upon phosphorylation CDC25A is degraded by the proteasome, a process that is describe in detail in the following sections of this work. In addition to the CDC25 phosphatases, CHK1 directly targets and activates WEE1, which is the kinase responsible for the inhibitory phosphorylation of CDK1 and CDK2 on Tyr15 thus promoting cell cycle arrest.

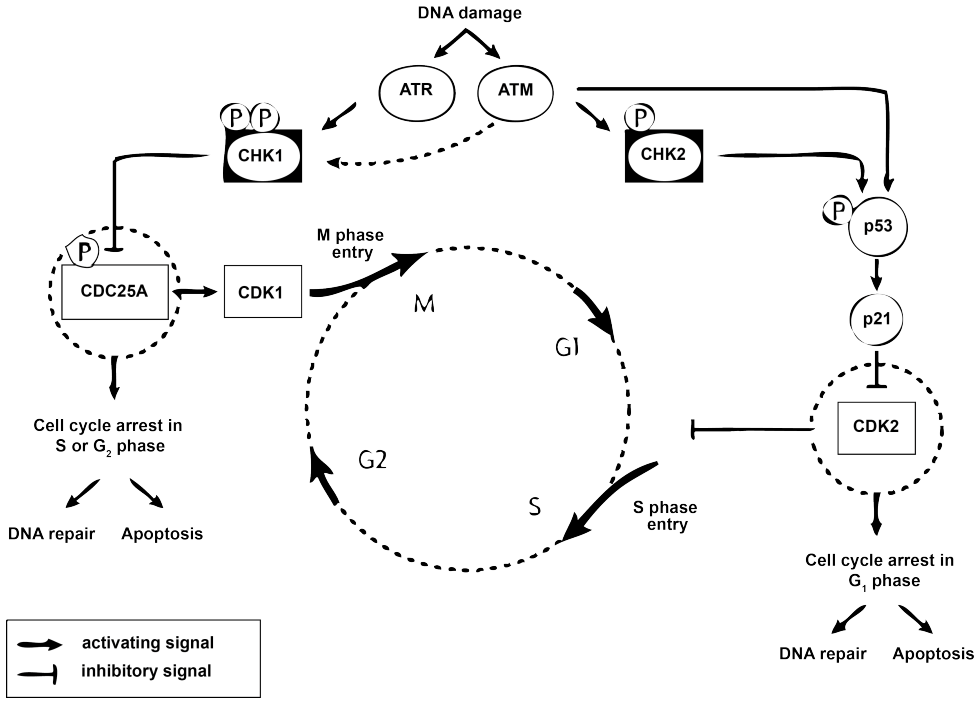

Figure 1.1: Cell cycle control after DNA damage induction.
Upon DNA damage the ATR/ATM kinases phosphorylate and activate the checkpoint kinases CHK1 and CHK2. Activated CHK1 and CHK2 promote the DNA damage response and subsequent cell cycle arrest by phosphorylation of the two key regulators: the CDC25 phosphatases and the p53 transcription factor. Upon phosphorylation p53 is active and promotes the transcription initiation of the CDK inhibitor p21 finally leading to cell cycle arrest. Phosphorylation of the CDC25 phosphatases result in their functional inactivation with subsequent cell cycle arrest, allowing the cell to repair DNA damage (modified from (Lapenna and Giordano, 2009)).

In addition to the activation of the checkpoint kinases, ATM also activates the tumour suppressor p53 leading to the transcription of the CDK inhibitor p21 and subsequent cell cycle arrest (Lobrich and Jeggo, 2007). The coordinated activation of the checkpoint kinases and tight regulation of cell cycle promoters and inhibitors mediates the controlled cell cycle arrest and recovery from DNA damage and subsequent progression in the cell cycle (Figure 1.1).

1.2 Ubiquitin-dependent cell cycle control

In addition to phosphorylation, ubiquitination and ubiquitin dependent proteolysis are important key events in the regulation of cell cycle progression. The ubiquitin proteasome system (UPS) plays a critical role in a wide variety of cellular processes, as it controls the abundance of cellular proteins. Ubiquitin is a highly conserved, small (8 kDa) protein that is covalently attached to substrates in a cascade manner. In the first step ubiquitin is linked to an ubiquitin-activating enzyme (E1) dependent on ATP hydrolysis. The activated ubiquitin is transferred to an ubiquitin-conjugating enzyme (E2), which cooperates with a E3 ubiquitin ligase that attaches ubiquitin to specific lysine residues of the target substrate (Hershko and Ciechanover, 1998) (Teixeira and Reed, 2013). The E3 ligases mediate the attachment of either only one ubiquitin to a specific lysine (monoubiquitination), the attachment of single ubiquitins to different lysines (multimonoubiquitination) or the attachment of ubiquitin-chains extending from a particular lysine residue (polyubiquitination). The ubiquitin can be linked to any of the seven lysine residues (Lys6, Lys11, Lys27, Lys29, Lys33, Lys48 and Lys63) as well as to the N-terminal methionine (Met1) (Johnson et al., 1995) (Peng et al., 2003) (Behrends and Harper, 2011). The different ubiquitin linkages create different types of ubiquitin chains and result in a wide range of molecular signals in the cell. Lys48-linked ubiquitin chains serve as a destruction tag for degradation of substrate proteins by the 26S proteasome (Baboshina and Haas, 1996), whereas Lys63-linked chains are considered to play an essential role in signalling processes like the NF-κB pathway, endocytosis or DNA repair processes (Lamothe et al., 2007) (Kim et al., 2007) (Sobhian et al., 2007). The regulation of the ubiquitination state of a protein is additionally modulated by deubiquitinating enzymes (DUB) that hydrolyse ubiquitin-protein bonds reversing ubiquitination of target proteins and recycling ubiquitin (Reyes-Turcu et al., 2009).

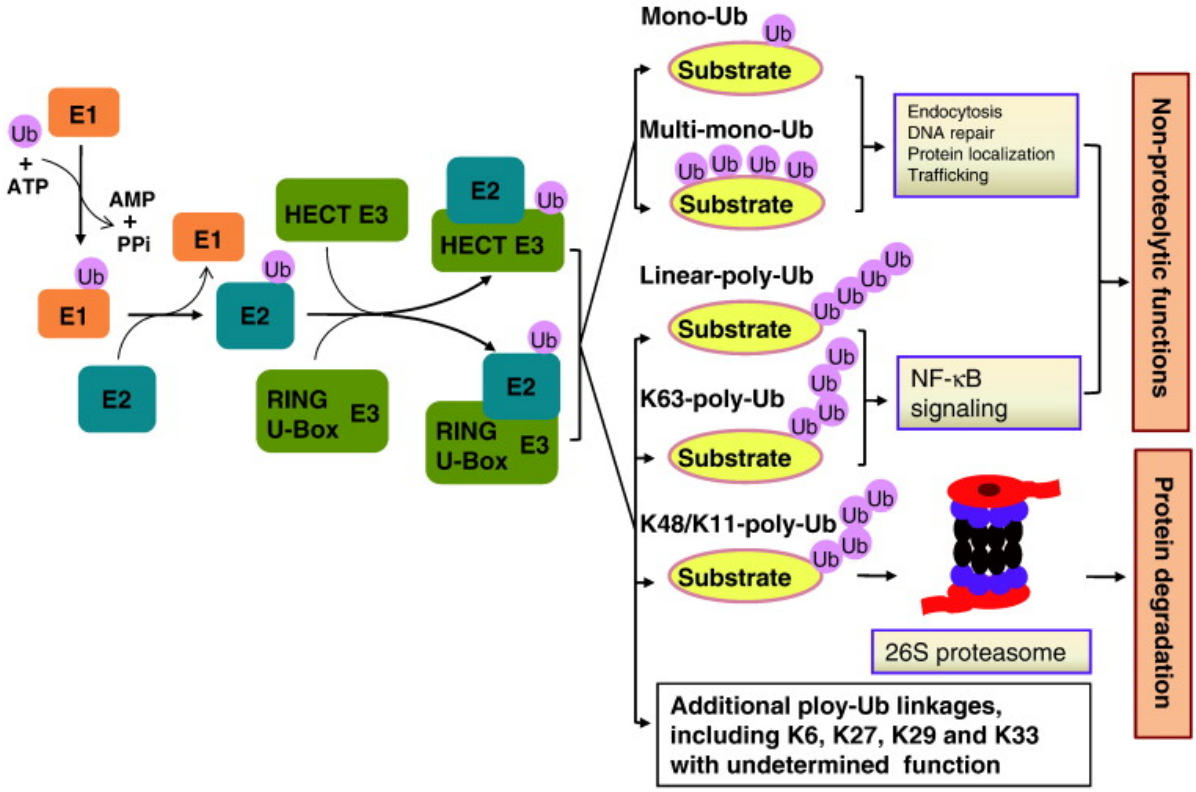

Figure 1.2: Schematic illustration of the ubiquitin-proteasome system.
In the first step ubiquitin (Ub) is linked to an ubiquitin-activating enzyme (E1) depending on ATP hydrolysis. The active ubiquitin is covalently linked to the target substrate by an E2 (ubiquitin-conjugating) and E3 ligase complex. The E3 ligases belong to the HECT E3 ligase family or to the RING E3 ligase family. The target substrate can be linked with monoubiquitin or ubiquitin chains at any of the seven lysine's found on target substrates. Depending on the type of ubiquitination, the biological outcome can range from protein degradation to non-proteolytical functions. (Zhang et al., 2014)

In eukaryotes two major classes of E3 ligase´s families exists: the homologous to the E6-AP carboxyl-terminus (HECT) and the really interesting new gene (RING)-domain containing E3 ligases (Rotin and Kumar, 2009). HECT E3 ligases form a transient and covalent linkage with ubiquitin at the conserved cysteine before they transfer ubiquitin to the substrate. In contrast, RING E3 ligases catalyse the transfer of ubiquitin from the E2 enzyme to the target substrate without direct substrate binding (Metzger et al., 2012). The RING-finger thereby serves as a scaffold, which brings the E2 enzyme and the substrate together (Ozkan et al., 2005). The mammalian genome encodes more than 600 potential RING E3 ligases (Li et al., 2008). These are further subcategorized into monomers, dimers and multi-subunit complexes, in which the RING-domain containing subunit and the substrate-binding domain are part of distinct proteins (Metzger et al., 2012). The best understood E3 ligases that are involved in the regulation of the cell cycle progression are the cullin-RING (CRL) ligases (Petroski and Deshaies, 2005) and their relative, the anaphase promoting

complex/cyclosome (APC/C). CRLs are characterized by their cullin-domain, which binds to the RING finger protein RING-box protein 1 (Rbx1). The human cullin family consists of seven cullins (Cul1, Cul2, Cul3, Cul4A, Cul4B, Cul5 and Cul7) and one more distinct member APC2 that functions in the APC/C complex. CRLs and the APC/C E3 ligases ubiquitinate various key cell cycle regulators like cyclins, WEE1, CDC25 phosphatases, p21, p27 as well as mitotic kinases Polo-like kinase 1 (PLK1), Aurora A and B (Carrano et al., 1999) (Koepp et al., 2001) (Strohmaier et al., 2001) (Sumara et al., 2007) (Beck et al., 2013). In the following sections, the cell cycle regulation by the APC/C complex and the CRL complexes is described in more detail.

1.2.1 Anaphase promoting complex

The APC/C complex is an important regulator of the cell cycle progression and is implicated in regulating processes including apoptosis, metabolism and development through degradation of specific substrates. The APC/C complex consist of three sub-complexes, namely the scaffolding sub-complex, the catalytic and substrate-recognition sub-complex and the tetra-tricopeptide repeat (TRP) arm (Foe and Toczyski, 2011) (Schreiber et al., 2011) (Schreiber et al., 2011). The TRP arm itself provides binding sites for the scaffolding unit and the co-activators Cdc20 and Cdh1 (Vodermaier, 2004). The cell cycle regulation is controlled by the temporal coordination of the co-activators Cdc20 and Cdh1, which form APC/C^{Cdc20} or APC/C^{Cdh1}, respectively. APC/C^{Cdc20} regulates the metaphase to anaphase transition as well as mitotic exit, whereas APC/C^{Cdh1} is active during the end of mitosis and early G_1 phase. In G_2 phase, Cdc20 is phosphorylated by CDK1 and other mitotic kinases promoting the interaction between APC/C and Cdc20 and thus partially activating APC/C^{Cdc20} (Kramer et al., 2000) (Kraft et al., 2003). Mitotic aberrations, like misaligned spindle or improper attachment of kinetochores on the sister chromatids, inhibit the APC/C^{Cdc20} activity due to the activation of the spindle assembly checkpoint (SAC). The SAC thereby negatively regulates the ability of Cdc20 to activate the APC/C-mediated proteolysis of downstream key regulators. Upon activation of the SAC, both BUBR1-BUB3 and Mad2 bind Cdc20 directly and inhibit its ability to activate the APC/C. The transient formation of BUBR1-BUB3-Cdc20 and Mad2-Cdc20 complexes lead to the formation of the BUBR1-BUB3-Mad2-Cdc20 mitotic checkpoint complex (MCC), which efficiently inhibits APC/C-mediated degradation of downstream key regulators and arrest mitotic progression (Musacchio and Salmon, 2007) (Yu, 2002). After satisfaction of the SAC, the APC/C^{Cdc20} complex becomes active and promotes the ubiquitin-dependent degradation of securin, an inhibitor of separase. Separase is a protease that cleaves the cohesin complex and thereby triggers sister chromatid separation (Michaelis et al., 1997) (Nasmyth et al., 2001). The APC/C^{Cdc20} complex also targets cyclin B for

degradation, which leads to reduced activity of CDK1 and promotes mitotic exit. Upon exit of mitosis the inhibitory phosphorylation of Cdh1 by CDK1 is reduced leading to an exchange of Cdh1 with Cdc20 and thus the APC/C^{Cdh1} complex becomes more active (Lukas et al., 1999) (Keck et al., 2007) (Harper et al., 2002). The APC/C^{Cdh1} complex in turn promotes the degradation of CDC20, PLK1, Aurora A and B (Huang et al., 2001) (Lindon and Pines, 2004) (Littlepage and Ruderman, 2002) (Stewart and Fang, 2005).
In contrast to APC/C^{Cdc20}, the APC/C^{Cdh1} complex is important for the cell cycle progression through G_1 phase by sustaining low CDK1 activity mediated by the degradation of mitotic cyclins, CDC25A, Skp2 and CSK1 (Irniger and Nasmyth, 1997) (Donzelli et al., 2002) (Bashir et al., 2004). Additionally, the APC/C^{Cdh1} complex promotes the ubiquitin-mediated degradation of geminin, Cdc6 and its own E2 enzyme UBCH10 (McGarry and Kirschner, 1998) (Petersen et al., 2000) (Rape and Kirschner, 2004). This leads in turn to stabilization of cyclin A and inactivation of APC/C^{Cdh1} leading to the timely limitation of G_1 phase.

1.2.2 SKP1/CUL1/F-box (SCF) protein complexes

In addition to the APC/C complex, the CRLs are another major group of E3 ligase complexes regulating cell cycle progression. Cullin1 RING ligases (also known as SCF complex) consist of the cullin 1- scaffold unit, Rbx1 (RING)-protein, which recruits the E2 enzyme and the S phase kinase associated protein 1 (Skp1), which serves as an adaptor to bind the F-box protein, the substrate-binding unit (Figure 1.3) (Zheng et al., 2002). F-box proteins are named after the F-box, a 40 amino acids motif that was first identified in cyclin F (Fbxo1) (Bai et al., 1996). Additionally to the F-box, these proteins contain extra motifs that contribute to substrate binding. Depending on these motifs F-box proteins are classified into three subgroups: the WD40 containing Fbxws proteins, the leucine-rich repeats (LRR) Fbxls proteins and the remaining F-box proteins with other motifs like tetratrico-peptide repeats, kelch repeats and prolin-rich motifs called Fbxos (Cenciarelli et al., 1999) (Cardozo and Pagano, 2004) (Jin et al., 2004). The human genome encodes 69 F-box proteins, which recognize individual substrates and thereby determine the broad functional bandwidth of SCF ligases. A biological function has been assigned only to a few F-box proteins. Three F-box proteins are connected to functions in the regulation of cell cycle progression: Skp2, Fbw7 and βTrCP.

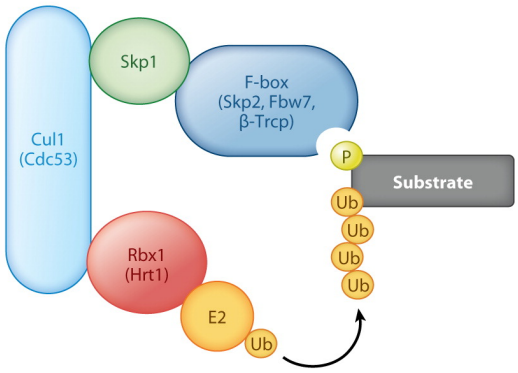

Figure 1.3: Schematic representation of the SCF E3 ligase complex.
SCF ligases contain a cullin-scaffold unit (light blue), Skp1 protein (green) and the Rbx1 (RING)-protein (red), which recruits the E2 enzyme (yellow). Skp1 recruits the different F-box proteins (dark blue), which recognize specific phosphorylates sequences on target substrates triggering their ubiquitylation and degradation. Abbreviations: Ub- ubiquitin, P- phosphate (Teixeira and Reed, 2013)

Skp2 binds substrates through its C-terminal LRR domain that requires additional binding of the small and highly conserved co-factor Cks1, which forms a part of the substrate-binding surface (Spruck et al., 2001) (Hao et al., 2005). Skp2 accumulates during G_1 to S-phase as a consequence of APC/C^{Cdh1} inactivation (Bashir et al., 2004). Skp2 itself mediates the ubiquitin-dependent degradation of the CKIs $p27^{Kip}$, $p21^{Cip}$, $p57^{Kip2}$ and the pocket protein p130/RB2, which leads to the increased activity of S phase CDK–cyclin complexes (Ganoth et al., 2001) (Bornstein et al., 2003) (Nakayama and Nakayama, 2006) (Frescas and Pagano, 2008) (Tedesco et al., 2002). During replication the degradation of the origin licensing factors Orc1 and Cdt1 is induced by Skp2, preventing origins from becoming re-licensed and thus re-replicated (Mendez et al., 2002) (Li et al., 2003).
In contrast to Skp2, Fbw7 levels are constant throughout cell cycle and its dimerization increases the efficiency to bind to its substrates. Fbw7 mediates the ubiquitin-dependent degradation of cell cycle activators like cyclin E, c-myc, c-Jun and Notch (Welcker and Clurman, 2008) (Crusio et al., 2010). Fbw7 binds to its substrates phosphodegrons via a domain composed of 8 WD40 repeats (Hao et al., 2007). The activity of Fbw7 depends not only on the phosphorylation state of its substrate but it is also regulated by glomulin. Glomulin is a CRL inhibitor that binds to Rbx1 and thereby blocks the association to the E2 enzyme Cdc34, what leads to accumulation of cyclin E and c-myc (Tron et al., 2012). Coupling CDK2-cyclin E activity to the abundance of cyclin E establishes a negative feedback loop that limits the maximal CDK2-cyclin E activity and defines the timely interval of the cell cycle.

The third F-box protein known to regulate cell cycle progression is βTrCP. Like Fbw7, βTrCP binds to substrate phosphodegrons via a C-terminal domain containing WD40 repeats. βTrCP mediates the ubiquitin-dependent degradation of the cell cycle inhibitor WEE1, which is phosphorylated by PLK1 and CDK1 on Ser53 and Ser123, respectively (Watanabe et al., 2004). This positive feedback loop ensures the rapid activation of CDK1 and mitotic entry. The activity of PLK1 itself is regulated by the synergistic actions of Aurora A and Bora. Accumulation of Bora during G_2 leads to the activation of Aurora A and thus to activation of PLK1. βTrCP also affects indirectly the chromosome segregation by regulating multiple aspects of the mitotic spindle. During mitosis, Bora regulates the localization and function of Aurora A at the spindle poles. The stabilization of Bora thus induces the formation of monopolar spindles and delays the metaphase to anaphase transition. Upon phosphorylation by PLK1, Bora is ubiquitinated by βTrCP and degraded (Seki et al., 2008a). In addition to Bora, βTrCP regulates the degradation of the repressor element 1 silencing transcription factor (REST) during G_2 phase and ensures full activation of the SAC (Guardavaccaro et al., 2008). The βTrCP protein further promotes mitotic progression by inducing the degradation of the APC/C inhibitor Emi1 during early mitosis (Margottin-Goguet et al., 2003). In addition to its functions in mitosis, βTrCP is an important player in the regulation of the cell cycle progression in response to DNA damage, which is described in more detail in the last part of this section.

In addition to the SCF complex, also other CRLs are involved in the regulation of cell cycle progression. The CRL3 complex controls mitotic progression through ubiquitination of Aurora B, which is then targeted to mitotic chromosomes to control their alignment (Sumara et al., 2008). CRL4 contains Cul4, Rbx1 and the DNA damage binding protein 1 (DDB1) domain and is implicated in the DNA replication and DDR. $CRL4^{Cdt2}$ interacts with the ubiquitin-conjugating enzymes (UBCs) UBCH8, UBE2G1 and UBE2G2, to mediate the ubiquitination of various substrates (Shibata et al., 2011). $CRL4^{Cdt2}$ mediates the degradation of the replication-licensing factor Cdt1 as well as degradation of p21 in normal cell cycle and after DNA damage induction (Hu and Xiong, 2006) (Abbas et al., 2008). In addition, CRL4 also mediates the ubiquitin-dependent degradation of the histone methytransferase Set8 and thereby regulates the H4Lys20me1 histone mono-methylation, which promotes the compaction of chromatin during G_2 phase. After DNA damage induction, Set8 is targeted for proteolysis by $CRL4^{Cdt2}$ in a PCNA-dependent manner (Jorgensen et al., 2011). The availability of Cdt2 itself is regulated by another CRL, the SCF^{Fbxo11}. The CDK-mediated phosphorylation of Cdt2 on Thr464 inhibits binding and degradation by SCF^{Fbxo11} and therefore delays cell cycle exit (Rossi et al., 2013).

βTrCP-mediated regulation of cell cycle checkpoints

Besides it functions in regulation of mitotic progression, βTrCP is a component of the DNA damage response (DDR) and mediates the degradation of CDC25A and CDC25B (Kanemori et al., 2005) (Uchida et al., 2009). βTrCP1 and its ortholog βTrCP2 (Fbxw11) are biochemically indistinguishable and are referred as βTrCP1/2 or βTrCP. Inhibition of βTrCP leads not only to a defective intra-S phase checkpoint but also to mitotic catastrophe (Busino et al., 2003). Unlike other βTrCP substrates, CDC25A contains a different phosphodegron ^{76}SSESTDSG^{83} with three phosphorylated serines instead of two (DSGxxS). Interestingly, the exact mechanism how βTrCP binds to the CDC25A degron is not clear, as no crystal structure is yet available. Upon DNA damage induction, the checkpoint kinases CHK1 and CHK2 phosphorylate CDC25A on Ser76, which serves as a priming event for further phosphorylation of CDC25A by other kinases (Jin et al., 2008). CHK1 activation additionally leads to phosphorylation of NEK11, which then in turn further phosphorylates CDC25A at Ser82 leading to its degradation (Melixetian et al., 2009). In addition to CHK1 and CHK2, several other kinases can phosphorylate CDC25A. The glycogensynthetase kinase 3 (GSK3)-β also phosphorylates CDC25A on position Ser76 after the priming of CDC25A by PLK3 (Kang et al., 2008). Phosphorylation of CDC25A on Ser76 by CHK1, CHK2 or GSK3β is followed by further phosphorylation on Ser79 and Ser82 by the casein kinase Iα (CKIα) leading to its ubiquitination by βTrCP and subsequent degradation (Honaker and Piwnica-Worms, 2010). Degradation of CDC25A leads to an arrest in cell cycle progression, as inhibitory phosphorylations are not removed from the CDKs (Figure 1.4).

βTrCP also mediates the MDM2-independent degradation of p53, which is phosphorylated on Ser362 and Ser366 by IκB kinase 2 (IκK2/IκKβ) (Xia et al., 2009). In addition to the functions in the DDR, βTrCP is also involved in the recovery from genotoxic stresses by regulation of claspin and WEE1 degradation. After DNA damage, the activity of PLK1 is inhibited by APC/C^{Cdh1}-mediated degradation (Macurek et al., 2008). During recovery the PLK1 levels increase and PLK1 is activated by Aurora A and Bora (Seki et al., 2008b). PLK1 and CDK1 then phosphorylate WEE1 leading to its βTrCP-mediated degradation (Watanabe et al., 2004). Additionally, PLK1 also phosphorylates claspin, which is then ubiquitinated by βTrCP and degraded. The degradation of claspin decreases CHK1 activity leading to termination of the checkpoint (Peschiaroli et al., 2006) (Mamely et al., 2006) (Mailand et al., 2006).

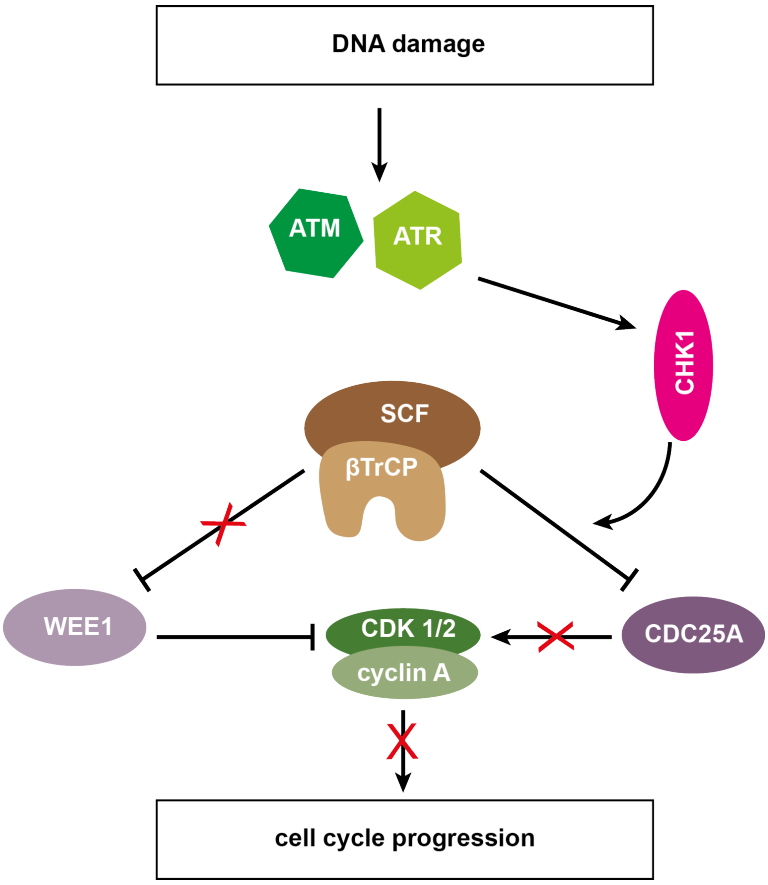

Figure 1.4: Role of SCF ligase complex in the DNA damage response.
Upon DNA damage ATR/ATM activate CHK1 leading to βTrCP-mediated degradation of Cdc25A, which inhibits CDK1 activity. In contrast, Wee1 is stabilized during the DNA damage response to promote arrest in the cell cycle progression. (adapted from (Bassermann et al., 2014))

1.3 The AAA$^+$ ATPase p97

An important component of the ubiquitin-proteasome system is the vasolin-containing protein (VCP)/p97, which belongs to the family of ATPases associated with various cellular activities (AAA$^+$-ATPases) (Neuwald et al., 1999). p97 (also called Cdc48 in yeast, CDC-48 in *Caenorhabitis elegans* and Ter94 in flies) is an essential and highly abundant protein that shares 69 % sequence identity from yeast to human (Frohlich et al., 1991). It catalyses the hydrolysis of ATP to generate energy, which is transferred into mechanical forces. Accounting for more than 1 % of the total amount of cellular proteins, p97 is involved in a wide variety of cellular functions ranging from membrane fusion events and endoplasmatic reticulum-associated degradation (ERAD) of proteins to the regulation of cell cycle progression and the DNA damage response (Meyer et al., 2012) (Wolf and Stolz, 2012) (Vaz et al., 2013). Mutations of the p97 gene are linked to neurodegenerative diseases like amyotrophic lateral sclerosis (ALS) and inclusion body myopathy associated with Paget disease of bone and fronttemporal dementia (IBMPFD) (Johnson et al., 2010) (Watts et al., 2004).

1.3.1 Structure and activity

The p97 ATPase is a homohexamer with a barrel-like structure. Thereby, each p97 monomer consists of two conserved ATPase domains, D1 and D2, which contain a Walker A (P-loop) and a Walker B (DEXX box) motif for ATP binding and hydrolysis, respectively (Neuwald et al., 1999) (Ogura and Wilkinson, 2001). The Walker B motif contains a second region of homology (SRH), which is required for efficient ATP hydrolysis. The D1-domain is important for the formation of a stable hexamer, whereas the D2-domain exhibits the major ATPase activity (Wang et al., 2003a) (Wang et al., 2003b). The N-domain of p97 is mostly flexible and is important for substrate and co-factor binding. A recent study proposes a model where the N-domain adopts either of two conformations: a flexible conformation compatible with ATP hydrolysis or a coplanar conformation that is inactive (Niwa et al., 2012). Another study identified conformational heterogeneity within two major p97 conformations depending on the nucleotide binding state and existing simultaneously in solution. In conformation one, the D1-domain forms an open pore with the N-domain in a raised position above the D1-domain. Upon nucleotide binding and hydrolysis the D1 ring rotates relative to the D2 ring, which may be linked to the remodeling of target protein complexes. In the second conformation, the D1-domain is tightly packed and the D2-domain is more open independent on the nucleotide binding state (Figure 1.5) (Yeung et al., 2014).

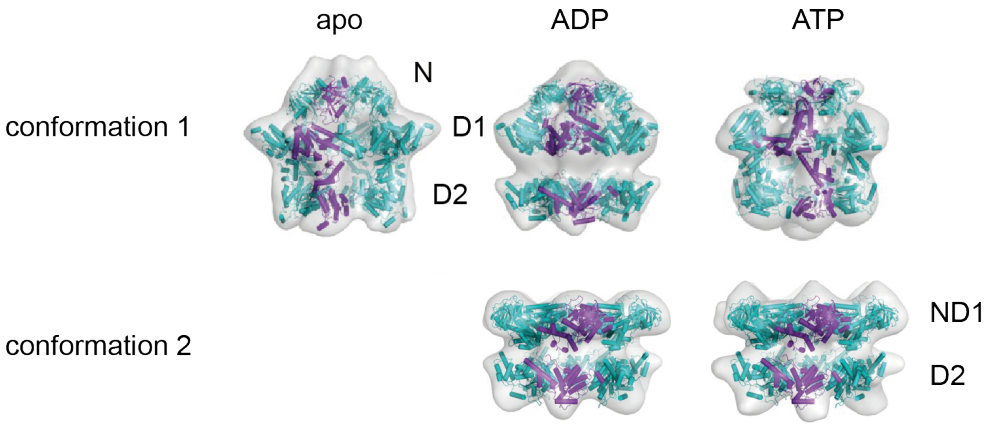

Figure 1.5: Three-dimensional reconstructions of p97^{E578Q} in different nucleotide states.
Conformation 1 has a three-layered structure with the N-domain above the D1 ring in the apo state, in an intermediate state in ATP bound state or as a flat cap in the ADP bound state. The D1 ring is expanded whereas the D2 domain shows conformational changes depending on the nucleotide state. Conformation 2 has a two-layered architecture with the ND1 domain in the first layer and the D2 domain in the second layer. There are only slight changes in the structure in the different nucleotide states. (modified from (Yeung et al., 2014))

The C-terminus of p97 is highly disordered and contains a tyrosine that regulates p97 activity in membrane fusion and nuclear translocation through its phosphorylation state (Lavoie et al., 2000) (Madeo et al., 1998).
Mutations of p97 are referred to as subtle as the disease forms of p97 are “late onset” diseases with associated defects in intracellular protein degradation pathways including UPS, autophagy and endosome-lysosome fusion (Tresse et al., 2010) (Ritz et al., 2011). Up to date there are 20 miss-sense mutations know from clinical studies with patient material. The majority of the mutation is located in the N-domain and in the ND1-linker. The highest occurrence in patients has the mutation of the residue R155 (Hubbers et al., 2007). Also mutation of R155H does not lead to major changes in the p97 structure and does not abolish the ATPase activity of p97, it displays a number of alterations in the interaction of p97 and its adaptor proteins (Fernandez-Saiz and Buchberger, 2010).
Another p97-modification, used in our experiments to confirm p97-interaction partners, is the p97EQ variant. Here the conserved glutamate (E) residue in the Walker B motif of the D2 domain is mutated to glutamine (Q), which abolishes the ATP hydrolysis and leads to a dominant negative variant of p97, termed p97EQ, that bind but cannot release substrates (DeLaBarre and Brunger, 2005) (Pye et al., 2006).

1.3.2 Model of p97 function

The p97 ATPase is an important component of the UPS that mediates the degradation of misfolded or damaged proteins to maintain the cellular homeostasis. Distinct from other classical ubiquitin-shuttling factors, p97 does not only bind to it substrates and the proteasome but uses the hydrolysis of ATP to structurally remodel or unfold its substrates to facilitate degradation by the proteasome (Yamanaka et al., 2012). As mentioned above, a well-established function of p97 in the ubiquitin-dependent degradation is the maintenance of protein homeostasis, as it facilitates the proteosomal degradation of misfolded proteins in different compartments, including the endoplasmatic reticulum (ER) and the outer mitochondrial membrane, as well as the ribosome-associated degradation of proteins (Figure 1.6). By facilitating the degradation of mitofusin, p97 protects the fusion of damaged and healthy mitochondria thereby facilitating the elimination of terminally defective mitochondria (Tanaka et al., 2010). In the ER-associated degradation (ERAD), p97 bind to misfolded ubiquitinated substrates and mediates their proteosomal degradation. Interfering with p97 function and thus accumulation of misfolded proteins in the ER leads to subsequent activation of the unfolded protein stress response (Meyer et al., 2012) (Kothe et al., 2005). Recently, p97 was implicated in the ribosome-associated protein quality control and thus in the translational stress response. p97 thereby regulates the turnover of aberrant mRNAs as well as the

direct degradation of ubiquitinated ribosomal proteins by the proteasome (Brandman et al., 2012) (Verma et al., 2011) (Fujii et al., 2012). Besides protein quality control, p97 is implicated in the regulation of signalling processes by the procession of cytosolic proteins, including the degradation the NFκB inhibitor IκBα and the degradation of HIFα, which leads to the activation of NFκB and down-regulation of the hypoxic response, respectively (Li et al, 2014, Alexandru et al, 2008). Furthermore, p97 is connected to an emerging number of chromatin-associated functions, which governs the timely degradation of cell cycle regulators and thus ensures ordered cell cycle progression (Vaz et al., 2013). The multiple aspects of p97 in the cell cycle regulation will be described in more detail in the following sections.

Additionally to the proteasome-dependent degradation of proteins, p97 is also implicated in the lysosomal degradation, as it mediates the sorting of cargo proteins through the endosomal pathway as well as through autophagy, although the exact mechanism of p97 function in autophagy remains not fully understood (Ritz et al., 2011) (Kirchner et al., 2013) (Meyer et al., 2012).

In addition to protein quality control-related protein degradation, specific p97 complexes associate with mono-ubiquitinated substrates and facilitate proteasome-independent membrane trafficking events, including Golgi reassembly by promoting membrane-protein segregation (Meyer et al., 2002) (Kondo et al., 1997). Furthermore, p97 is also implicated in non-degradative processes, promoting the extractions of transcription factor precursors from membranes, leading to their subsequent activation.

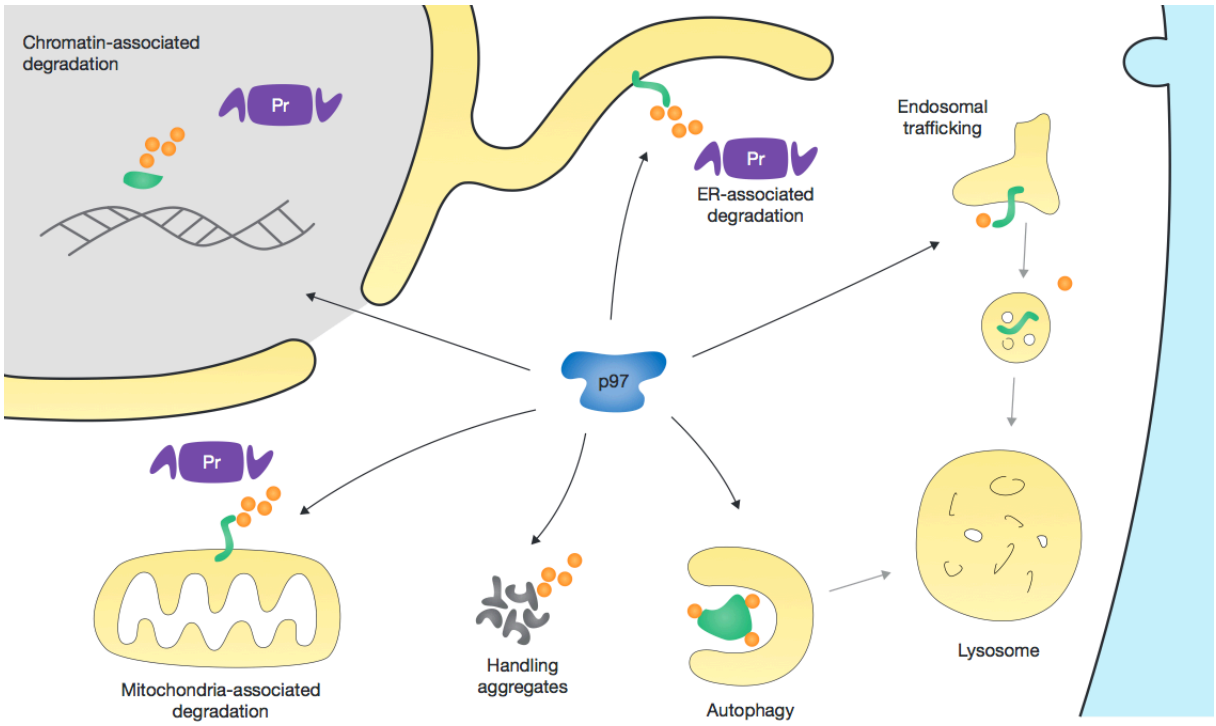

Figure 1.6 Cellular functions of p97 in interphase cells.
The best understood function of p97 is its function in ER-associated degradation (ERAD). In addition p97 is involved in the handling of protein aggregates, in the degradation of mitochondrial outer-membrane proteins and in the chromatin-associated degradation of proteins. p97 also facilitates the proteasome-independent degradation of proteins via the lysosomal pathway by mediating the endosomal sorting in endocytosis and the regulation of autophagy. Target substrates are coloured in green, proteasome in violet and ubiquitin in orange. (modified from (Meyer et al., 2012))

1.3.3 p97 adaptor protein system

As p97 is involved in a wide range of cellular processes, its activity needs to be specified for the distinct functions. Therefore p97 interacts with a large number of adaptor proteins, which contain different p97-binding domains or motif (Figure 1.7). The various p97 adaptor proteins are believed to bind to p97 in a hierarchical manner, meaning that p97 forms core complexes with mutually exclusive major co-factors including Ufd1-Npl4, p47 and UBXD1 (Meyer et al., 2012). The binding of additional co-factors modulates the localization of p97 or acquires additional enzymatic activity and thereby mediates specific p97 functions. Interestingly, p97 binds to ubiquitin directly *in vitro*, however it is believed that *in vivo* p97requires the binding of substrate recruiting co-factors to obtain optimal activity (Rape et al., 2001). Since p97 acts on ubiquitinated substrates, the substrate recruiting factors contain ubiquitin-binding domains to mediate a more stable enzyme-substrate complex formation (Meyer et al., 2002). Some adaptor proteins like VIMP and Derlin-1 do not bind to ubiquitin but are still considered to be substrate-recruiting factors as they tether p97 to the ER membrane at the sites of ERAD and thereby allow a more efficient degradation of ubiquitinated substrates. Two distinct models describe the

sequential p97-substrate complex formation. In the first model, the complex assembly starts with the binding of an adaptor protein to the substrate. The adaptor-substrate complex recruits p97. Such a mechanism was shown for UBXD7 and SAKS1, where the p97 activity is regulated by the availability of the substrate (Madsen et al., 2009). In the second model of p97-substrate complex formation, the binding of the adaptor protein to p97 creates a complex that is able to bind to ubiquitinated substrates. After the formation of a p97-substrate complex, p97 can also bind additional substrate-processing co-factors. Substrate-processing co-factors often equip p97 with additional enzymatic activity or inhibit the p97 activity. Some substrate-processing factors display DUB activity preventing p97 substrates from degradation. The yeast enzyme OTU1 removes ubiquitin chains from Ufd1-Npl4 recruited p97 substrates and thereby prevents their degradation (Rumpf and Jentsch, 2006). In addition to preventing ubiquitinated substrates from proteasomal degradation, DUBs can also promote degradation of substrates by cutting polyubiquitin branches into ubiquitin chains that can be recognized by the proteasome.

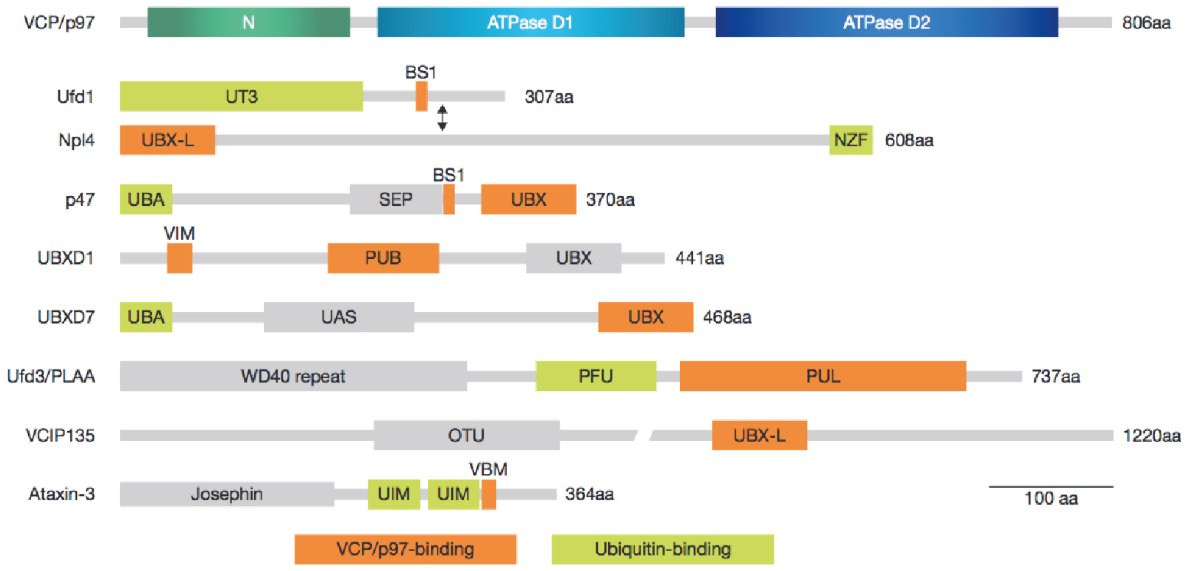

Figure 1.7: p97 and p97 co-factor domain structure.
The p97 monomer consists of a N-domain and the two ATPase-domains D1 and D2. The D1-domain is believed to be important for ATP binding whereas the D2 domain is mostly important for ATP hydrolysis. p97 co-factors bind to the N-domain of p97 via their UBX, UBX-L domains or via short binding motifs like the BS1, VBM and VIM motif. PUB or PUL domains bind to the C-terminus of p97. With the ubiquitin-binding domains like UBA, NZF in Npl4 and PFU in Ufd3/PLAA p97 adaptors bind to ubiquitin. UAS: ubiquitin-associating, UT3: Ufd1 truncation 3 domain, SEP: Shp1-eyc-p47 domain. The OTU and Josephin domains have deubiquitinating activity. (modified from (Meyer et al., 2012))

The majority of p97 co-factors bind to the N domain of p97 by interacting with either the UBX domain or the UBX-like (UBX-L) domain. In addition, adaptor proteins bind p97 via different binding motifs like the SHP box (also called Binding Site 1), the VCP binding motif (VBM) or the VCP interacting motif (VIM) (Buchberger 2010; Kloppsteck et al. 2012; Meyer et al. 2002; H. Meyer 2012). Some co-factors bind to the C-terminal tail of p97 by interacting with the PUB or PUL domains (Figure 1.7) (Madsen et al. 2009). Below, the p97 co-factors Ufd1-Npl4, DVC1 and UBXD7 are described in more detail.

Ufd1-Npl4

As mentioned above the p97 co-factors p47 and Ufd1-Npl4 bind to the N domain of p97 in a mutually exclusive manner (Bruderer et al., 2004) (Meyer et al., 2000). The nuclear protein localization-4 (Npl4) was first identified in a yeast screen for temperature-sensitive mutants that accumulate nuclear proteins in the cytoplasm upon shift to the semi-permissive temperature (DeHoratius and Silver, 1996). Npl4 binds to the ubiquitin fusion degradation 1 protein (Ufd1) in a 1:1 stoichiometry and exists either as heterodimer or bound to p97 (Meyer et al., 2000) (Bruderer et al., 2004). It was shown that Ufd1 is unstable in the absence of Npl4, and that the heterodimer Ufd1-Npl4 is the only essential cofactor in yeast (DeHoratius and Silver, 1996) (Johnson et al., 1995). The N domain of Ufd1 is structurally similar to the N domain of p97 and contains binding-sites for both mono- and polyubiquitin (Park et al., 2005). The structure of Npl4 is less understood also NMR studies resolved a N-terminal UBX-L domain and a C-terminal zinc-finger (NZF), which binds to polyubiquitin (Isaacson et al., 2007) (Meyer et al., 2002). The interaction of Ufd1-Npl4 with p97 has been described as bipartite with two different p97-interacting sites located at the UBX-L domain of Npl4 and the C-terminal BS1 motif of Ufd1 (Bruderer et al, 2004). Recent studies revealed different conformational states of the $p97^{Ufd1\text{-}Npl4}$ complex, in which the positions of Ufd1-Npl4 differ relative to the p97 ring, displaying the dynamic behaviour of the complex (Bebeacua et al., 2012). Ufd1-Npl4 directs the p97 function to disperse cellular functions like ERAD, activation of transcription factors and chromatin-associated degradation of proteins. Previous findings implicate the $p97^{Ufd1\text{-}Npl4}$ complex in the regulation of cell cycle progression and the regulation of the DNA damage response, which will be described in detail in the following section.

UBXD7

UBXD7 belongs to the p97 co-factors that bind p97 via an UBX domain. Based on their domain composition UBX-proteins are divided into two major groups. The UBX-UBA proteins contain an ubiquitin-binding ubiquitin-associated (UBA) domain and a

p97-binding UBX domain, whereas UBX-only proteins lack the UBA domain and the ability to bind ubiquitin. UBXD7 belongs together with UBXD8, FAF1, SAKS1 and p47 to the group of UBX-UBA containing proteins (Hurley et al., 2006). UBX-UBA proteins have the ability to interact with multiple E3 ligases, especially with CRL but also with HECT-E3 ligases (Alexandru et al., 2008). The individual UBX-UBA proteins thereby do not strictly interact with only one particular E3 ligase as UBXD7 for example interacts preferentially with CUL2 and CUL4 ligases but also to lesser extend with CUL1 and CUL3 (den Besten et al., 2012) (Alexandru et al., 2008). Together with p97 and Ufd1-Npl4, UBXD7 forms a higher-ordered complex connected to the function of CRL E3 ligases. UBXD7 directly binds to CRL through its ubiquitin-interacting motif (UIM) that is located between the UBX and the UBA domain (Bandau et al., 2012) (den Besten et al., 2012). The UIM of UBXD7 recognizes the ubiquitin-like small modifier NEDD8, whose dynamic conjugation to the CRL is required to activate the ligase activity (Saifee and Zheng, 2008). UBXD7 links p97 to the CRL2-VHL substrate HIF1-α that is constantly degraded in normoxic conditions (Alexandru et al., 2008). The yeast homolog of UBXD7, Ubx5, binds to CRL3 and mediates together with Cdc48, Ufd1-Npl4 and Ubx4 the extraction and degradation of the RNA polymerase subunit 2 in response to UV-light (Verma et al., 2011) (Schuberth and Buchberger, 2008). A recent study links UBXD7 in complex with $p97^{Ufd1\text{-}Npl4}$ to the degradation of the CUL4A substrates DDB2 and XPC in response to UV light thus ensuring the proper activation of the nucleotide excision repair (NER) pathway (Puumalainen et al., 2014).

DVC1

DVC1, also called Spartan or C1orf124, is a multi-domain protein and contains a SprT-like domain at its N-terminus, a SHP box motif and a PIP box in the middle region and a ubiquitin-binding zinc-finger (UBZ) domain at its C-terminus (Kim et al., 2013) (Juhasz et al., 2012) (Ghosal et al., 2012) (Centore et al., 2012). It belongs to the family UBZ4-type domain- containing proteins, whose UBZ4- domain is important for the recruitment to sites of DNA damage or stalled replication forks (Davis et al., 2012). The first studies identified DVC1 as a protein that localizes to the sites of stalled replication forks after UV-light and is involved in the process of TLS. It interacts with ubiquitinated PCNA, also the exact mechanism remains unclear. Ghosal and colleagues found that DVC1 interacts with PCNA via its PIP domain and UBZ domain dependent on the ubiquitination of PCNA, whereas others did not find ubiquitination of PCNA to be important for the interaction (Ghosal et al., 2012) (Mosbech et al., 2012). DVC1 is expressed in human cell lines during S- and G_2 phase and is rapidly degraded upon mitotic exit (Mosbech et al., 2012). It interacts with Cdh1 and is ubiquitinated by the APC/C^{Cdh1} complex *in vitro* suggesting that

APC/C^{Cdh1} targets DVC1 for degradation. Recently, DVC1 was discovered to bind to p97 via its SHP box motif (Mosbech et al., 2012) (Davis et al., 2012). Both studies propose a model where p97 is recruited by DVC1 to the sites of DNA damage to promote the extraction of TLS polymerase η leading to polymerase switch after bypass of the DNA lesion. Unclear is, whether DVC1 binding to p97 requires Ufd1-Npl4 as both studies reveal opposite results. DVC1 is conserved in humans and *C.elegans,* also in *C.elegans* it lacks the PIP domain but is conserved in its function to recruit p97 to sites of DNA lesions (Mosbech et al., 2012).

1.3.4 p97 function in cell cycle regulation

In addition to the above-mentioned processes, p97 also facilitates the degradation of chromatin-associated proteins by extracting them from the chromatin and thus regulate their activity. The chromatin is a large protein integration platform with dynamic association of proteins involved in the regulation of various processes like transcription, replication and mitosis. The chromatin-associated degradation of proteins plays an important role in maintaining genomic integrity and cellular homeostasis by the timely removal and degradation of proteins and protein-complexes from the chromatin. The inactivation of p97 leads to the accumulation of its substrates on the chromatin and thus causes protein-induced chromatin stress, which negatively affects multiple DNA metabolic processes like DNA replication, DNA damage response and mitosis promoting genome instability (Figure 1.8). The following sections describe the detailed role of p97 in the single cell cycle phases and in response to DNA damage.

G_1 to S phase transition

The p97 homolog Cdc48 was first identified in yeast in a genetic screen for cell cycle division mutants. Ccdc48 attaches to the ER, but upon phosphorylation it shuttles into the nucleus in a cell cycle dependent manner (Madeo et al., 1998). Mutations in the Cdc48 gene lead to a delay in the G_1/S transition and to an arrest in the G_2/M phase of the cell cycle. The yeast homolog of CDK1-cyclin ,Cdc28 – Cln, is important for the regulation of G_1/S transition. The inhibitor Far1p, which is degraded in a Cdc48-dependent manner, regulates Cdc28 activity. Mutation of Cdc48 leads to the accumulation of ubiquitinated Far1, which than leads in turn to persisting activity of Cdc28. The additional mutation of Far1 can rescue the delayed G_1/S phase transition (Fu et al., 2003). Additionally the $Cdc48^{Ufd1\text{-}Npl4}$ complex controls the G_1/S transition by the regulation of the cell wall integrity pathway in yeast. The exact mechanism of Cdc48 in this pathway is not completely understood also Cdc48 regulates the activity of Mpk1, a MAP kinase family member important for the cell wall integrity in response to stress (Hsieh and Chen, 2011).

S phase/DNA replication

In *Caenorhabditis elegans* (*C. elegans*) the depletion of Cdc48 or Ufd1-Npl4 delays the progression through S phase due to the activation of the Atr1 and CHK1-dependent intra-S phase replication checkpoint (Mouysset et al., 2008). DNA replication is initiated by the loading of a pre-replicative complex to each origin of replication (pre-RC). As mentioned before, the pre-RC consists of the origin recognition complex, CDC6, Cdt1 and MCM2-7. Upon phosphorylation the pre-RC recruits essential replication factors like MCM-10, CDC45 and the GINS complex, which than recruit the DNA primase and polymerases to initiate DNA synthesis. p97 regulates Cdt1 turnover via two distinct pathways: the UV-dependent degradation of Cdt1 and during firing and elongation of the replication fork. After UV-induced DNA damage the nucleotide excision repair (NER) machinery recognizes distorted DNA and excises the damaged DNA strands. The arising gap is filled by DNA polymerases dependent on the actions of the E3 ligase complex Cul4-DDB2 and PCNA. Cdt1 associates with PCNA and initiates the gap filling and is removed from chromatin by $p97^{Ufd1\text{-}Npl4}$ to prevent re-initiation (Raman et al., 2011). In *C. elegans* and *Xenopus egg* extracts p97 removed Cdt1 from chromatin under physiological conditions. Depletion of p97, Ufd1 or Npl4 leads to the stabilization of Cdt1 on the chromatin and subsequent stabilization of CDC45 and GINS on Cdt1 in *C. elegans*, *Xenopus egg* extracts and human cell lines (Franz et al., 2011). Interestingly, depletion of p97, Ufd1 or Npl4 did not lead to a re-replication phenotype in the examined model systems.

The p97 ATPase also interacts directly with the DNA helicases Werner protein and HIM-6 (Blooms helicase) as well as the DNA unwinding factor (DUF), further promoting its crucial role in the regulation of DNA replication (Indig et al., 2004) (Yamada et al., 2000).

Mitosis

The p97 ATPase regulates multiple steps in the progression of mitosis. The first identified substrate of p97 in chromatin-associated degradation was the Aurora B kinase. In *Xenopus egg* extracts and *C. elegans* $p97/Cdc48^{Ufd1\text{-}Npl4}$ binds to polyubiquitinated Aurora B and extracts it from chromatin. Removal of Aurora B allows the chromatin decondensation and nuclear envelope reformation during mitotic exit (Ramadan et al., 2007). In human cells, p97 regulates the Aurora B activity in early stages of mitosis (Dobrynin et al., 2011). Depletion of Ufd1 or Npl4 causes an increase in Aurora B activity, which leads to defects in chromosome alignment and the miss-segregation of chromosomes. In this process, $p97^{Ufd1\text{-}Npl4}$ acts

as negative regulator of Aurora B. In *C. elegans,* Cdc48 is required for the proper localization of the Aurora B homolog AIR-2 at the regions between homologues chromosomes in meiosis I, thus ensuring proper condensation and segregation of meiotic chromosomes (Sasagawa et al., 2012). Depletion of Cdc48 leads to an increased AIR-2 substrate phosphorylation and causes defects in chromosome segregation. In yeast, the p47 homolog Shp1 in complex with Cdc48 facilitates the nuclear localization of Glc7, which counteracts the Ipl1 (Aurora) activity. Inactivation of Cdc48 or Shp1 causes cell cycle arrest in metaphase due to defects in the bipolar attachment of the kinetochores and thus activation of the SAC (Cheng and Chen, 2010). In *Xenopus egg* extracts, p97 is required for the spindle disassembly at the end of mitosis. Depletion of Ufd1 or Npl4 leads to defects in the spindle disassembly and the reformation of the interphase microtubles.

The $p97^{Ufd1\text{-}Npl4}$ complex interacts with the spindle assembly factors XMAP215, TPX2 and Plx1 at the end of mitosis promoting their extraction from the microtubles or sequestration into the cytosol (Cao et al., 2003). Also in yeast, Cdc48 is required for the degradation of the spindle assembly factors Ase1 and Cdc5.

In *C. elegans* and human cell lines, p97 together with it co-factor UBXN-2 is required for the regulation of Aurora A activity. In *C. elegans* embryos depleted of UBXN-2 more AIR-1 (Aurora A) is recruited to the centrosomes leading to precociously maturation and impairment of the alignment of the mitotic spindle with the axis of polarity. The depletion of the human homologues of UBXN-2 p37/p47 results in accumulation of Aurora A at the centromeres and a delay of the centrosome segregation (Kress et al., 2013).

In yeast, Cdc48 is crucial for the proper transition through mitosis by modulating the turnover of key proteins or the localization of the proteasome to the nucleus. In *Schizosaccharomyces pombe,* Cdc48 is required for the stabilization of Cut1, the yeast homolog of separase, in the metaphase to anaphase transition and thus ensures cell viability (Ikai and Yanagida, 2006). In *Saccharomyces cerevisiae* depletion of Cdc48 and its adaptor UBX4 leads to an arrest in mitosis and the accumulation of Cbl2 and Cdc20, which are normally degraded in anaphase allowing the mitotic exit of the cell. Cdc48-UBX4 interacts with the proteasome and is thought to localize it to the nucleus, where it facilitates degradation of ubiquitinated Cbl2 and Cdc20 (Chien and Chen, 2013).

DNA damage response

Apart from its functions in the regulation of cell cycle progression under physiological conditions, p97 is also important for various processes in the DNA damage response. During DNA replication, the cell is extremely sensitive to DNA damage induction, as lesions cannot be accommodated at the sites of replicative DNA polymerases. This

leads to a stalled progression of the DNA replication fork and to the activation of the DNA damage response (Lehmann, 2011). Upon activation of the DDR translesional DNA polymerases are recruited to the stalled replication fork. In a process called translesional DNA synthesis, the replicative DNA polymerases are switched to translesional DNA polymerases depending on the ubiquitination status of PCNA (Lehmann et al., 2007). The recently identified p97 co-factor, DVC1, links p97 to the process of TLS through the direct interaction with p97 as well as with PCNA. DVC1 interacts with p97 through its SHP box and recruits it to stalled replication forks upon ubiquitination of PCNA, however the exact mechanism remains still unclear. Recent studies provide controversial results whether recruitment of p97 depends on the action of the Rad18 E3 ligase. Two groups provide evidence that DVC1 recruits Rad18 to the chromatin leading to enhanced ubiquitination of PCNA (Centore et al., 2012) (Ghosal et al., 2012). Juhasz and colleagues found that DVC1 is recruited itself to stalled replication forks depending on Rad18 and mono-ubiquitination of PCNA and protects PCNA from de-ubiquitination (Juhasz et al., 2012). The second controversial point is the actual function of DVC1 and p97 at the sites of stalled replication. Two groups provide evidence that DVC1 recruits p97 to stalled replication forks to remove DNA polymerase η and thus allow the switch to the replicative DNA polymerases (Davis et al., 2012) (Mosbech et al., 2012). In contrast, Ghosal and colleagues show that DVC1 leads to the removal of the replicative DNA polymerase δ to switch to the translesional DNA polymerase η (Ghosal et al., 2012).

As replication fork collapse can also occur due to stalled transcription at the sites of DNA lesions, transcription-coupled nucleotide excision repair (TC-NER) is activated and lesions from the transcribed DNA strand are removed (Fousteri and Mullenders, 2008). Stalled transcription leads to the recruitment of the Cul3 E3 ligase, which mediates the ubiquitination the RNA polymerase II complex and its degradation (Ribar et al., 2007). In yeast the Cdc48-Ubx4-Ubx5 (UBXD9 and UBXD7) complex is involved in the turnover of RNA polymerase II after UV-induced DNA damage by targeting the RNA polymerase subunit Rbp1 for degradation (Verma et al., 2011).

As mentioned before, unrepaired DNA damage in S phase can manifest as DNA double strand breaks (DSB) during cell cycle progression. Also the exposure of cells to ionizing radiation (IR) or DNA damaging agents like doxorubicin induces the formation of DSB. In recent studies, p97 was connected to the DNA damage response pathway after DSB induction. In response to DSB, the E3 ligase RNF8 creates Lys48-linked ubiquitin chains, which in turn recruit the $p97^{Ufd1\text{-}Npl4}$ complex to the sites of DNA damage. Processing of Lys48-linked substrates by p97 allows DNA repair proteins like 53BP1, BRAC1 and Rad51 to bind to the DNA lesions (Meerang et al., 2011). In undamaged chromatin L3MBTL1 can bind via its Tandem-Tudor domains with high affinity to methylated Lys20 of histone 4 (H4Lys20Me2). After DNA

damage L3MBTL1 is removed from the chromatin in a p97-dependent manner and 53BP1 can bind to H4Lys20Me2 with its own Tudor domain (Acs et al., 2011).
In yeast, Cdc48 together with Ufd1-Npl4 is, in addition to processing ubiquitinated substrates, also involved in the processing of sumoylated substrates at the site of DNA damage (Nie et al., 2012). The yeast variant of Ufd1 contains a sumo-interacting motif (SIM) that binds to sumoylated conjugates and recruits the $Cdc48^{Ufd1\text{-}Npl4}$ complex to STUbL targets. Cdc48 complex acts in concert with STUbL to remove stalled covalent DNA topoisomerase 1 DNA adducts. Also Rad52 is sumoylated in response to DNA damage. Sumoylated Rad52 interacts with $Cdc48^{Ufd1}$ leading to the removal of the Rad51/Rad52 complex from sites of DNA damage and thus to regulation of the Rad51 recombinase activity (Bergink et al., 2013).
Recent results demonstrated the clinical relevance of the p97 function in the DNA DSB repair, as the interference with the p97 function is the basis for the pathology of neurodegenerative diseases. p97 binds to polyglutaminated (polyQ) disease proteins like Huntington, ataxin-1 and ataxin-7. It can thereby bind to the wild type form and mutant form of polyQ. Binding of mutant polyQ to p97 leads to impaired p97 accumulation and interaction with related DSB repair proteins and thus to an increase in unrepaired DSB, which is a critical factor for the pathology of neurons (Fujita et al., 2013).

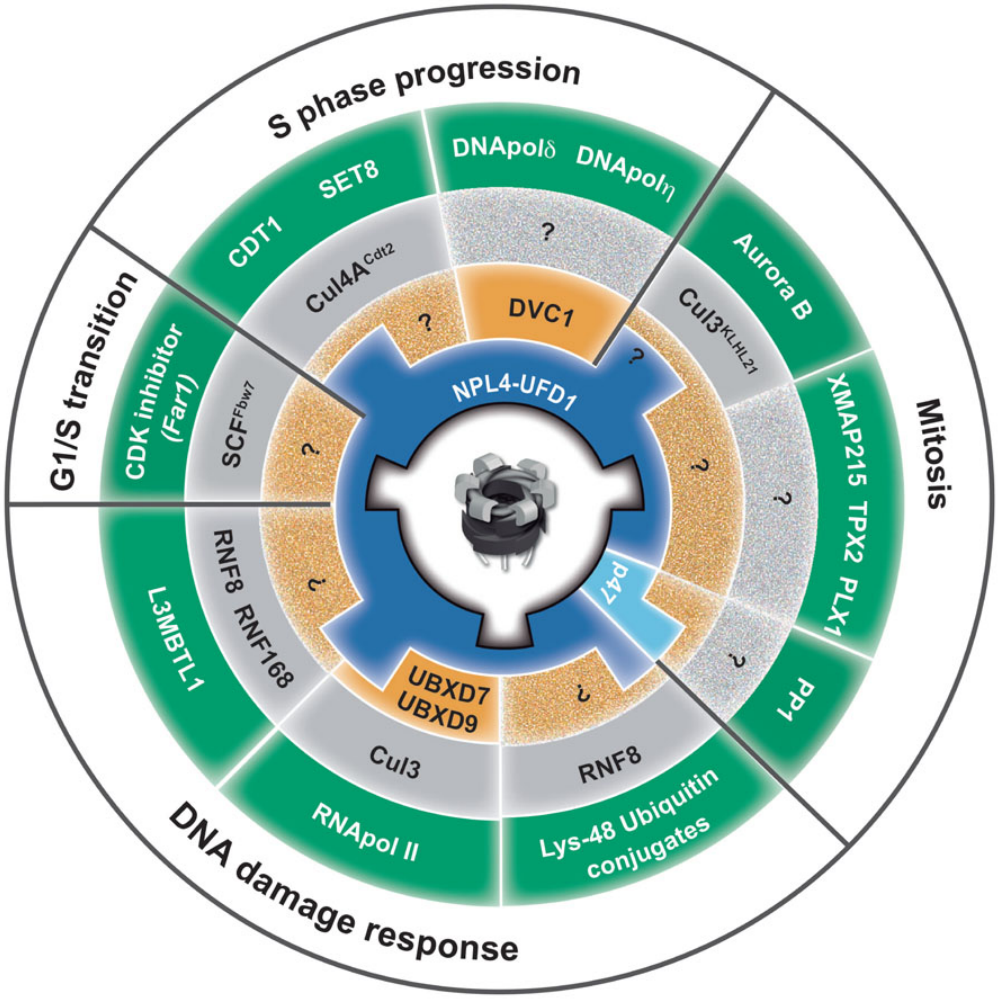

Figure 1.8: Role of p97 ATPase in the cell cycle progression.
The circle represents the current understanding of p97 function in the regulation of cell cycle progression and genome stability in different model systems (Yeast, *C. elegans*, human). The p97 core is extended by different adaptor proteins like Ufd1-Npl4 or p47 (blue layer). The binding of substrate-recruiting factors like DVC1 further directs the function of the p97 complex (orange layer). DVC1 directs $p97^{Ufd1\text{-}Npl4}$ towards TLS whereas UBXD7-UBXD9 promotes the function in stalled transcription and TC-NER. The third layer (Gray) of complexity is the interaction with different E3 ligases that ubiquitinate p97 substrates (green ring). The outer layer represents the cell cycle stages in which p97 plays essential role to promote cell cycle progression and maintenance of genomic stability. (modified from (Vaz et al., 2013))

1.3.1 Aim of thesis

Depletion of the $p97^{Ufd1\text{-}Npl4}$ complex causes severe chromosome segregation defects in mitosis. In addition to the established function in the regulation of mitosis progression, $p97^{Ufd1\text{-}Npl4}$ is implicated in an increasing number of interphase functions, including regulation of S phase progression as well as regulation and promotion of the DNA damage response, which makes p97 an integral component to suppress chromosome instability and thus maintain genomic integrity.

In this study, we aimed at elucidating the relevance of $p97^{Ufd1\text{-}Npl4}$ interphase functions on the manifestation of chromosome segregation defects in mitosis.

We demonstrated that the $p97^{Ufd1\text{-}Npl4}$ complex ensures proper activation of the G_2/M checkpoint in response to DNA insults, and thus prevents the cells from entering mitosis with damaged DNA. Therefore, then we aimed at elucidating the molecular basis of the role of the $p97^{Ufd1\text{-}Npl4}$ complex in the regulation of mitotic entry in response to DNA damage in human somatic cells.

2 Results

2.1 Part I: The p97$^{Ufd1\text{-}Npl4}$ complex ensures robustness of the G_2/M checkpoint by facilitating CDC25A degradation

2.1.1 Pre-mitotic defects in DNA repair lead to severe chromosome segregation defects in Ufd1-Npl4 depleted cells

As mentioned above, the p97 together with its adaptor Ufd1-Npl4 has been linked to several aspects of the cell cycle regulation and thus maintaining genomic stability. Recent studies demonstrated that depletion of p97$^{Ufd1\text{-}Npl4}$ leads to chromosome segregation errors caused by improper regulation of Aurora B kinase (Dobrynin et al. (2011). In addition, an increasing number of interphase functions have been connected to p97$^{Ufd1\text{-}Npl4}$ that are important to maintain genomic stability. To investigate to what extent pre-mitotic functions of the p97$^{Ufd1\text{-}Npl4}$ complex affect chromosome stability in human somatic cells, we analysed segregation errors caused by depletion of Ufd1-Npl4, p97 or DVC1. Segregation errors were classified into pre-mitotic or mitotic according to the centromere staining: misaligned chromosomes in metaphase and lagging chromosomes in anaphase containing a centromere were considered to be caused by defects in mitotic functions whereas chromosome fragments without centromere and anaphase bridges were considered to be of pre-mitotic origin (Figure 2.1 a). Depletion of CHK1 served as a positive control. To induce additional DNA damage, cells were treated with a dose of 3 Gy of ionizing irradiation (IR) or mock treated 8 h prior fixation. Fixed cells were analysed and confocal pictures of metaphase and anaphase cells were acquired. In metaphase cells without IR, depletion of Ufd1-Npl4 as well as p97 or DVC1 results in an increase of misaligned chromosomes over control depleted cells. Interestingly, p97 and DVC1 depleted cells as well as CHK1 depleted cells show a small fraction of cells containing chromosome fragments lacking a centromere. Also in anaphase, a small fraction of cells showed chromosome bridging and chromosomes lacking centromere, indicating a low level of pre-mitotic errors (Figure 2.1 b/c). Moreover, after challenging cells with additional DNA damage induced by gamma radiation, the fraction of pre-mitotic errors drastically increased in Ufd1-Npl4, p97 or DVC1 depleted cells (Figure 2.1 b/c). Notably cells depleted of p97 did not enter anaphase after IR, indicating high levels of damage.

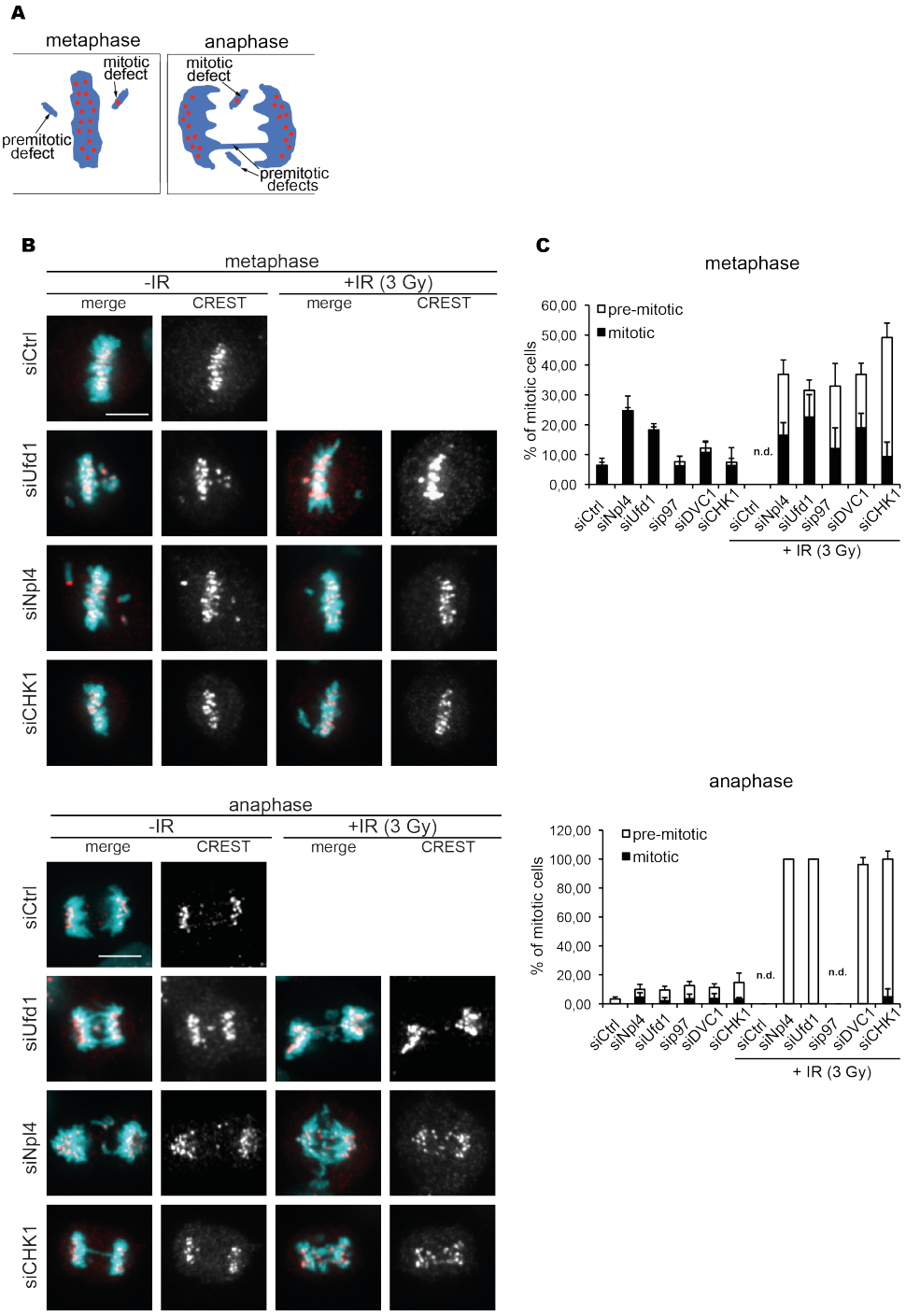

Figure 2.1: Unrepaired DNA damage leads to severe chromosome segregation errors in Ufd1-Npl4 deficient cells.

(A) Schematic illustration of mitotic and pre-mitotic defects in metaphase and anaphase. Blue depicts chromatin, red dots depict centromeres. (B) Confocal micrographs of mitotic HeLa cells depleted with indicated siRNAs and treated with ionizing radiation (IR) or mock-treated as depicted. Cells were fixed 8 hours after IR and stained with DAPI or CREST antibodies to visualize chromatin and centromeres, respectively. Luciferase siRNA served as control. Merge: DAPI – cyan, CREST – red; Scale bar: 5 µm. (C) Quantification of B according to classification in A. Shown are means of 3 independent experiments with at least 40 cells per condition. Error bars: s.d., n.d.: not determined due to low number of mitotic cells. Note the mitotic defects in unchallenged cells and the increase in pre-mitotic defects in irradiated cells.

To confirm that cells depleted of Ufd1-Npl4, p97 or DVC1 enter mitosis despite unrepaired DNA damage, HeLa cells were depleted of the mentioned proteins and DNA damage was induced by irradiation with 3 Gy. 8 h after IR cells were fixed and stained for DAPI and γ-H2AX, a marker for DNA double strand breaks. For the quantification of γ-H2AX foci on mitotic chromatin, confocal images of mitotic cells were acquired. The main population of mock irradiated mitotic cells contain less than five γH2AX foci per cell for all depletion conditions. Importantly however, after irradiation the number of cells with more than 5 foci per cell largely increased, meaning that cells enter mitosis despite unrepaired DNA damage (Figure 2.2 a/b).

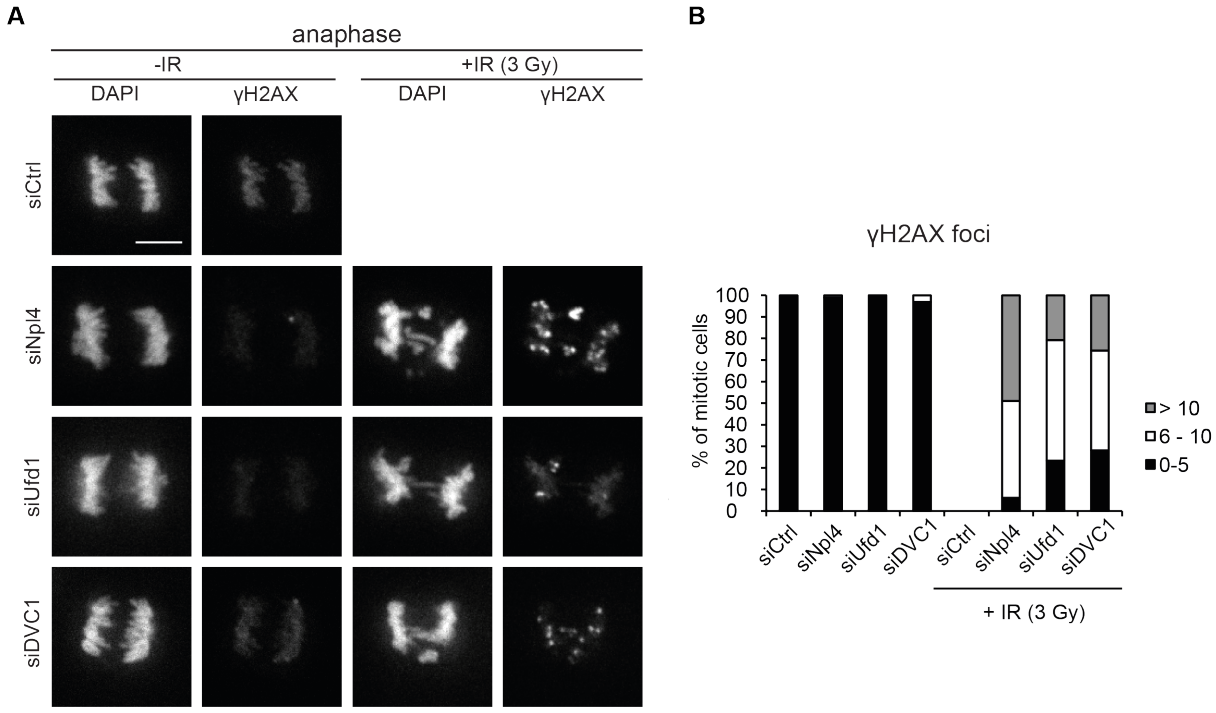

Figure 2.2: Cells depleted of Ufd1, Npl4 or DVC1 enter mitosis despite unrepaired DNA damage. (A) Representative images of mitotic HeLa cells depleted with the indicated siRNAs and treated with ionizing radiation (IR) or mock-treated as depicted. Cells were fixed 8 hours after IR and stained with DAPI and γH2AX. Luciferase siRNA served as control. Scale bar: 5 µm (B) Quantification of γH2AX foci in A. Shown are means of 3 independent experiments. n.d.: not determined due to low number of mitotic cells. Note that cells depleted of Ufd1, Npl4 or DVC1 enter mitosis despite DNA damage marked by γH2AX.

2.1.2 Depletion of the $p97^{Ufd1\text{-}Npl4}$ complex leads to a compromised G_2/M checkpoint

To further analyse the observation that cells depleted of Ufd1-Npl4 enter mitosis despite DNA damage, we ask whether that is due to a non-functional G_2/M checkpoint. To do so, HeLa cells were treated with siRNA against p97, Ufd1 or Npl4 and irradiated with 3 Gy or mock irradiated. Cells were fixed 8 h after IR and stained for DAPI and the Ser10 phosphorylated form of histone 3 (pH3 (S10)), a marker for mitotic cells. Indeed, we could frequently observe pH3 (S10) positive cells after IR while they were virtually absent in control depleted cells (Figure 2.3 c). The increase of mitotic cells can result from cells arrested in mitosis after IR or due to a defect in the G_2/M checkpoint. To confirm that the observed mitotic cells indeed entered mitosis after IR and were not arrested in mitosis we depleted HeLa cells of the mentioned proteins and treated them with 3 Gy dose of IR. CHK1 depletion served as a positive control. 30 min after IR, we scored cells entering mitosis by brightfield live cell imaging and followed them over a time period of 10 h. Indeed, cells depleted of Ufd1-Npl4 kept entering mitosis after irradiation whereas control-depleted cells efficiently arrested their cell cycle progression (Figure 2.3 a). Cells entering mitosis were cumulatively added up over the complete time course of imaging. Quantification of 3 independent experiments showed that almost 15 % of the cells depleted of Ufd1-Npl4 enter mitosis within 10 h after IR, which is about half the amount of mitotic cells of the CHK1 depleted population (Figure 2.3b). However, cells depleted of p97 or the E3 ligase subunit βTrCP showed an intermediate effect in these experiments.

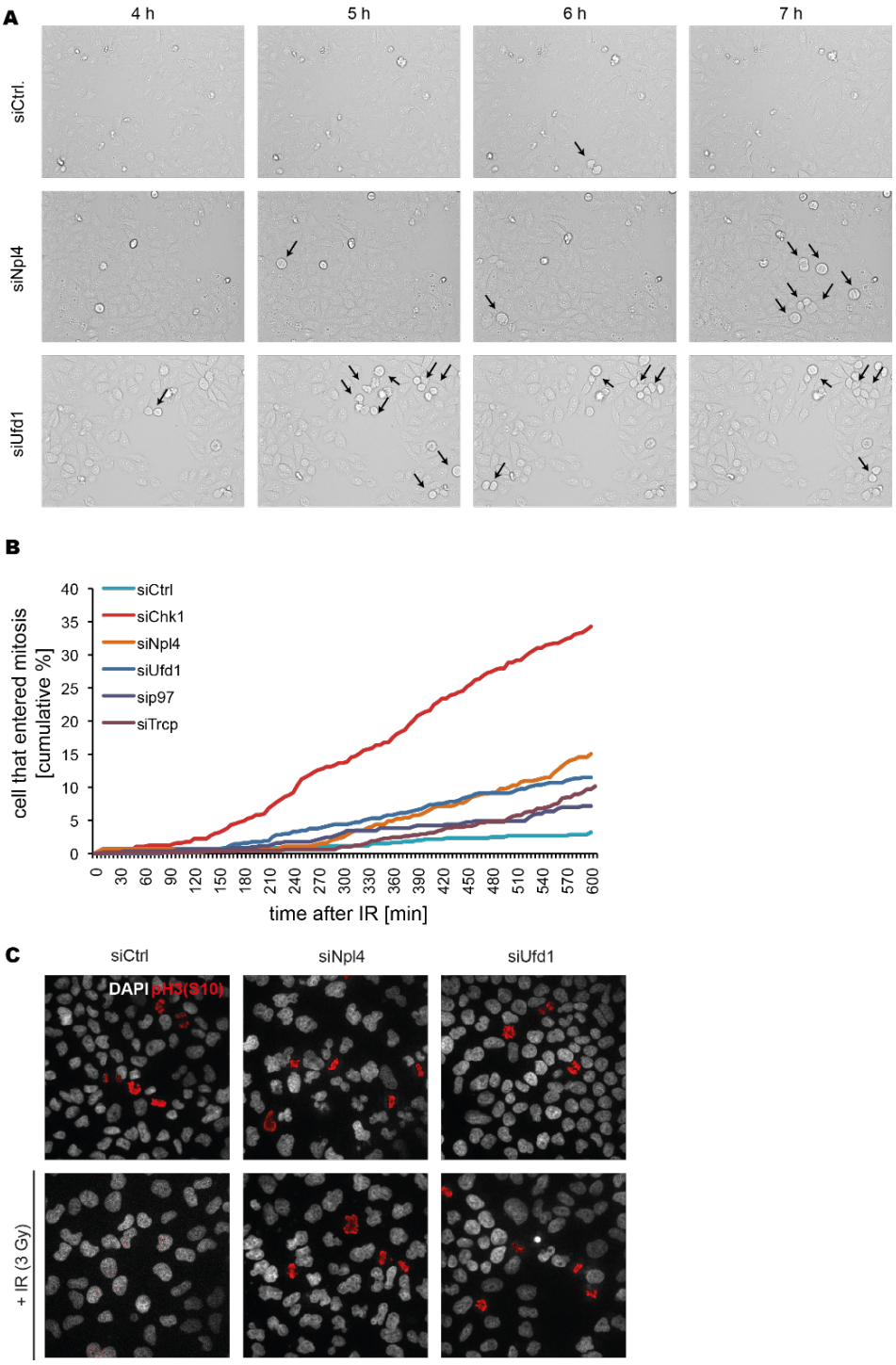

Figure 2.3: Ufd1-Npl4 depleted cells enter mitosis after ionizing radiation.
(A) HeLa cells were treated with the indicated siRNAs for 48 h and irradiated with 3 Gy. 30 min after IR cells were imaged over a time course of 10 h. Arrowheads indicate mitotic cells. Note that Ufd1 or Npl4 deficient cells enter mitosis already 4 h after IR. (B) Quantification of A. The number of cells that enter mitosis is plotted cumulatively over a period of 10 h. The graph shows means of 3 independent experiments with at least 200 cells per condition. Note that 15 % of Ufd1-Npl4 depleted cells enter mitosis after 10 h. (C) Representative micrographs of unsynchronized HeLa cells fixed 8 h after mock or IR (3 Gy) treatment. Cells were fixed and stained with DAPI and pH3 (S10) antibodies. Shown are overlay images. Note the presence of pH3 (S10)-positive mitotic cells in Ufd1- or Npl4-depleted populations despite irradiation.

To further examine whether $p97^{Ufd1\text{-}Npl4}$ is involved in the regulation of the G_2/M checkpoint we applied a quantitative FACS approach. To do so, HeLa cells were depleted of Ufd1, Npl4, p97 or DVC1 and irradiated with 3 Gy or mock irradiated. To monitor any cell that passed the G_2/M checkpoint, cells were treated with 100 ng/mL nocodazole (nocodazole-trap) 1 h after IR. 10 h after IR cells were fixed, stained with propidium iodine and pH3 (S10) and subjected to FACS analysis. We again observed that Ufd1-Npl4 depleted cells failed to arrest properly in the G_2/M checkpoint after IR. About 10 % of the IR treated Ufd1-Npl4 depleted cells entered mitosis compared to only 2-3 % of cells in the control-depleted population. This result was then further confirmed by depleting Ufd1-Npl4 with additional oligonucleotides (Figure 2.4 c).

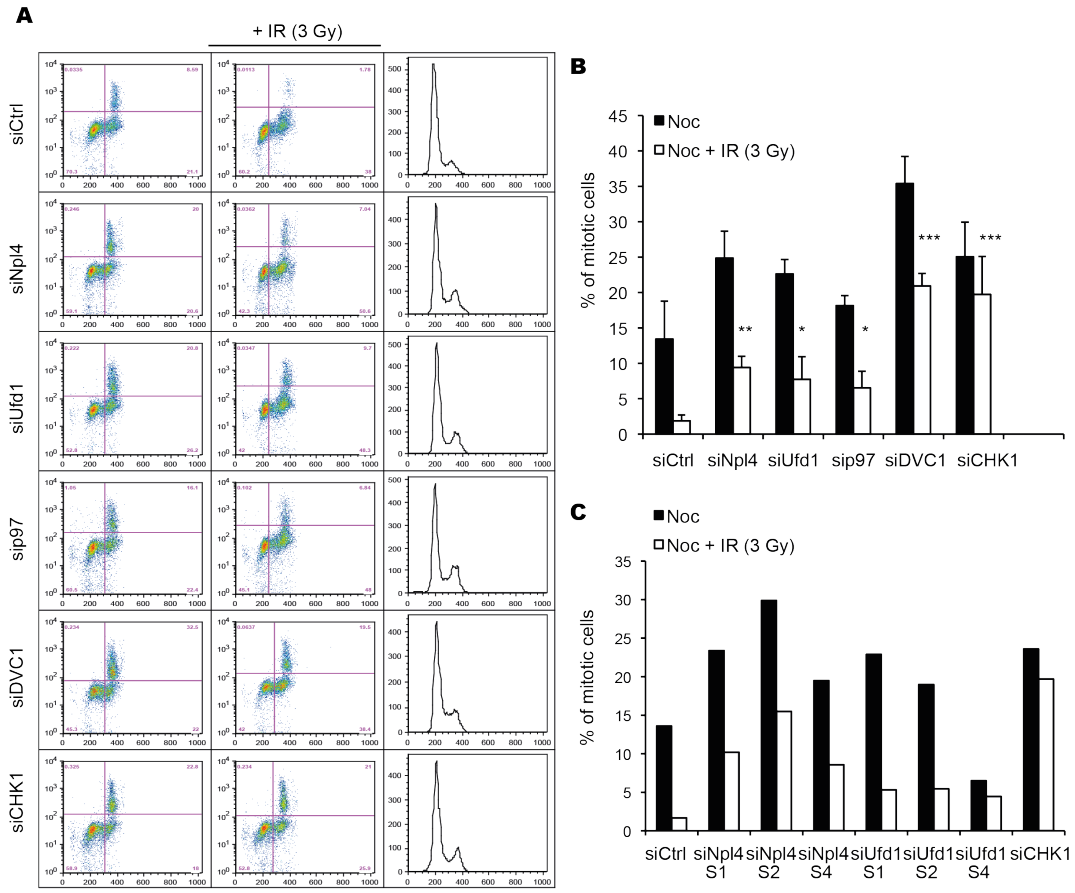

Figure 2.4: Quantitative FACS analysis of cell cycle progression after irradiation confirms compromised G_2/M checkpoint in Ufd1-Npl4, p97 or DVC1 depleted HeLa cells.
(A) Flow cytometry data of HeLa cells stained with propidium iodide and pH3 (S10) antibodies. Cells were depleted with indicated siRNAs, mock-treated or irradiated as indicated and then subjected to a nocodazole trap for 10 h prior to analysis. Note that none of the depletions has a major effect on the cell cycle profile. (B) Quantification of mitotic indices based on A. Shown are means of 3 independent experiments with n=10.000 cells per condition. Note that depletion of p97 or Ufd1-Npl4 leads to a significantly reduced drop in mitotic cells after IR compared to control cells. ** p< 0.01; * p< 0.05. (C) Cells were treated as in A. Graph shows the quantification of mitotic indices. Note that depletion of Ufd1 and Npl4 with different siRNAs leads to compromised G_2/M checkpoint after irradiation.

Likewise, also the p97 depleted populations failed to arrest in G_2 phase with about 10 % mitotic cells after IR. Interestingly, almost 20 % of cells depleted of DVC1 entered mitosis after IR, which was comparable to the effect in the CHK1 depleted population (Figure 2.4 a/b). Notably, none of the depletions led to major changes in the cell cycle profile of otherwise untreated cells compared to control depletion (Figure 2.4 a).

2.1.3 The $p97^{Ufd1\text{-}Npl4}$ complex ensures proper degradation of CDC25A downstream of ubiquitination by the $SCF^{\beta TrCP}$ complex

Upon DNA damage induction by IR, cells activate a signalling cascade to arrest in the cell cycle progression and prevent entering mitosis with damage DNA. The previous results indicate that the G_2/M checkpoint is compromised in cells depleted of the $p97^{Ufd1\text{-}Npl4}$ complex. To investigate at which step of the IR induced checkpoint response the function of the $p97^{Ufd1\text{-}Npl4}$ complex is required, we investigated the phosphorylation status and total protein levels of components of the checkpoint response pathway. To do so, we depleted HeLa cells of Ufd1-Npl4 and treated them with a 6 Gy dose of IR or mock treated them. Cells were lysed 30 min after IR and the lysates were subjected to SDS-PAGE and Western blotting. The membranes were probed for different marker proteins of the DDR. Notably, none of the depletion conditions affected the activation of CHK1 after IR as it was phosphorylated to the full extends at serine 317 (pCHK1 (S317)) as well as at serine 345 (pCHK1 (S345)) (Figure 2.5). In parallel, full activity of CHK1 was further confirmed by increased levels of the phosphorylated from of CDC25C (pCDC25C (S216)) upon IR in all conditions (Greg Dobrynin). As expected, the CDC25A phosphatase was degraded in control-depleted cells within 30 min after IR whereas depletion of the SCF F-box protein βTrCP clearly stabilized CDC25A after IR, since the $SCF^{\beta TrCP}$ complex ubiquitinates CDC25A and mediates subsequent degradation of CDC25A. Importantly, Ufd1-Npl4 depleted cells also showed persistence of CDC25A after IR compared to control cells. Interestingly, the steady-state levels of CDC25A are increased in Ufd1-Npl4 depleted cells compared to control cells (Figure 2.5), indicating that the $p97^{Ufd1\text{-}Npl4}$ complex is mediates CDC25A degradation independently of IR.

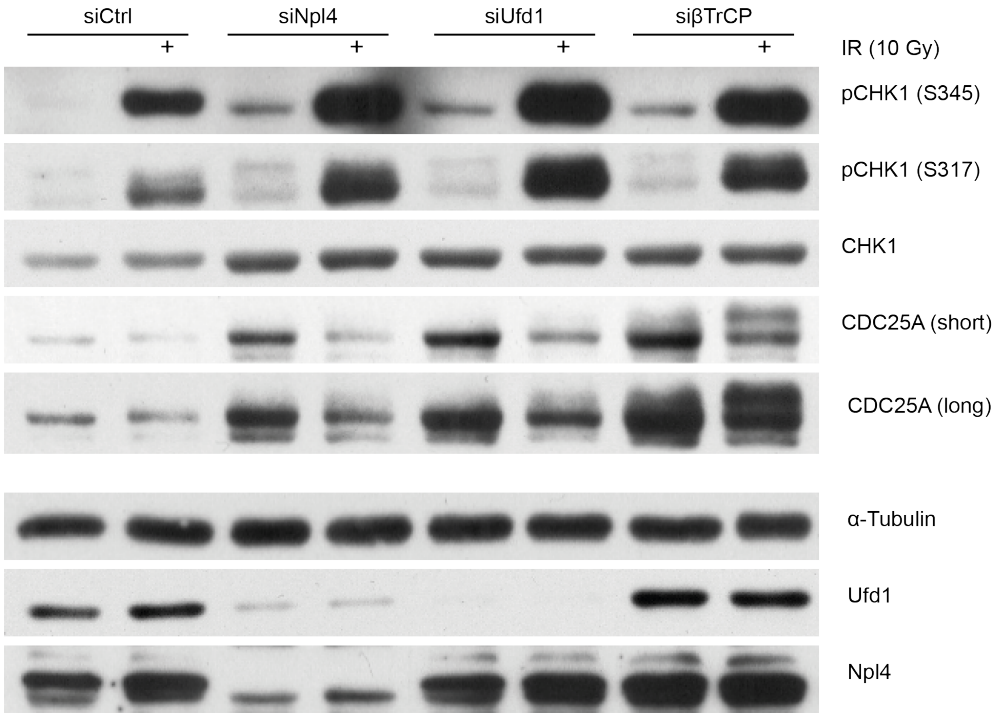

Figure 2.5: Depletion of Ufd1-Npl4 leads to compromised CDC25A degradation upon IR-induced DNA damage.

HeLa cells were depleted of the indicated proteins and treated with 6 Gy dose of IR or mock treated. Cells were lysed 30 min after IR and subjected for SDS-PAGE and Western blotting. Membranes were probed with the indicated antibodies. Note that depletion of Ufd1-Npl4 leads to increased levels of CDC25A in general and to persistence of CDC25A after IR compared to control depletion.

To further confirm that the $p97^{Ufd1\text{-}Npl4}$ complex governs CDC25A degradation we turned to HEK293 cells, which inducibly express HA-CDC25A and depleted p97, Ufd1 or Npl4 in these cells. Depletion of βTrCP served as a positive control. Expression of HA-CDC25A was induced 24 h after siRNA transfection. CDC25A degradation was induced by irradiation with 6 Gy. To block protein re-synthesis, 50 µg/mL cyclohexamide (CHX) was added to the cells directly after IR. Cells were lysed at 0, 10, 20 and 30 min after IR and lysates were subjected to SDS-PAGE and Western blotting. As expected, depletion of βTrCP led to stabilization of HA-CDC25A after IR-induced DNA damage. Notably, depletion of Ufd1- Npl4 or p97 led to significantly increased steady state levels of HA-CDC25A compared to HA-CDC25A levels in control depleted cells (Figure 2.6 a/b). Additionally, in cells depleted of the $p97^{Ufd1\text{-}Npl4}$ complex, HA-CDC25A was still present in the lysates 40 min after IR whereas it was virtually absent in control depleted cells (Figure 2.6 a).

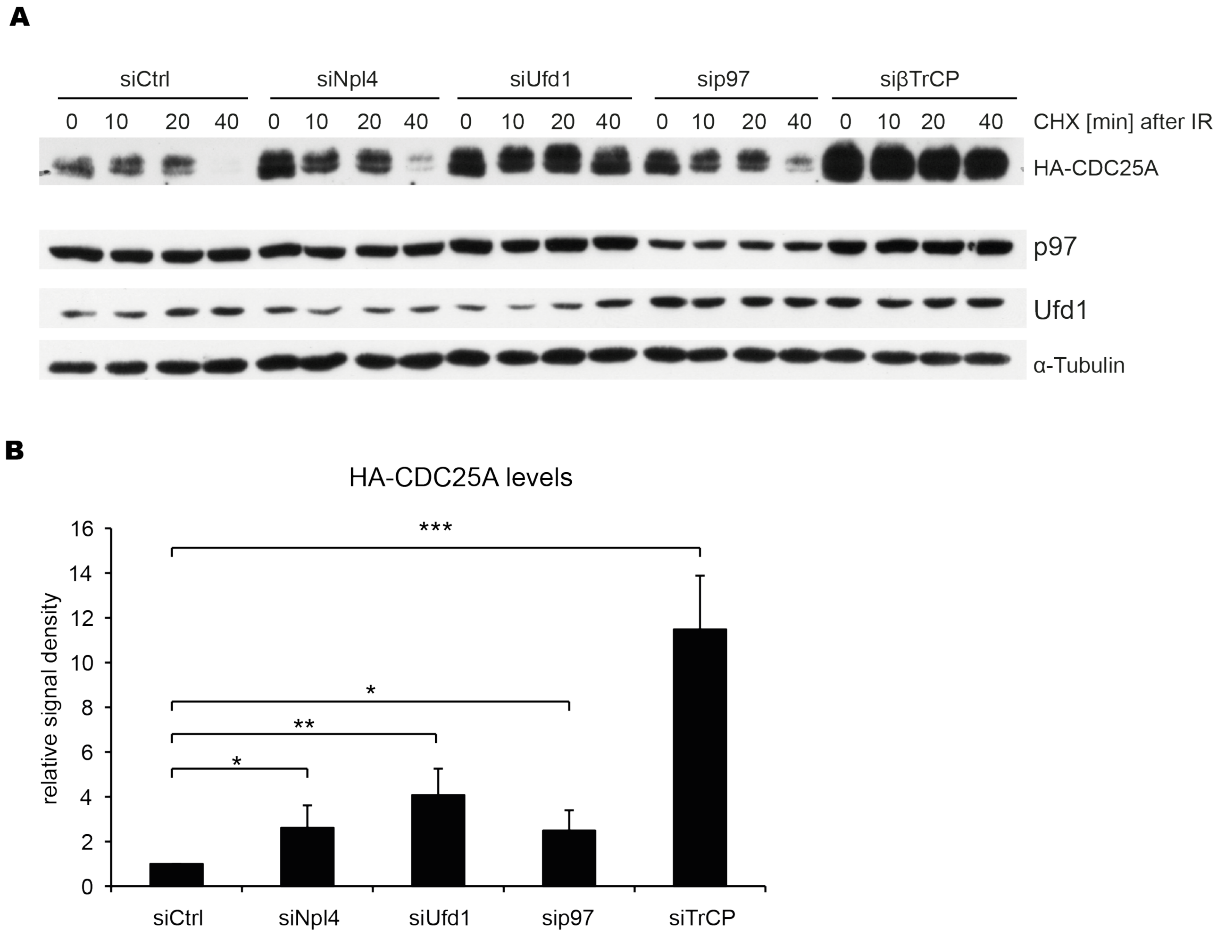

Figure 2.6: Depletion of the p97$^{Ufd1\text{-}Npl4}$ complex leads to an increase in HA-CDC25A levels and to persistence of HA-CDC25A after irradiation.

(A) HEK293 cells inducibly expressing HA-CDC25A were depleted of the indicated proteins and subjected to 6 Gy dose of IR or mock-treated. Protein re-synthesis was inhibited by adding 50 µg/mL CHX to the cells. Lysates were taken at the indicated time points and subjected to SDS-PAGE and Western blotting. Membranes were probed with the indicated antibodies. Note that in Npl4, Ufd1 or p97-depleted cells, HA-CDC25A is still present in the lysates 40 min after IR. (B) Quantification of A. Shown is the mean value of 3 independent experiments. Note that depletion of Ufd1, Npl4 or p97 leads to an increase of HA-CDC25A protein levels compared to control depletion. Chemiluminescence signal was detected with a CCD camera and the signal density was quantified using ImageJ. Signal density of CDC25A band in control-depleted cells was set to 1. Error bars: s.d.; ***, p< 0.001; **, p< 0.01; * p< 0.05.

To further confirm that the p97$^{Ufd1\text{-}Npl4}$ complex plays a role in the degradation of endogenous CDC25A, HeLa cells were treated with siRNA against Ufd1 or Npl4. CDC25A degradation was induced by irradiation with 6 Gy and CHX was added to the cells directly after IR. 0, 15 and 30 min after IR cells were lysed and subjected to SDS-PAGE and Western blotting. In control-depleted cells CDC25A was degraded within 30 min after IR, whereas depletion of βTrCP led to stabilization of CDC25A. Interestingly, Ufd1-Npl4 depletion resulted in increased levels of endogenous CDC25A at time point 0 h. Notably, CDC25A was stabilized in the slower migrating

form (Figure 2.7 a), indicating that CDC25A was fully phosphorylated but not further processed. To follow the degradation rate of CDC25A, we quantified the signal density of CDC25A using ImageJ. In control-depleted cells CDC25A levels were reduced by 50 % within 30 min after IR whereas CDC25A was fully stabilized in cells depleted of βTrCP. Notably, Ufd1-depleted cells showed about 75 % residual CDC25A 30 min after IR. However, Npl4 depletion has only a minor effect on the CDC25A stabilization after 30 min IR compared to control depletion. Yet, Npl4 depletion led to increased CDC25A levels compared to control at time point 15 min after IR (Figure 2.7 b).

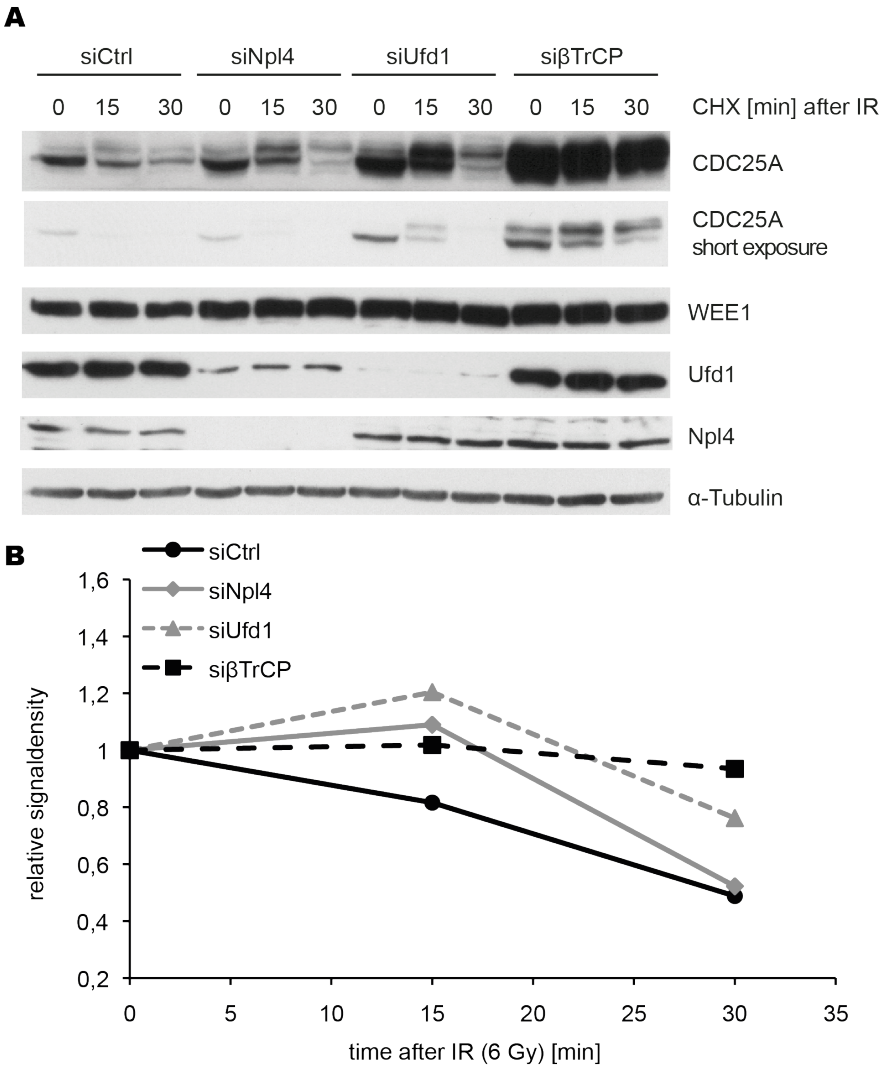

Figure 2.7: The p97$^{Ufd1\text{-}Npl4}$ complex ensures proper degradation of CDC25A after irradiation.
(A) HeLa cells were transfected with the indicated siRNAs and irradiated with 6 Gy or mock irradiated. Additionally, cells were treated with 50 µg/mL CHX directly after IR and lysed at the indicated time points. Lysates were subjected to SDS-PAGE and Western blotting. Membranes were probed with the indicated antibodies. (B) Quantification of A. Note that depletion of Ufd1-Npl4 leads to stabilization and delayed degradation of CDC25A. Density of the signals on X-ray films was quantified using ImageJ and time point 0 h was set to 1.

Reconsidering the observation that also DVC1 depleted cells enter mitosis after IR, we ask whether DVC1 functions in the same pathway or distinct from Ufd1-Npl4. To do so, we depleted HeLa cells of DVC1 and βTrCP and treated cells with 6 Gy dose of IR or mock treated them. CHX was added directly after IR and cells were lysed 0, 15 and 30 min after IR. Lysates were subjected to SDS-PAGE and Western blotting and membranes were probed with CDC25A and WEE1 antibodies. The specificity and efficiency of DVC1 siRNA was shown by Mosbach et al (Mosbach et al., 2012). Again control-depleted cells degraded CDC25A within 30 min after IR whereas it was strongly stabilized in the βTrCP-depleted population. Interestingly, DVC1 depleted cells did not show an increase in CDC25A protein levels. On the contrary, WEE1 protein levels were strongly reduced independent of IR (Figure 2.8 a). Importantly, also depletion of p97 leads to reduction of WEE1 independent of IR (Figure 2.8 b).

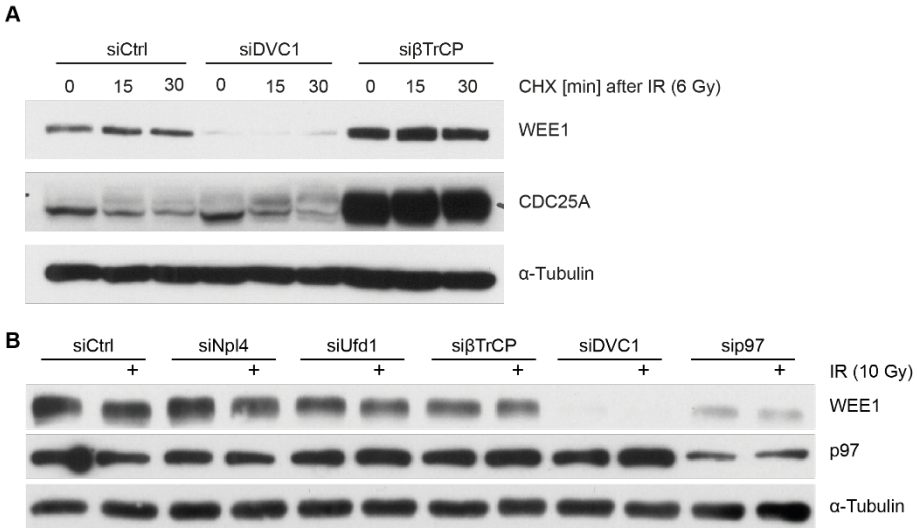

Figure 2.8: Depletion of DVC1 results in reduction of WEE1 levels independent of irradiation.
(A) HeLa cells were depleted of DVC1 or βTrCP and treated with 6 Gy or mock irradiated. Protein synthesis was blocked directly after IR by adding 50 µg/mL CHX to the cells. Lysates were taken at 0, 15 and 30 min after IR and subjected to SDS-PAGE and Western blotting. Membranes were probed with the indicated antibodies. Note that depletion of DVC1 leads to strong reduction of WEE1 levels independent of IR. (B) HeLa cells were treated with the indicated siRNAs and subjected to 10 Gy dose of IR. Cells were lysed 30 min after IR and subjected to SDS-PAGE and Western blotting. Membranes were probed with the indicated antibodies. Note that depletion or p97 or DVC1 leads to reduced WEE1 protein levels independent of IR.

In the next step we ask for the functional interactions of the $p97^{Ufd1\text{-}Npl4}$ complex to ensure proper CDC25A degradation. Experiments carried out by Grzegorz Dobrynin in the laboratory, showed that p97 physically interacts with HA-CDC25A and that the ATPase function of p97 is required for proper degradation of HA-CDC25A (Grzegorz Dobrynin). Overexpression of the ATPase inactive p97 E587Q (EQ) variant led to an increase of p97-bound HA-CDC25A as well as an increase in its ubiquitinated fraction. In parallel, we ask whether p97 interacts with βTrCP as CDC25A degradation is mediated via its ubiquitination by the $SCF^{\beta TrCP}$ ligase complex (Figure 2.9).

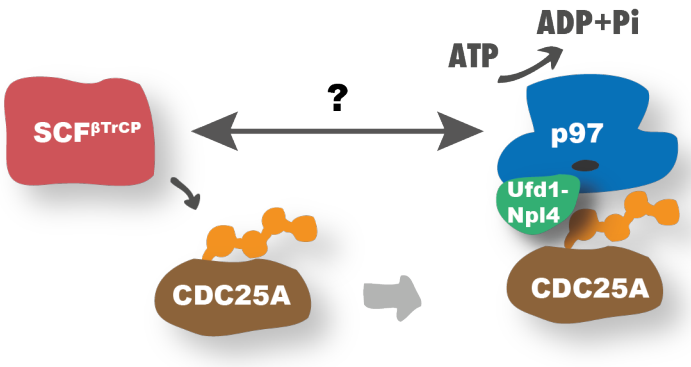

Figure 2.9: Hypothesized model of the functional interaction of $p97^{Ufd1\text{-}Npl4}$ complex.
Experiments done by Greg Dobrynin in the laboratory demonstrate the physical interaction of the $p97^{Ufd1\text{-}Npl4}$ complex with CDC25A. Additionally the ATPase function of p97 is required for proper degradation of CDC25A as overexpression of kinase dead p97 variant leads to an increased interaction with increase in the ubiquitinated fraction. In parallel we ask for a direct interaction between the SCF F-box protein βTrCP and the $p97^{Ufd1\text{-}Npl4}$ complex.

To test the possible interaction between p97 and βTrCP, HEK293 cells inducibly expressing p97 WT or p97 EQ variant were transfected with either GFP-βTrCP or GFP alone. Expression of p97 was induced 16 h before cell lysis. Cells were lysed in IP buffer and subjected to GFP pull down. IP samples together with 1 % inputs were analysed by SDS-PAGE and Western blotting. Indeed, GFP-βTrCP interacts with p97 and its cofactors Ufd1 and Npl4. Notably, the interaction was increased in the p97EQ background (Figure 2.10).

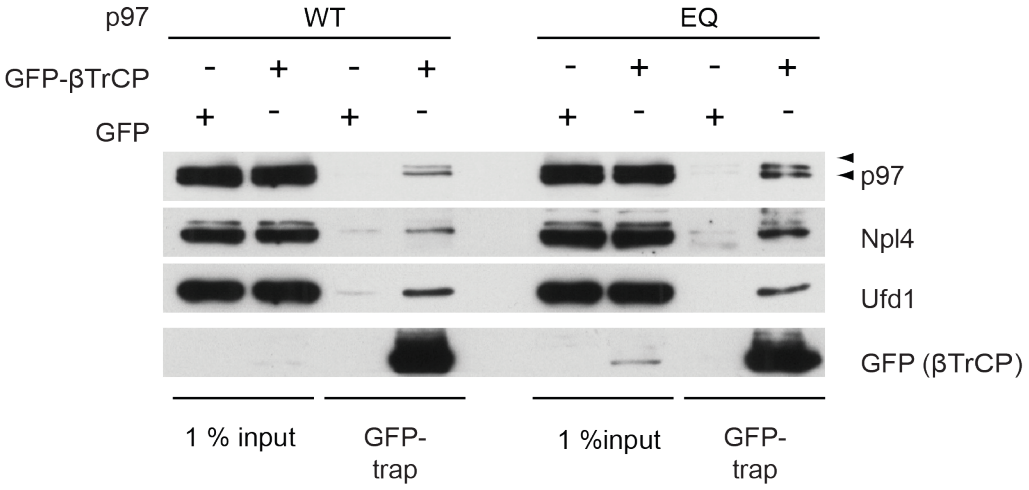

Figure 2.10: The p97$^{Ufd1\text{-}Npl4}$ complex interacts with the SCF F-box protein βTrCP.
(A) HEK293 cells inducibly expressing either mycSTREP tagged p97 (WT) or ATPase inactive p97 E587Q (EQ) were transfected with GFP-βTrCP or GFP empty vector. 24 h after transfection cells were lysed in IP buffer and lysates were subjected to GFP pull down. IP samples together with 1 % inputs were analysed by SDS PAGE and Western blotting. Membranes were probed with the indicated antibodies. Arrowheads indicate the mycSTREP p97 and endogenous p97. Note that βTrCP binds to the p97$^{Ufd1\text{-}Npl4}$ complex and binding is increased in cells expressing the substrate trapping p97 EQ variant.

To further confirm that the compromised G_2/M checkpoint results from persistence CDC25A, we investigated whether inhibition of CDC25A can restore the proper function of the checkpoint. Therefore HeLa cells were depleted of p97, Ufd1 or Npl4 and irradiated with 3 Gy or mock irradiated. To arrest mitotic cells, 100 µg/mL nocodazole was added to the cells 30 min after IR. 2 h before cell fixation, CDC25 phosphatases were inhibited by adding 10 µM NSC663284 or vehicle alone to the cells. Cells were stained with propidium iodine and pH3 (S10) and the fraction of mitotic cells was determined by FACS analysis. Consistent with the results above, cells depleted of Ufd1-Npl4 entered mitosis after IR in contrast to the control-depleted population. However, additional inhibition of CDC25A, using the CDC25 phosphatase inhibitor NSC663284, fully reduced mitotic indices comparable to control-depleted cells (Figure 2.11 a/b). Intriguingly, while p97 depletion also caused a checkpoint failure, NSC663284 treatment only partially prevented cells from entering mitosis.

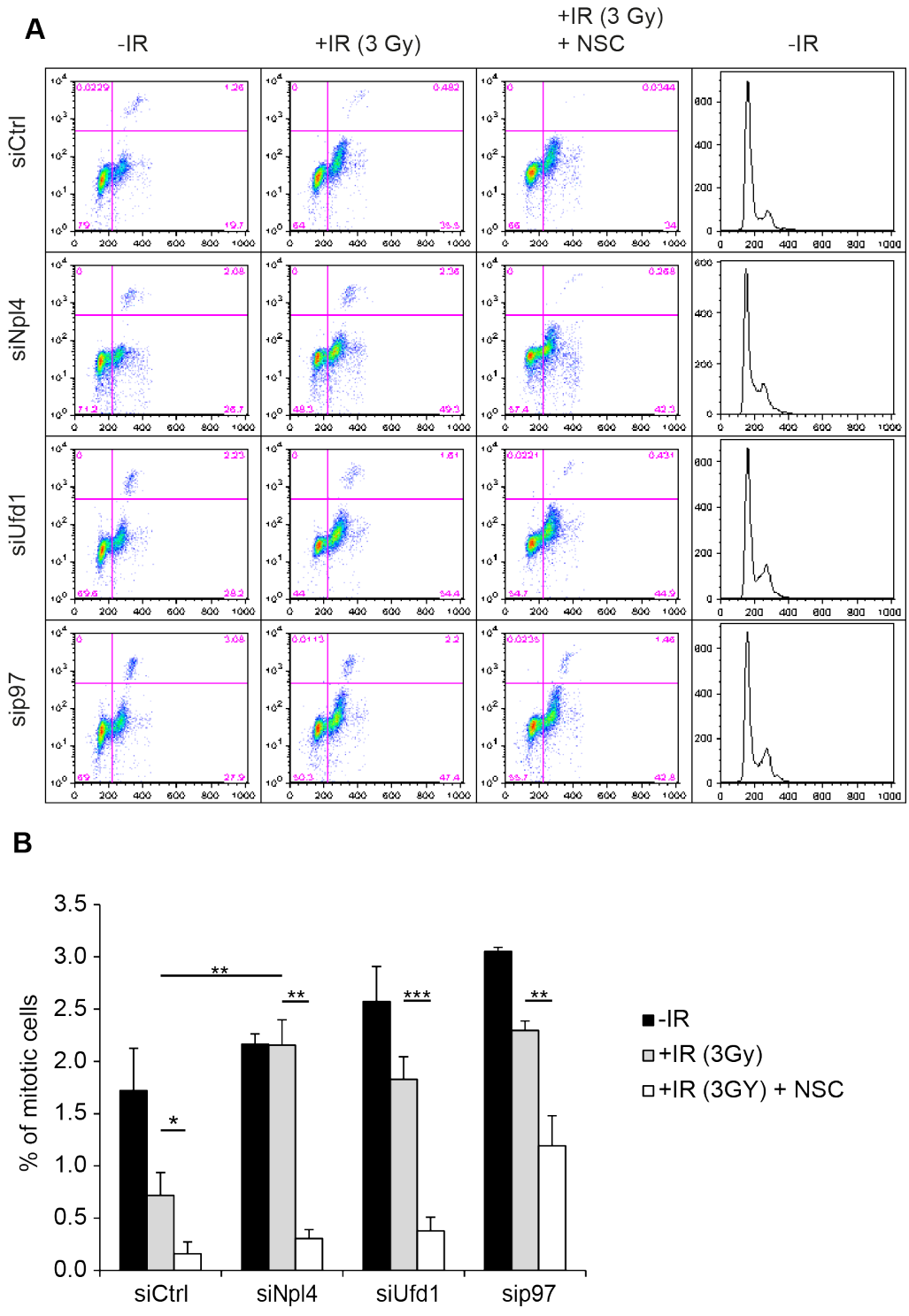

Figure 2.11: G_2/M checkpoint failure in Ufd1-Npl4 depleted cells is caused by persistent CDC25A activity.

(A) HeLa cells were transfected with the indicated siRNAs for 48 hours and exposed to IR (3 Gy) or left unchallenged. 6 h after IR, cells were treated with the CDC25-specific phosphatase inhibitor NSC663284 (NS(C) or vehicle alone for further 2 h before processing for flow cytometry of propidium iodine and pH3 (S10). (B) Quantification of A. Shown are mean values of 3 independent experiments with 10.000 cells per condition. Note that p97- and Ufd1-Npl4-depleted cells fail to block entry into mitosis, but this is restored with the CDC25 inhibitor. Error bars: s.d.; ***, p< 0.001; **, p< 0.01; * p< 0.05.

2.1.4 G_2/M checkpoint failure in Ufd1-Npl4 depleted cells depends on p53 function

As the previous experiments were performed in HeLa cells, which lack functional p53, we assumed that p53 proficient cells would be still able to halt cell cycle progression despite the lack of CDC25A inactivation after Ufd1-Npl4 depletion. To confirm this, we turned to the colon carcinoma cell line HCT116, which were either p53-proficient ($p53^{+/+}$) or p53-deficient ($p53^{-/-}$). HCT116 $p53^{+/+}$ or HCT116 $p53^{-/-}$ cells were depleted of p97, Ufd1 or Npl4 and treated with 3 Gy ionizing radiation or mock treated. Cells passing the G_2/M checkpoint were arrested in mitosis by adding 100 ng/mL nocodazole 30 min after IR to the medium. Cells were fixed 8 h after IR and stained with propidium iodine and pH3 (S10) and the fraction of mitotic cells was determined by FACS. Similar to the result obtained in HeLa cells, HCT116 $p53^{-/-}$ cells depleted of Ufd1 or p97 failed to fully arrest in the G_2/M checkpoint after IR. However, Npl4 depleted cells did not show a significant increase in the mitotic index after IR compared to control depletion. Importantly, moreover, HCT116 $p53^{+/+}$ cells depleted of p97, Ufd1 or Npl4 all stopped cell cycle progression comparable to control-depleted cells after IR (Figure 2.12 a). To further confirm that in HCT116 cells the $p97^{Ufd1\text{-}Npl4}$ complex indeed acts on CDC25A, HCT116 $p53^{+/+}$ and $p53^{-/-}$ cells were depleted of the mentioned proteins and treated with 6 Gy irradiation or mock irradiated. Cells were lysed 30 min after IR and lysates subjected to SDS-PAGE and Western blotting. In both cell lines, CDC25A was strongly degraded within 30 min after IR in control depletion, whereas it was stabilized in βTrCP depletion. Again, depletion of p97, Ufd1 or Npl4 led to increased levels of CDC25A in untreated cells and persisting levels after IR compared to control depletion. In contrast, the effect was generally less pronounced in HCT116 $p53^{+/+}$ cells (Figure 2.12 b).

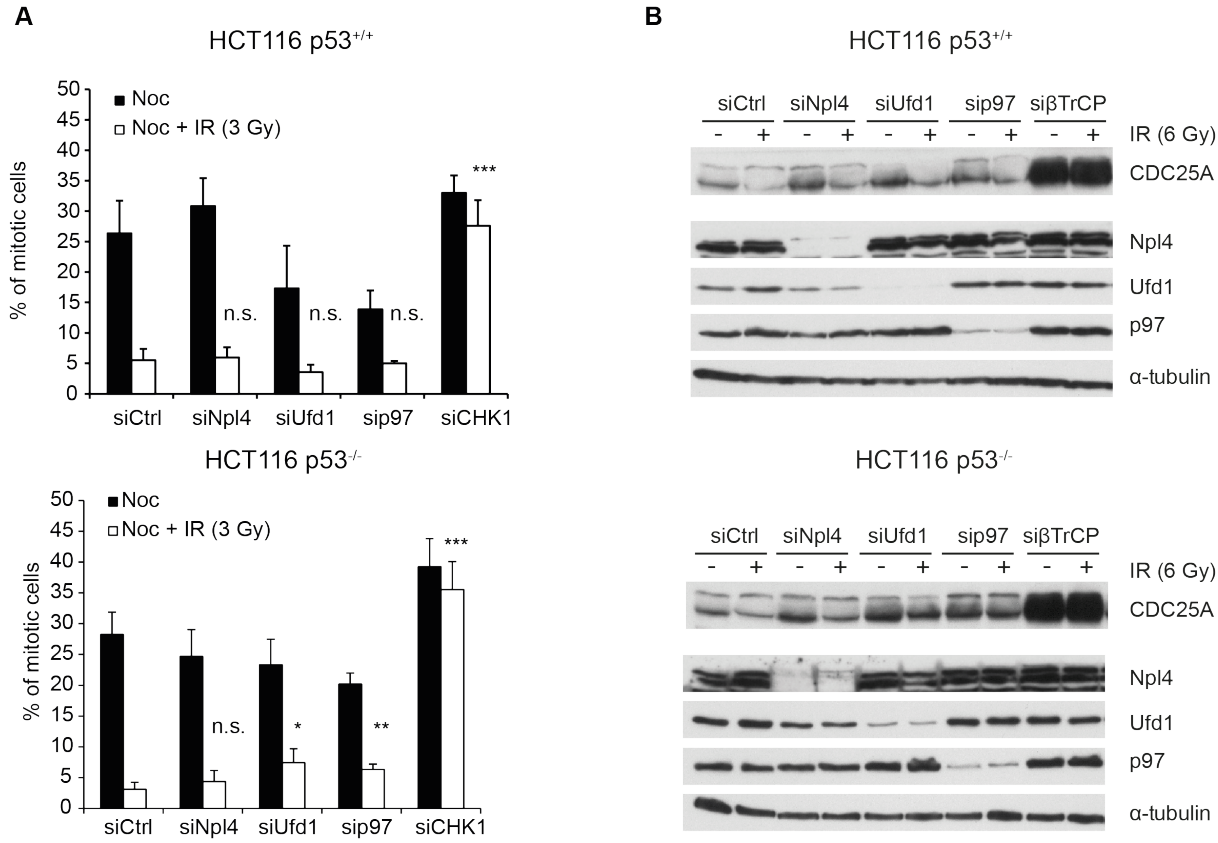

Figure 2.12: G_2/M checkpoint failure in Ufd1-Npl4 depleted cells depends on p53 deficiency. (A) HCT116 ($p53^{+/+}$) or ($p53^{-/-}$) cells were depleted of the indicated proteins and treated with 3 Gy or mock treated. 30 min after exposure to IR, cells were treated with 100 µg/mL nocodazole for 10 h to arrest any cells in mitosis that passed through the G_2/M checkpoint. Cells were fixed and processed for flow cytometry of propidium iodine and pH3 (S10) staining. Shown are mean values of 3 independent experiments with 10.000 cells per condition. Note that p97 or Ufd1 depletion leads to significantly more mitotic cells after IR compared to control-depleted cells in p53-/-, but not in $p53^{+/+}$ cells. Error bars: s.d.; ***, p< 0.001; **, p< 0.01; * p< 0.05. (B) HCT116 ($p53^{+/+}$) or ($p53^{-/-}$) cells were depleted of the indicated proteins, and mock-treated (-) or exposed to IR (6 Gy) (+) 25 min prior to lysis. Lysates were subjected to immunoblot analysis with indicated antibodies. Alpha-tubulin served as loading control. Note that Ufd1 is again co-destabilized in Npl4-depleted cells. Also note that CDC25A is stabilized in p97-, Ufd1- or Npl4-depleted cells.

2.1.5 Impairment of the G_2/M checkpoint after irradiation is dependent on specific p97 adaptor proteins

In the next step we ask whether the compromised G_2/M checkpoint by $p97^{Ufd1\text{-}Npl4}$ is specific for certain p97 adaptor proteins. Recently, the UBX domain containing p97 adaptor proteins came into focus to target p97 complex for specific cellular functions. UBXD1 is implicated to function in endocytosis, whereas UBXD6 and UBXD8 are related to ERAD functions of p97. UBXD7 was recently implicated to connect p97 to ubiquitin E3 ligases ((Ritz et al., 2011); (Madsen et al., 2011); (Glinka et al., 2014); (Alexandru et al., 2008) (Puumalainen et al., 2014)). To evaluate to what extent UBX

domain containing proteins are involved in the degradation of CDC25A and thereby the regulation of the G_2/M checkpoint, we depleted HeLa cells of the mentioned proteins and treated cells with 3 Gy or mock irradiated them. Cells passing the G_2/M checkpoint were arrested by nocodazole-trap 30 min after IR. Cells were fixed 8 h after IR and stained with propidium iodine and pH3 (S10) and then analysed by FACS. None of the depletions led to major changes in otherwise untreated cells (Figure 2.13 a). Again, control-depleted cells failed to enter mitosis after IR. The same is true for UBXD6-and UBXD8-depleted cells. UBXD1-depleted cells had no significant effect on mitotic entry after IR compared to control depletions in these experiments (Figure 2.13 a/b). However and importantly, depletion of UBXD7 led to a significant increase of the mitotic fraction after IR compared to control depletion. Consistently, UBXD7 depletion also led to increased protein levels of CDC25A compared to control depletion (Figure 2.13 a/b/c).

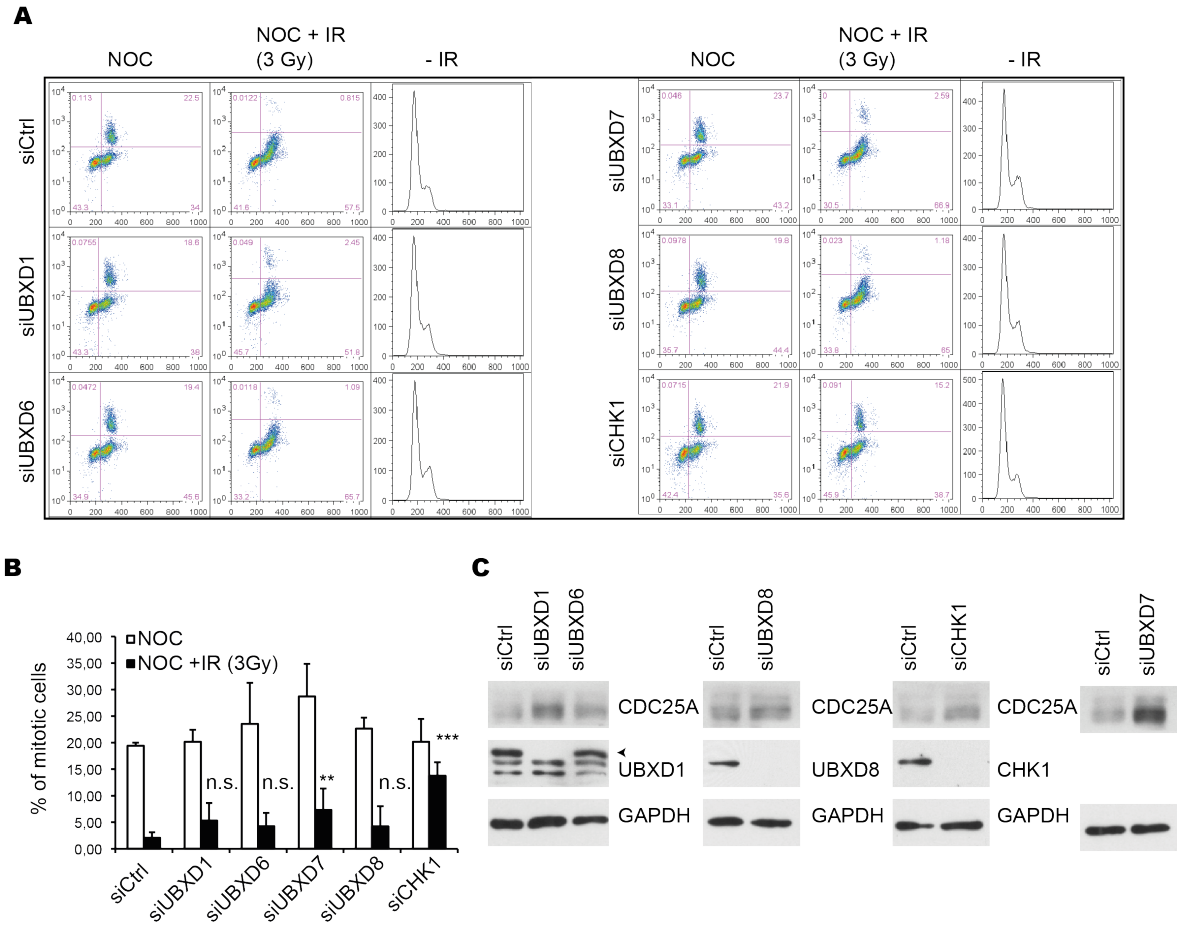

Figure 2.13: Impairment of the G_2/M checkpoint after irradiation is dependent on specific p97 adaptor proteins.

(A) Flow cytometry of HeLa cells stained with propidium iodine and pH3 (S10) antibodies. Cells were depleted of indicated proteins, mock-treated or irradiated as indicated and then subjected to a nocodazole trap for 7 h prior to analysis. Arrowhead indicates UBXD1.

Figure legend (Figure 2.13) continued: (B) Quantification of mitotic indices based on A. Shown are means of 3 independent experiments with n=10.000 cells per condition. Note that only depletion of UBXD7 from the tested p97 UBX domain-containing adaptor proteins leads to a significant increase in the mitotic index after IR compared to control depletion. Error bars: s.d.; ***, p< 0.001; **, p< 0.01; * p< 0.05. (C) HeLa cells were depleted of the indicated proteins and cell lysates subjected to SDS-PAGE and Western blotting. Membranes were probed with the indicated antibodies. Note that depletion of UBXD7 leads to increased CDC25A protein levels compared to control depletion.

2.2 Part II: The role of p97 in the DNA replication

The primary goal of this thesis was examine the functional and molecular basics of p97 regulating the cell cycle progression and ensuring genomic stability. On previous part I, we have shown that $p97^{Ufd1\text{-}Npl4}$ ensures proper CDC25A degradation and G_2/M checkpoint function. Recent studies link p97 to many processes within the cell cycle, which regulate cell cycle progression under physiological conditions and in response to DNA damage. Besides regulating the progression through mitosis by modulating Aurora B kinase activity (Dobrynin et al. (2011), the $p97^{Ufd1\text{-}Npl4}$ complex regulates degradation of the replication-licensing factor Cdt1 in unperturbed interphase cells and in response to DNA damage (Raman et al., 2011). Studies in *C. elegans* linked the function of the $p97^{Ufd1\text{-}Npl4}$ complex to DNA replication and cell cycle progression (Mouysset et al., 2008).

2.2.1 Depletion of Ufd1-Npl4 leads to a delay in recovery from replication stress

In the next step, we further investigated the function of Ufd1-Npl4 in the regulation of cell cycle progression by performing cell synchronization experiments and checking for alterations in the cell cycle profiles after release from the S phase block. Therefore HeLa cells were depleted of Ufd1 or Npl4 and blocked in S phase by double thymidine block. Thymidine induces replication stress by specifically depleting deoxycytidine triphosphate (dCTP) from the cellular pool and thus to an early S phase block. 11 h after the release from the double thymidine block, cells reached G_2 phase and were treated with 3 Gy dose of IR to selectively hit G_2 phase cells. Unsynchronized cells served as reference for the cell cycle profile and protein levels. Cells were collected 0, 6 and 12 h after release from second thymidine block and either fixed for FACS or lysed to analyse the protein levels. Fixed cells were stained with propidium iodine and the cell cycle profile was analysed by FACS. Control-depleted cells peaked in G_2 phase 6 h after release from second thymidine block. IR treatment caused the cells to arrest in G_2/M phase. Depletion of Ufd1-Npl4 did not lead to major changes in the cell cycle profiles compared to control (Figure 2.14 b).

Cell lysates were subjected to SDS-PAGE, Western blotting and membranes were probed with antibodies against pCHK1 (S317) to check for activation of the DNA damage response pathway. Depletion of Ufd1-Npl4 in otherwise untreated cells did not lead to phosphorylation of CHK1 at S317. In control-depleted cells, which were lysed directly after the release from the double thymidine block, CHK1 was activated upon thymidine treatment and cells recovered from the induced replication stress within 6 h. Treatment of the cells with IR led to activation of the DNA damage response and phosphorylation of CHK1 at Ser317. Similarly, Ufd1-Npl4-depleted cells activate the DNA damage response upon thymidine-induced replication stress as well as after IR resulting in full phosphorylation of CHK1 at Ser317. Importantly however, depletion of Ufd1-Npl4 led to persistent phosphorylation of CHK1 6 h after release from the double thymidine block (Figure 2.14 a), indicating a delay in recovery.

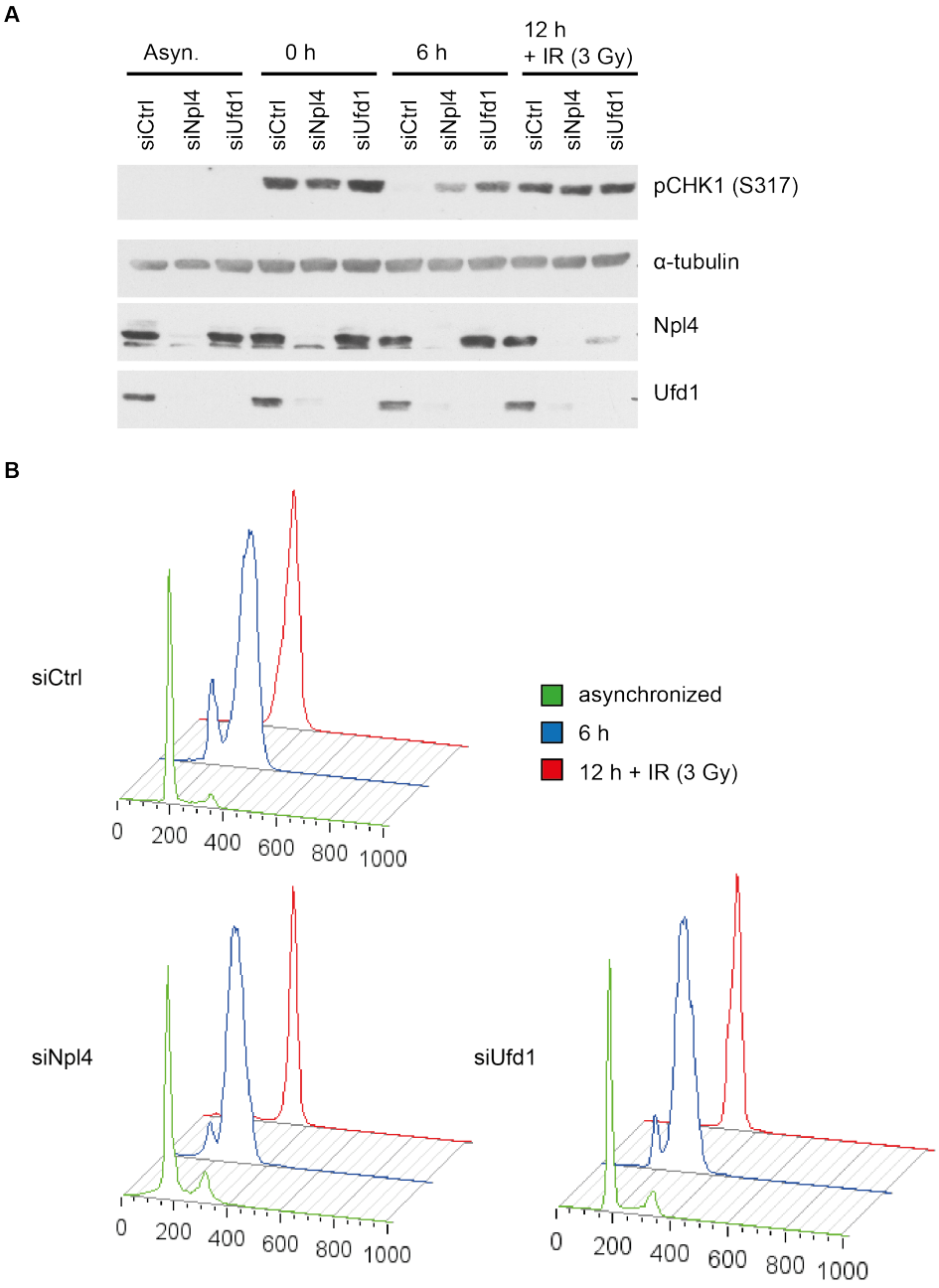

Figure 2.14: Cells deficient of Ufd1-Npl4 show persistent activation of CHK1 after double thymidine-induced replication stress.

(A) HeLa cells depleted of the indicated proteins were left untreated or treated with double thymidine block. Cells were lysed at the indicated time points after release from double thymidine block and the lysates were subjected to SDS-PAGE and Western blotting. 11 h after release from double thymidine block, cells were treated with 3 Gy ionizing radiation dose before lysis. Note that cells depleted of Ufd1-Npl4 show prolonged activation of CHK1 compared to control-depleted cells, which completely recovered from replication stress 6 h after release from the double thymidine block. (B) Cells were treated as in A and fixed in 4 % PFA. The DNA content of the cells was determined by propidium iodine staining and FACS. Note that Ufd1-Npl4 depleted cells do not show major changes in the cell cycle profiles compared to control-depleted cells.

2.2.2 Npl4 depletion causes prolonged activation of CHK1 after low dose aphidicolin-induced replication stress

To further investigate the findings described in the previous section, we changed to low dose aphidicolin-induced replication stress. Aphidicolin inhibits the DNA polymerases α and δ and thereby inhibits DNA replication. Low dose of aphidicolin however selectively impairs the progression replication forks (Durkin and Glover, 2007). HeLa cells were depleted of p97, Ufd1 or Npl4 and treated with 0.2 µM aphidicolin (APH) for 24 h or left untreated. To investigate the activation of the DNA damage response pathway after aphidicolin treatment, we analysed the levels of phosphorylated CHK1. Therefore cells were lysed 0 and 6 h after release from the aphidicolin-induced replication stress. Lysates were subjected to SDS-PAGE and Western blotting and membranes were probed with antibodies against phosphorylated CHK1. Control-depleted cells showed strong increase in phosphorylation of CHK1 at S317 as well as S345 upon APH treatment, which was largely reduced 6 h after release from APH. Cells depleted of p97 showed similar phosphorylation pattern as control cells. Interestingly, Npl4-depleted cells had slightly higher levels of pCHK1 (S317 and S345) and CHK1 at all time points compared to control. Additionally, Npl4-depleted cells showed persistent phosphorylation of CHK1 at S317 and S345 6 h after release from APH-induced replication stress (Figure 2.15). In contrast, Ufd1-depleted cells showed no increase in CHK1 phosphorylation upon treatment with APH.

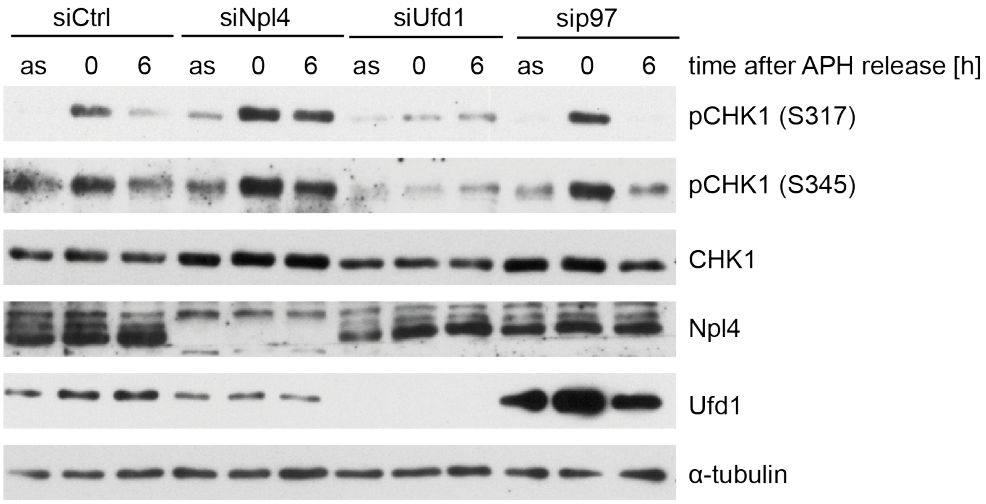

Figure 2.15: Depletion of Npl4 but not Ufd1 leads to persistent activation of CHK1 aphidicolin-induced replication stress.

U2OS cells depleted of the indicated proteins were treated with 0.2 µM aphidicolin (APH) for 24 h or left untreated (as). Cells were lysed after the indicated time points after release from APH. Cell lysates were subjected to SDS-PAGE and Western blotting. Note that only cells deficient of Npl4 show persistent activation of CHK1 after release from APH-induced replication stress. Note also that cells depleted of Ufd1 do not show activation of CHK1 at all.

2.2.3 Depletion of DVC1, UBXD7 or Npl4 leads to accumulation of γH2AX and 53BP1 positive foci

Unresolved replication intermediates induced by low doses of aphidicolin are transferred into mitosis and converted into DNA/chromatin lesions. In the following G_1 phase these unrepaired lesions are shielded by 53BP1 against further excessive DNA/Chromatin degradation (Lukas et al., 2011). Therefore the increase of 53BP1 positive foci in G_1 phase cells serves as an indicator for perturbation of DNA replication. To further investigate the role of p97 and its cofactors in DNA replication, we analysed the accumulation of 53BP1 positive foci in G_1 phase cells. To do so, U2OS cells were depleted of p97, Ufd1, Npl4, DVC1 or UBXD7 and treated with 0.2 µM APH for 24 h or left untreated. Cells were fixed and stained with DAPI and 53BP1 antibodies. To recognize G_1 cells, cells were stained additionally for Cyclin A, which is expressed during S and G_2 phase but is absent in G_1 phase. To quantify the number of 53BP1 foci in G_1 cells, confocal images were acquired and the number of 53BP1 foci per cyclin A-negative cell was counted using CellProfiler. In the control-depleted population about 15 % of the cells had more than four 53BP1 foci per G_1 cell, which did not further increase upon aphidicolin treatment. Surprisingly, the amount of 53BP1 positive foci in p97-depleted cells was comparable to control-depleted cells. Ufd1 depletion led to general more cells with more than four foci per cell compared to control, which was however not significantly different from control. Importantly, depletion of Npl4, DVC1 or UBXD7 significantly accumulated 53BP1 positive foci upon aphidicolin treatment with over 30 % of cells containing more than four foci per cell (Figure 2.16 a/b). However, only cells depleted of DVC1 show a significant increase in 53BP1 positive foci per cell upon aphidicolin treatment compared to DVC1-depleted cells without aphidicolin treatment.

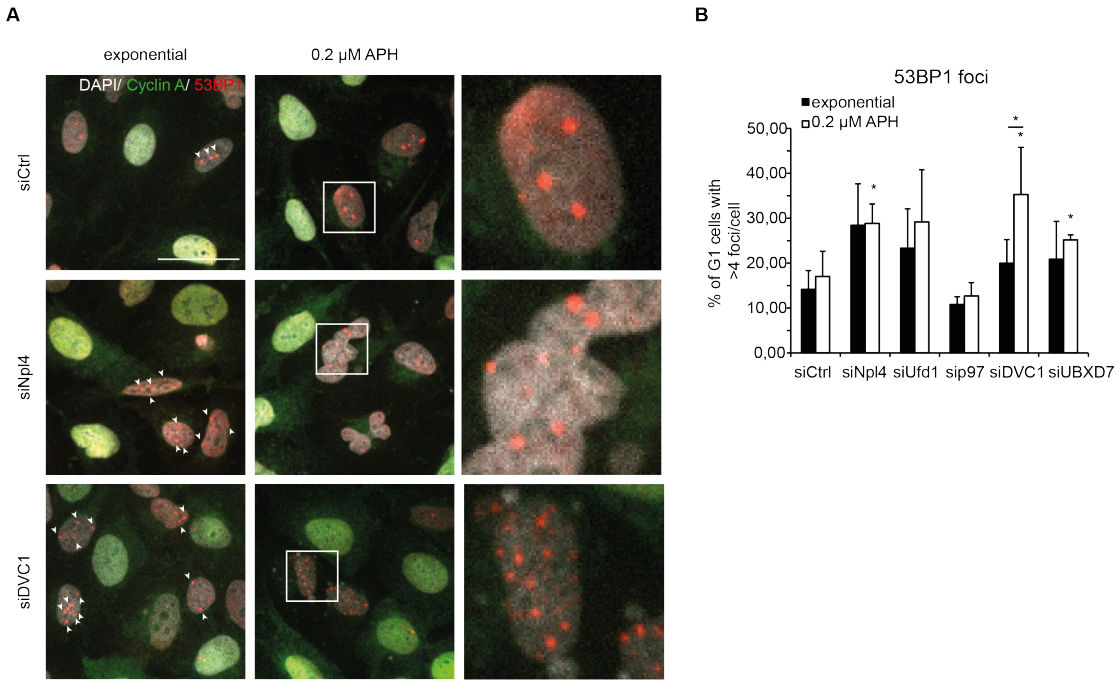

Figure 2.16: Depletion of Npl4, DVC1 or UBXD7 causes an increase of replication errors which result in an increase of 53BP1 positive foci in G_1 cells after APH treatment.
(A) Representative images of U2OS cells depleted of the indicated proteins and treated with 0.2 µM APH for 24 h or left untreated. After fixation cells were stained for DAPI, cyclin A and 53BP1. As a marker for replication stress 53BP1 foci in G_1 cells were quantified. Arrowheads indicate 53BP1 foci; enlarged picture of the ROI is shown in the right panel; scale bar represents 10 µm (B) Quantification of A. Shown are means of 3 independent experiments with at least 120 cells per condition. Note that depletion of Npl4, DVC1 or UBXD7 leads to a significant increase of cells with more than 4 foci/cell after APH treatment compared to control depletion. Error bars: s.d. ***, p< 0.001; **, p< 0.01; * p< 0.05.

Additionally to the formation of 53BP1 foci in G_1 cells, unresolved replication errors also result in the formation of γH2AX foci on mitotic chromatin (Durkin and Glover, 2007). To confirm our previous results with yet another marker for replication stress, U2OS cells were depleted of p97, Ufd1, Npl4, DVC1 or UBXD7. Cells were treated with 0.2 µM APH for 24 h and stained for DAPI and γH2AX. In control-depleted cells, we observed an increase in cells with more than four foci per cell from 20 % to around 40 % after aphidicolin treatment. Again, p97-depleted cells showed comparable result to control depletion with around 30 % of cell containing more than three foci per cell after aphidicolin treatment. In contrast, depletion of Npl4-Ufd1 as well as DVC1 or UBXD7 led to a significant increase in the cell population of cells containing more than four foci per cell compared to control depletion (Figure 2.17 a/b). Additionally, depletion of Npl4, DVC1 or UBXD7 led to an increase in the mean

number of γH2AX foci per cell compared to control-depleted cells. On the contrary, depletion of p97 did not result in major changes of the mean foci number per cell compared to control-depleted cells.

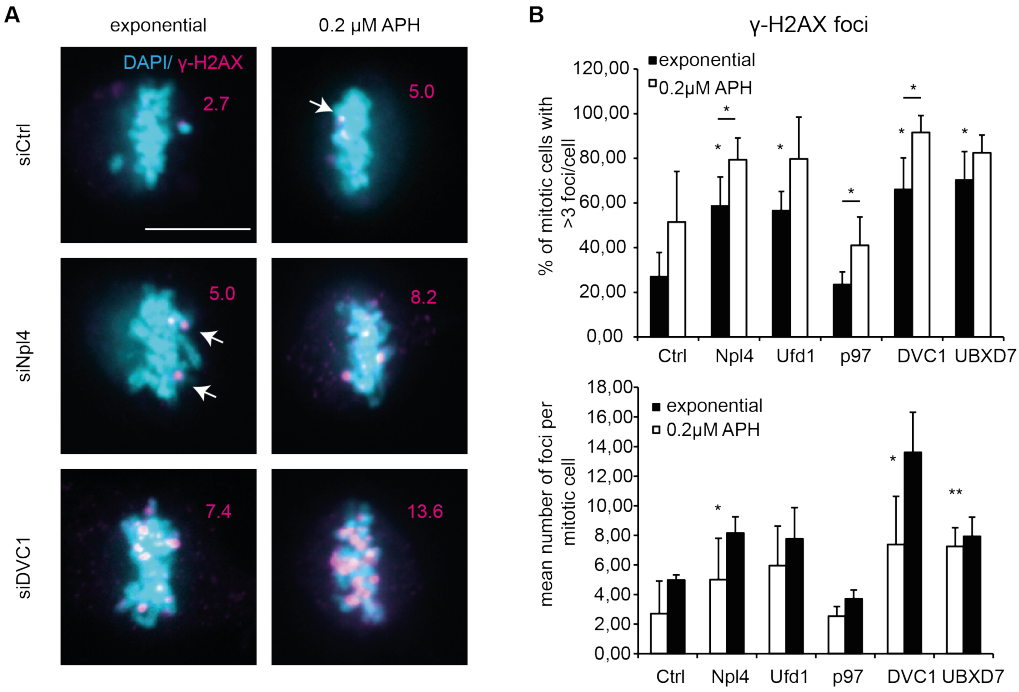

Figure 2.17: Npl4, DVC1 or UBXD7 depletion result in an increased number of γ-H2AX positive foci on mitotic chromatin.

(A) Representative images of U2OS cells depleted of the indicated proteins and treated with 0,2 µM APH for 24 h or left untreated. After fixation cells were stained for DAPI and γ-H2AX. In magenta the mean γ-H2AX foci number per cell is depicted. Arrowheads indicate γ-H2AX foci on the mitotic chromatin. Scale bar represents 10 µm (B) Quantification of A. Note that depletion of Npl4, DVC1 or UBXD7 leads to a significant increase in the mean number of γ-H2AX foci per cell as well as increased number of cells with more than 3 foci/cell. Shown are means of 3 independent experiments with at least 60 cells per condition. Error bars: s.d. ***, p< 0.001; **, p< 0.01; * p< 0.05.

2.3 Part III: Characterization and verification of mitotic phenotypes of Npl4 depletion

In the previous parts I and II, we focused on the role of $p97^{Ufd1\text{-}Npl4}$ complex in S phase and G_2 phase of the cell cycle. In the third part of the thesis we focused on the mitotic functions of the $p97^{Ufd1\text{-}Npl4}$ complex. In former studies, we and others described a role for p97 in regulating progression of mitosis by regulating mitotic kinases Aurora A and Aurora B (Kress et al., 2013). Depletion of $p97^{Ufd1\text{-}Npl4}$ leads to missregulation of Aurora B kinase and results in chromosome congression and chromosome segregation defects (Dobrynin et al., 2011). Additionally, our lab observed the loss of BUBR1 protein on mitotic chromatin as well as on the total protein level upon Npl4 depletion in HeLa cells. BUBR1 is an essential member of

the mitotic checkpoint complex, which becomes activated upon the activation of the spindle assembly checkpoint by unattached microtubules.

2.3.1 Depletion of Npl4 leads to chromosome misalignment and chromosome segregation errors in mitosis

As the loss of BUBR1 occurred not in Ufd1-depleted cells, but only after depletion of Npl4 with one of the tested siRNAs, we set out to verify whether the observed effect is specific for Npl4-depletion or due to an off-target effect of the used siRNA. In the first step, I reproduced the above-mentioned loss of BUBR1 on mitotic chromatin upon Npl4 depletion in HeLa cells. To do so, HeLa cells were depleted of Ufd1, Npl4 or BUBR1 for 48 h, fixed and stained with BUBR1 antibodies. Consistently with previous results, depletion of Npl4 with siNpl4 S2, but not with siNpl4 S1, led to loss of BUBR1 in pro-metaphase cells (Figure 2.18).

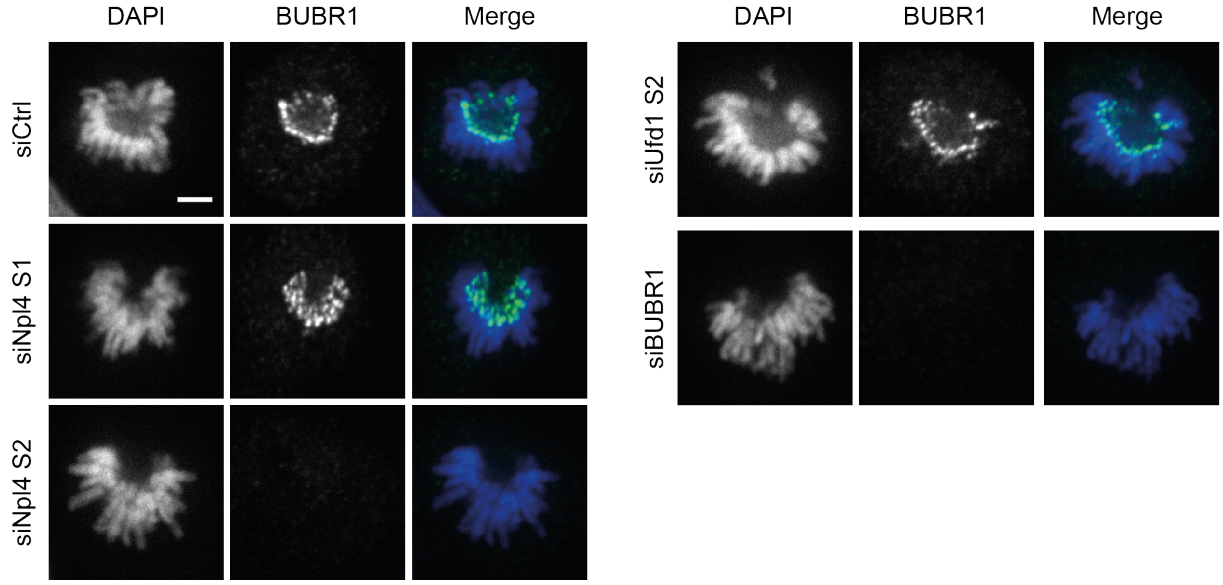

Figure 2.18: Depletion of Npl4 with siNpl4 S2 leads to loss of BUBR1 localization on pro-metaphase chromatin.

HeLa cells were treated with the indicated siRNAs for 48 h and fixed. Fixed cells were stained with DAPI and BUBR1 antibodies and analysed for BUBR1 localization in pro-metaphase cells. Note that depletion of Npl4 with siNpl4 S2 led to loss of BUBR1 on mitotic chromatin. Scale bar represents 5 µm

However, this phenotype was only observed with one of the tested oligonucleotides against Npl4. To rule out a direct off-target effect of the used siRNA oligonucleotide, we compared the used siRNA sequences to the nucleotide sequences of Npl4 and BUBR1 using the BLAST tool. The used siRNA sequences showed 100 % sequence similarity only to the nucleotide sequence of Npl4, but no significant sequence similarity BUBR1 (data not shown). Therefore, we set out to verify the mitotic

phenotypes observed upon Npl4 depletion. To do so, we generated a HeLa cell line, which inducibly expresses a siRNA-resistant Npl4-3myc construct (Figure 2.19 a). For this purpose, we cloned rat Npl4 cDNA fused to 3myc-tag into a pcDNA5/FRT/TO vector and the generated pcDNA5/FRT/TO/reNpl4-3myc vector was transfected into HeLa Flip-in cells. The rat Npl4 cDNA does not show 100 % sequence similarity with the used siRNA oligonucleotides, as it has three nucleotide mismatches for Npl4 S2 oligonucleotide and two for Npl4 S1 oligonucleotide and is resistant to the used Npl4 siRNA oligonucleotides. From the transfected HeLa cells single cell clones were selected and tested for expression of reNpl4 upon doxycyclin treatment. Indeed expression of reNpl4 was induced upon treatment with 1 mg/mL doxycyclin (Dox) for 24 h and reNpl4 localized to the cytoplasm as well as to the nucleus (Figure 2.19 b). In the next step, we investigated whether reNpl4 binds to endogenous p97 and Ufd1. To do so, we induced expression of reNpl4 with doxycycline for 24 h or left the cells uninduced. Cells were lysed in IP-buffer and used for immunoprecipitation with anti-myc antibodies, pulling on the exogenous reNpl4 or anti-Ufd1 antibodies to pull out the endogenous $p97^{Ufd1\text{-}Npl4}$ complex. IP samples together with 1% inputs (In) and 1% flowthroughs (FT) were subjected to SDS-PAGE and Western blotting. Membranes were probed with p97, Npl4 and Ufd1 antibodies. Indeed, reNpl4 binds to p97 and Ufd1. Moreover, reNpl4 can be found in complex with endogenous Npl4 together with Ufd1 and p97 (Figure 2.19 c). In further experiments, we tested whether the generated reNpl4-3myc-expressing cells respond to siRNA transfection. For that purpose, HeLa reNpl4-3myc cells were treated with siRNA for 48 h and expression of reNpl4 was induced 24 h before cell lysis. Cell lysates were subjected to SDS-PAGE and Western blotting. Endogenous Npl4 protein levels were reduced upon siRNA treatment. Furthermore, the protein levels of reNpl4 were not affected by siRNA depletion. Again, depletion of Npl4 with siNpl4 S2 led to loss of BUBR1 on protein level. In addition, Ufd1 was destabilized in Npl4 depleted cells as previously shown (Dobrynin et al. 2011). However, cells expressing reNpl4 showed a slight increase in the overall levels of endogenous Npl4, which might result from degradation products of the overexpressed 3myc-tagged Npl4 variant (Figure 2.19 d).

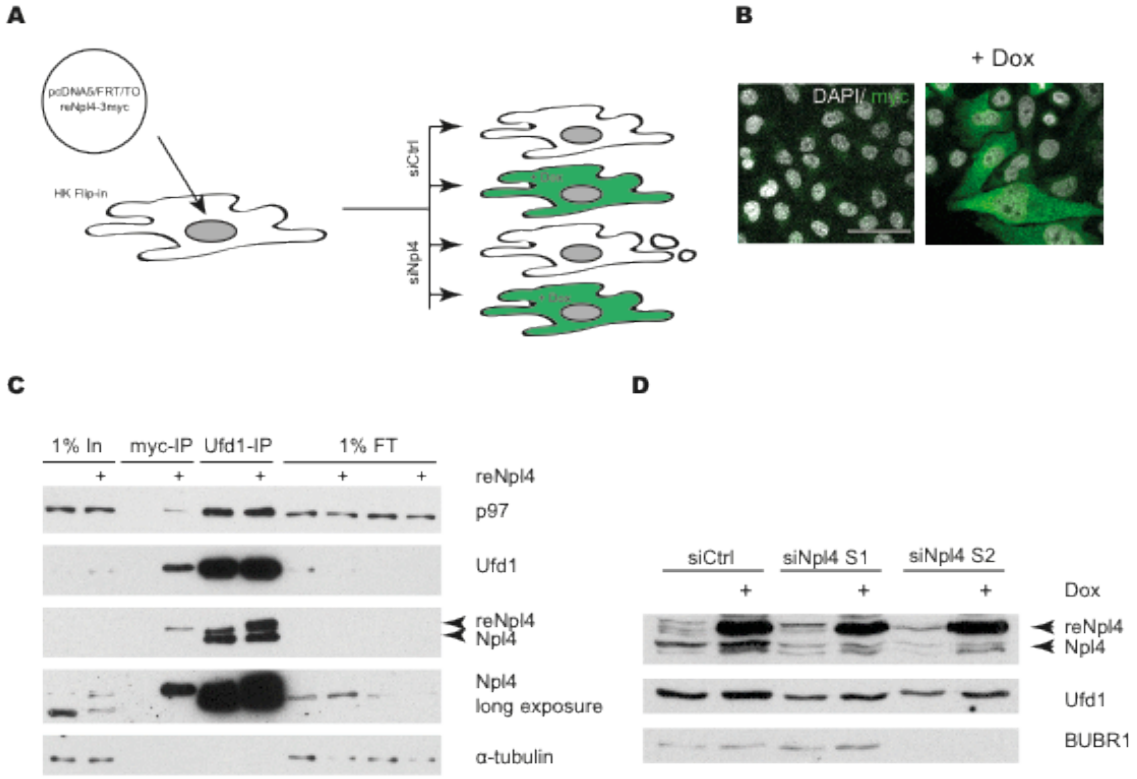

Figure 2.19: Generation of an inducible HeLa cell line expressing siRNA resistant Npl4-3myc (reNpl4).

(A) Schematic illustration of the generation of a HeLa cell line. (B) HeLa reNpl4-3myc cells were treated with 1 mg/mL doxycyclin (Dox) or left untreated. After 24 h cells were fixed and stained with anti-myc antibody. Note that the expression of reNpl4 is induced upon doxycyclin treatment and that reNpl4 localizes to the cytoplasm as well as to the nucleus. Scale bar represents 50 µm. (C) Expression of reNpl4 in the generated cells was induced 24 h before cell lysis. Lysates were subjected to immunoprecipitation with anti-myc antibodies (myc-IP) or anti-Ufd1 antibodies (Ufd1-IP). IP samples, together with 1 % inputs (In) and flowthroughs (FT) were analysed by SDS PAGE and Western blotting. Membranes were probed with the indicated antibodies. Note that reNpl4 binds to endogenous p97 and Ufd1. (D) HeLa reNpl4-3myc cells were treated with the indicated siRNAs for 48 h. Expression of reNpl4 was induced 24 h before cell lysis. Cell lysates were subjected to SDS-PAGE and Western blotting. Note that Ufd1 is co-depleted in siNpl4 treated cells and that reNpl4-3myc levels are not affected by siNpl4 depletion.

In the next step we aimed at confirming the mitotic phenotypes of Npl4 depletion in the generated cell line. Therefore the cells were depleted for endogenous Npl4 and the expression of reNpl4 was induced for 24 h. Luciferase served as control depletion. 48 h after siRNA transfection cells were fixed and stained for DAPI and BUBR1. Depletion of Npl4 with S1 oligonucleotide as well as control depletion did not affect the localization of BUBR1 on the mitotic chromatin. In contrast, cells depleted

for Npl4 using S2 oligonucleotide did not show any BUBR1 on mitotic chromatin in pro-metaphase cells (Figure 2.20 a). Induction of the reNpl4 protein in control- and Npl4-depleted cells using S1 oligonucleotide did not affect the proper localization of BUBR1. Interestingly, overexpression of the reNpl4 protein in cell depleted of endogenous Npl4 using S2 oligonucleotide did not show restoration of the BUBR1 localization on mitotic chromatin. Instead, the BUBR1 signal in these cells is still strongly reduced compared to control-depleted cells (Figure 2.20 b). This indicates, that the observed loss of BUBR1 protein in Npl4 depleted cells is due to an off-target effect and not specific for Npl4 depletion.

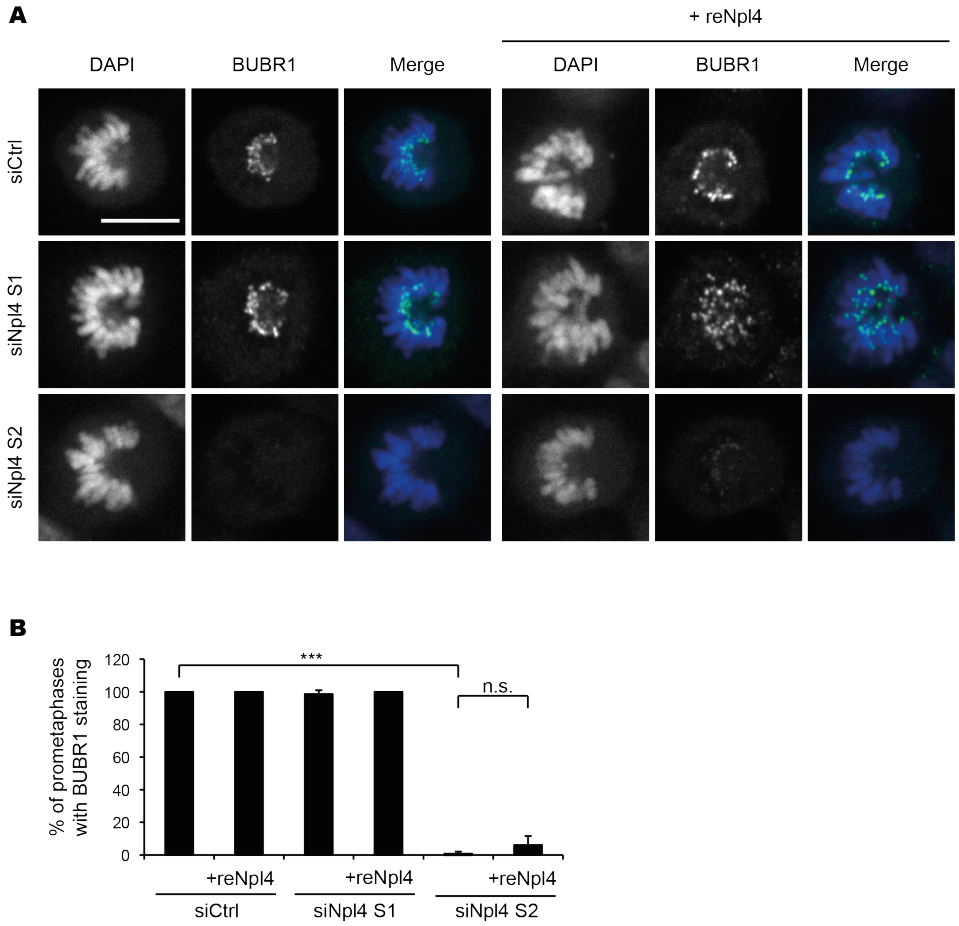

Figure 2.20: Loss of BUBR1 protein upon Npl4 depletion can not be restores by overexpression of reNpl4.

(A) Representative images for siRNA depletion phenotypes in prometaphase. HeLa –reNpl4-3myc cells were depleted for endogenous Npl4 using the indicated siRNAs. Luciferase depletion served as control depletion. 24 h after siRNA transfection the expression of 3myc-tagged exogenous reNpl4 was induced by treatment with doxycyclin for 24 h. Afterwards, cells were fixed and stained with BUBR1 antibodies. Scale bar represents 10 µm (B) Quantification of A. Shown are mean values of 3 independent experiments with at least 80 cells per condition. Error bars indicate standart error, *** = p-value < 0,001; n.s. = not significant. Note that depletion of endogenous Npl4 using S2 oligonucleotide leads to loss of BUBR1 protein on mitotic chromatin, which is not restored by overexpression of reNpl4, indicating non-specific off-taget effect of the used siRNA oligimer.

Depletion of Npl4 in the generated cell line resulted in an identical phenotype to the one that was observed previously in HeLa cells. Npl4-depleted cells showed misaligned chromosomes in metaphase as well as lagging chromosomes in anaphase. Upon induction of reNpl4 expression the chromosome misalignment was significantly reduced in cells treated with siNpl4 S1 oligonucleotide (Figure 2.21 a/b). Also chromosome segregation errors were significantly reduced upon expression of reNpl4. In conclusion, only the defects in chromosome alignment and segregation defects were considered to be specific for Npl4 depletion.

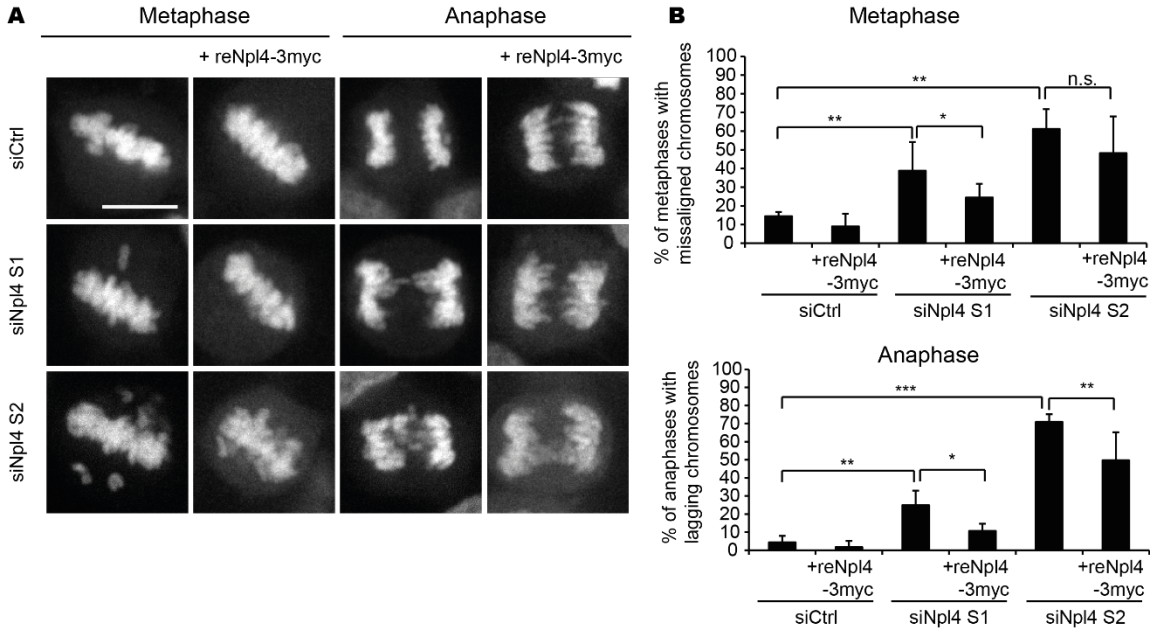

Figure 2.21: Depletion of Npl4 leads to chromosome misalignment and chromosome segregation defects in mitosis.

HeLa cells inducibly expressing siRNA resistant Npl4 (reNpl4) were transfected with the indicated siRNAs and expression of reNpl4 was induced 24 h after siRNA transfection. Cells were fixed 48 h after siRNA transfection and stained with DAPI. (A) Representative images for siRNA depletion phenotypes in metaphase and anaphase. Scale bar represents 10 µm (B) Quantification of A with at least 80 cells/condition. Note that the chromosome misalignment in metaphase and the chromosome segregation defects in anaphase can be restored by overexpression of reNpl4. Error bars indicate standart error, *** = p-value < 0,001, **= p-value < 0,01; *= p-value < 0,05; n.s. = not significant.

3 Discussion

The Cell cycle is a tightly regulated process that governs faithful replication and segregation of DNA material into two daughter cells during proliferation. To ensure ordered and directed cell cycle progression and thus maintain genomic integrity, the mammalian cell cycle harbours a number of checkpoints. Among them, the G_2/M checkpoint is activated by damaged or unreplicated DNA to prevent the cells from committing to mitosis, which leads to deleterious effects on chromosome segregation. The timely and efficient degradation of cell cycle effector proteins, including the CDC25A phosphatase, by the ubiquitin-proteasome pathway (UPS) is an essential step for robust activation of the G_2/M checkpoint. CDC25A degradation is triggered by its phosphorylation and ubiquitination by CHK1 and βTrCP, respectively. However, the exact molecular mechanism by which ubiquitinated CDC25A is targeted for degradation is not described so far.

The AAA – ATPase p97 is a well-known component of the UPS and is involved in a wide variety of cellular processes including the regulation of S phase and mitosis progression as well as modulating the DNA damage response by targeting ubiquitinated substrates for degradation. Therefore, in this study we ask whether p97 is involved in the regulation of CDC25A degradation in human somatic cells. Our results confirmed, that indeed p97 together with its adaptor Ufd1-Npl4 facilities the degradation of CDC25A downstream of βTrCP mediated ubiquitination under physiological conditions and in response to DNA damage. Furthermore, we showed evidence that the p97 co-factor UBXD7 acts together with Ufd1-Npl4 in facilitating CDC25A degradation. In contrast, we identified an additional p97 co-factor, DVC1, involved in the regulation of the G_2/M checkpoint. Interestingly, DVC1 does not act in the same pathway as $p97^{Ufd1\text{-}Npl4}$ but through a mechanism distinct from the degradation of CDC25A. Moreover, we showed that depletion of $p97^{Ufd1\text{-}Npl4}$ leads to a diminished G_2/M checkpoint after IR and that this is due to the stabilization of CDC25A. More importantly, we demonstrated that $p97^{Ufd1\text{-}Npl4}$ is essential to maintain genomic stability as depletion of the complex leads to mitotic entry despite the presence of DNA damage with an increase of mitotic aberrations and subsequent segregations errors.

In the following sections I will discuss the role of p97 in the regulation of the cell cycle progression and the DNA damage response focussing on the regulation of the G_2 to M transition. Furthermore, I will review the modulation of p97 function in the regulation of cell cycle progression by its different adaptor proteins. In the last two parts of the discussion, I will consider the more general role of p97 in the regulation of S phase and mitosis progression.

3.1 Part I: The $p97^{Ufd1\text{-}Npl4}$ complex ensures robustness of the G_2/M checkpoint

The pre-mitotic and mitotic functions of p97 contribute to the manifestation of segregation errors in mitosis

It has been previously shown that p97 is connected to multiple processes in the regulation of mitosis progression and, moreover, is recently implicated in a growing number of interphase functions, including the regulation of S phase progression and the modulation of the DNA damage response. Thereby the majority of p97 functions in the regulation of cell cycle progression are mediated by its co-factor Ufd1-Npl4. In mitosis, depletion of Ufd1-Npl4 causes severe chromosome misalignment and segregation errors, whose origins are however so far only connected to the mitotic functions of $p97^{Ufd1\text{-}Npl4}$. Here we provide evidence that, especially after challenging cells with DNA damage, also the pre-mitotic interphase functions of $p97^{Ufd1\text{-}Npl4}$ contribute to the manifestation of chromosomal instability in $p97^{Ufd1\text{-}Npl4}$ –depleted cells. Our experiments show that depletion of $p97^{Ufd1\text{-}Npl4}$ primarily leads to an increase in segregation errors with mitotic origin, as lagging chromosomes contain a centromere (Figure 2.1 b/c). According to the quantification published by Burrell and colleagues, lagging chromosomes containing centromeres indicate mitotic dysfunctions resulting in the improper attachment of chromosomes (Burrell et al., 2013). Indeed, it was shown previously that depletion of Ufd1-Npl4 leads to persisting Aurora B activity on the chromatin, which than results in defects in the microtubule-kinetochore attachment and thus to defects in chromosome alignment as well as in chromosome segregation during mitosis (Dobrynin et al., 2011). However, additionally to the segregation defects caused by mitotic dysfunctions, we observed a small fraction of chromosome fragments lacking a centromere and the formation of anaphase bridges in $p97^{Ufd1\text{-}Npl4}$ depleted cells, which drastically increased after challenging the cell with DNA damage by IR, indicating that errors from pre-mitotic functions were transferred into mitosis. In contrast to segregation errors with mitotic origin, pre-mitotic errors manifest as chromosome fragments without centromeres and anaphases bridges in mitosis (Burrell et al., 2013). Importantly, anaphase bridges are connected to DSB, as the incorrect fusion of the DNA strands manifest as anaphase bridge in mitosis (Geigl et al., 2008). Previous studies implicated $p97^{Ufd1\text{-}Npl4}$ in the DNA repair in response to DSB (Meerang et al., 2011). In this process $p97^{Npl4}$ orchestrates the response to DNA damage by extracting L3BMTL1 from the chromatin and thus facilitates the recruitment of the DNA repair protein 53BP1 to the sites of DNA damage (Acs et al., 2011). These studies further support our finding that indeed not only mitotic but also pre-mitotic functions of $p97^{Ufd1\text{-}Npl4}$ contribute to the formation of anaphase bridges and segregation defects in mitosis. However, anaphase bridges can also result due to errors in the microtubule

attachment, which finally lead to the generation of anaphase bridges (Maia et al., 2012). As Ufd1-Npl4 depletion lead to malfunction in the proper microtubule attachment, anaphase bridges in unirradiated cells might rather result from the mitotic functions of Ufd1-Npl4 than due to pre-mitotic functions. However, we additionally observed an increase in the formation of γH2AX foci on the mitotic chromatin after IR in Ufd1-Npl4 depleted cells, indicating that cells entered mitosis with damaged DNA (Figure 2.2 a/b). The generation of DNA damage-induced DNA double strand breaks leads to subsequent phosphorylation of H2AX (γH2AX). Phosphorylated H2AX is than recruited to sites of DNA damage to further transduce the DNA damage response signal (Lobrich and Jeggo, 2007). Unrepaired DNA damage that is transferred into mitosis, manifest as chromosomal aberrations, including chromosome fragments and acentric chromosomes (Asaithamby et al., 2011). Consistently with the above mentioned results, also the number of chromosomal aberrations in metaphase spreads after IR drastically increases in Npl4- or Ufd1-depleted cells compared to control-depleted cells, where mitotic cells were virtually absent (Grzegorz Dobrynin; (Riemer et al., 2014)).

In addition to Ufd1-Npl4 another p97 cofactor, DVC1, was implicated in the regulation of S phase progression. DVC1 recruits p97 to the sites of DNA damage in the process of translesion synthesis after UV light-induced DNA damage (Davis et al., 2012) (Mosbech et al., 2012). In contrast to Ufd1-Npl4, DVC1 is so far not implicated in any mitotic function. Surprisingly, in our experiments, depletion of DVC1, like Ufd1-Npl4, caused an increase of chromosome misalignment and chromosome segregation errors in mitosis. Moreover importantly, after induction of DNA damage by IR, the number of segregation errors with pre-mitotic origin in DVC1 depleted cells strongly increased (Figure 2.1 b/c), indicating that indeed DNA damage resulting from S phase functions of DVC1 was transferred into mitosis and manifested as anaphase bridges and chromosome fragments. However, the exact molecular mechanism, how the DNA damage is transferred into mitosis in DVC1-dpeleted cells is yet to be identified.

Depletion of $p97^{Ufd1\text{-}Npl4}$ leads to an impaired G_2/M checkpoint after IR.

The presence of pre-mitotic errors in Ufd1-Npl4 depleted cells raised the question why the cells did not arrest in the G_2/M DNA damage checkpoint, but instead entered mitosis despite the persistence of DNA damage. Upon induction of DNA damage the cell activates the ATM/ATR-dependent DNA damage response leading to subsequent cell cycle arrest (Lobrich and Jeggo, 2007). In our previous experiments with fixed cells and chromosomal spreads, we found evidence that cells depleted of Ufd1-Npl4 did not arrest in the cell cycle progression upon IR treatment. In live-cell imaging experiments, we showed that cells depleted of Ufd1-Npl4 indeed entered

mitosis after IR, indicating that the G_2/M checkpoint activating is impaired in these cells (Figure 2.3 a/b). Furthermore, quantitative FACS analysis confirmed our previous observation that cells depleted of Ufd1-Npl4 or DVC1 entered mitosis after IR, providing evidence for an impaired G_2/M checkpoint activation in response to IR in these cells (Figure 2.4 a/b). Interestingly, cells depleted of p97 as well as cells depleted of the SCF E3 ligase F-box protein βTrCP showed only a small number of cells entering mitosis after IR in the live-cell imaging analysis. This can result from pleiotropic effects, as both proteins are implicated in the regulation of a wide variety of cellular processes. It is known that depletion of βTrCP leads to a stabilization of the promoter of cell cycle progression, CDC25A (Busino et al., 2003). Interestingly, so far it has not been shown that depletion of βTrCP leads mitotic entry after IR, which might be due to the additional stabilization of WEE1, the counterpart of CDC25A.

$p97^{Ufd1\text{-}Npl4}$ facilitates the degradation of CDC25A and thus ensures robust activation of the G_2/M checkpoint after IR.

To cope with ionizing radiation-induced DNA damage, cells are equipped with a network of proteins that recognize it and subsequently lead to the activation of the G_2/M checkpoint to prevent cell from entering mitosis with damaged DNA material (Lobrich and Jeggo, 2007). As described previously, in response to IR-induced DNA damage, the CHK1/CHK2 kinases are rapidly phosphorylated by the ATM/ATR kinases and become highly activated. CHK1/CHK2 further transduce the DNA damage signal to multiple downstream effectors, including the CDC25 phosphatases and WEE1 kinase. In our experiments, we showed that depletion of Ufd1-Npl4 or DVC1 did not lead to impaired activation of the DNA damage response, as CHK1 was fully phosphorylated after IR (Figure 2.5). Furthermore, we showed that the CHK1 substrate CDC25C was phosphorylated at Ser316 in response to IR in Ufd1-Npl4 or DVC1 depleted cells, indicating that CHK1 was active in these cells (Grzegorz Dobrynin, (Riemer et al., 2014)). As described earlier, another CHK1 substrate, CDC25A, is degraded by the proteasome in response to IR-induced DNA damage (Melixetian et al., 2009). Importantly, in our experiments CDC25A is stabilized in cells depleted of Ufd1-Npl4 whereas it is fully degraded in control-depleted cells, indicating that Ufd1-Npl4 is involved in the regulation of CDC25A degradation (Figure 2.5).

Persisting CDC25A leads to the prolonged activation of CDK1-cyclinA complex and promotes mitotic entry (Timofeev et al., 2010). Parallel experiments carried out in our laboratory, showed reduced phosphorylation levels of CDK1 on Tyr15 in Ufd1-Npl4 depleted cells after IR, indicating persistent CDC25A activity in these cells (Grzegorz Dobrynin). Indeed in this work, we demonstrated that the impaired G_2/M checkpoint

in Ufd1-Npl4 depleted cells is caused by the persistence of CDC25A activity, as additional treatment of the cells with the CDC25 phosphatase inhibitor NSC663482 completely restored the G_2/M checkpoint after IR (Figure 2.11 a/b).
In cyclohexamide chase experiments we confirmed, that depletion of Ufd1-Npl4 lead to a stabilization of exogenous HA-CDC25A as well as endogenous CDC25A under physiological conditions as well as after DNA damage (Figure 2.6 a/b, Figure 2.7 a/b), indicating that Ufd1-Npl4 regulates CDC25A turnover on protein levels rather than CDC25A transcription rates. Consistently, parallel experiments in the laboratory, revealed the physical interaction of p97-Npl4 and HA-CDC25A, indicating that CDC25A is a direct substrate of $p97^{Ufd1\text{-}Npl4}$ (Grzegorz Dobrynin, (Riemer et al., 2014)). In line with the previous findings, we observed that expression of the substrate-trapping p97 EQ variant increases the amount of HA-CDC25A bound to p97 as well as the amount of ubiquitinated form of HA-CDC25A, further confirming a model, where $p97^{Ufd1\text{-}Npl4}$ targets ubiquitinated CDC25A for degradation. Importantly, induction of DNA damage in these cells led to further accumulation of ubiquitinated HA-CDC25A bound to p97EQ, providing evidence for the relevance of p97 in facilitating CDC25A degradation after IR and thus prevent cells to commit to mitosis with damaged DNA (Grzegorz Dobrynin, (Riemer et al., 2014)).

Does interact $p97^{Ufd1\text{-}Npl4}$ with UBXD7 and $SCF^{\beta TrCP}$ to facilitate CDC25A degradation?

The regulation of cell cycle progression is connected to the ubiquitination of target substrates by different E3 Cullin-RING-ligases complexes like the SCF- and APC/C E3 ligases (Vodermaier, 2004). As mentioned earlier, phosphorylated CDC25A is recognized by the F-box protein βTrCP and subsequently ubiquitinated by the $SCF^{\beta TrCP}$ E3 ligase, which than leads to it proteasomal degradation (Busino et al., 2003). Here, we show that $p97^{Ufd1\text{-}Npl4}$ physically interacts with the SCF F-box protein βTrCP, further confirming that $p97^{Ufd1\text{-}Npl4}$ acts downstream of $SCF^{\beta TrCP}$ (Figure 2.10). In recent studies, p97 was linked to the $SCF^{\beta TrCP}$ complex in drosophila as well as in human cell lines (Zhang et al., 2013) (Li et al., 2014), which supports a more general model of $p97^{Ufd1\text{-}Npl4}$ in targeting ubiquitinated substrates for degradation downstream of the $SCF^{\beta TrCP}$ E3 ligase.
Supporting our previous result, it has been shown that the p97 co-factor UBXD7 connects p97 to ubiquitinated substrates of CRL E3 ligases, as it interacts with p97 as well as with multiple E3 ligases (Alexandru et al., 2008). Recent studies demonstrated that UBXD7 binds to NEDD8 modified cullins via its UIM domain and subsequently facilitates the degradation of cullin substrates (den Besten et al., 2012) (Bandau et al., 2012). Importantly, UBXD7 directly links p97 to the degradation of the cullin2-E3 ligase substrate HIF1-α (Alexandru et al., 2008) (Bandau et al., 2012). In

this work, we provide evidence that UBXD7 links the $p97^{Ufd1\text{-}Npl4}$ complex to the $SCF^{\beta TrCP}$ E3 ligase in facilitating CDC25A degradation, as depletion of UBXD7 but not UBXD8 leads to an increase in the CDC25A protein levels (Figure 2.13 a/b/c). Moreover, we observed that depletion of UBXD7 but not UBXD8 lead to a significant increase in the mitotic fraction of cells after IR, indicating a defect in G_2/M checkpoint activation after IR. A recent study implicated UBXD7 in the DNA damage response, where it acts together with $p97^{Ufd1\text{-}Npl4}$ in facilitating the degradation of DDB2 and XPC after DNA damage induction (Puumalainen et al., 2014), further supporting the idea that UBXD7 acts together with $p97^{Ufd1\text{-}Npl4}$ in the regulation of protein turnover in response to DNA damage.

Taken together the data from this study propose a model where $p97^{Ufd1\text{-}Npl4}$ together with UBXD7 acts downstream of $SCF^{\beta TrCP}$ in the regulation of CDC25A (Figure 3.1). The exact mechanism, how UBXD7 facilitates CDC25A degradation still needs to be clarified. One possibility is that it recognizes neddylated $SCF^{\beta TrCP}$ and recruits the $p97^{Ufd1\text{-}Npl4}$ complex to the $SCF^{\beta TrCP}$ complex and its ubiquitinated substrate, CDC25A, thereby ensuring proper CDC25A degradation.

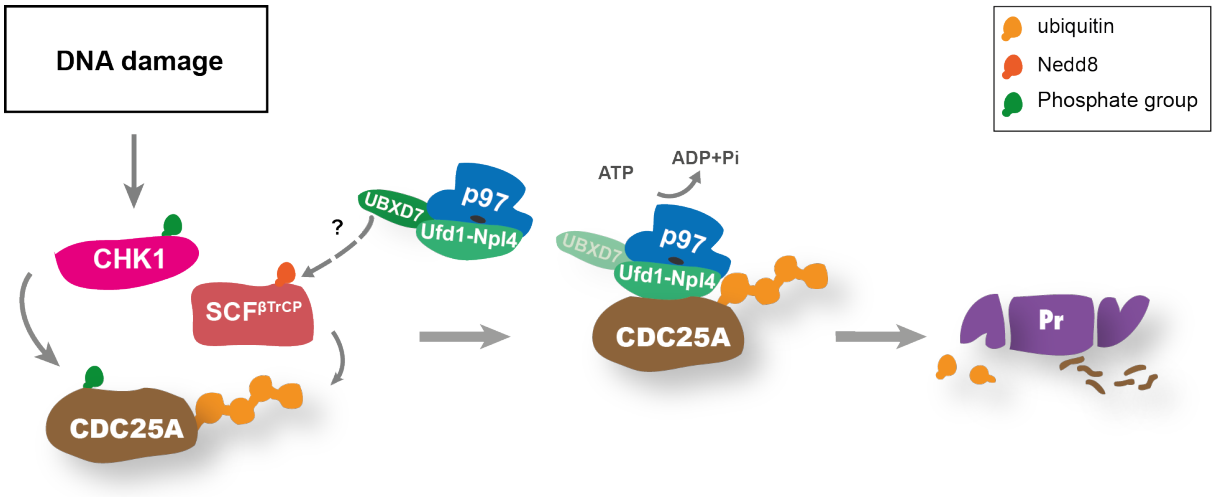

Figure 3.1: Model of $p97^{Ufd1\text{-}Npl4}$ complex facilitating CDC25A degradation in response to DNA damage.

Upon DNA damage CHK1 is phosphorylated and thus activated by ATM/ATR kinases. Activated CHK1 phosphorylates CDC25A at multiple serine-residues, which primes for further phosphorylation of CDC25A on Ser82 by NEK11 kinase and thus creating phosphodegron for recognition by βTrCP. The $SCF^{\beta TrCP}$ E3 ligase ubiquitinates CDC25A and targets it for proteosomal degradation. Experimental data indicate that UBXD7 acts in concert with $p97^{Ufd1\text{-}Npl4}$ and brings $p97^{Ufd1\text{-}Npl4}$ complex to the $SCF^{\beta TrCP}$ complex and ubiquitinated CDC25A. $p97^{Ufd1\text{-}Npl4}$ binds to ubiquitinated CDC25A and facilitates its degradation.

What is the molecular mechanism of p97 and DVC1 in the regulation of the G_2/M checkpoint in response to DNA damage?

As mentioned above, we showed that depletion of DVC1, like Ufd1-Npl4 depletion, leads to mitotic entry after IR, indicating an impaired G_2/M checkpoint in these cells. However interestingly, DVC1, in contrast to Ufd1-Npl4, did not lead to a stabilization of CDC25A, indicating that DVC1 acts via a distinct mechanism in regulating the G_2/M checkpoint after IR. Interestingly, we showed that depletion of DVC1 leads to strong reduction of WEE1 protein levels already under physiological conditions, indicating that DVC1 regulates WEE1 and not CDC25A (Figure 2.8 a/b). WEE1 is the counterpart of CDC25A as it modulates CDK1 with an inhibitory phosphate at Tyr15 leading to subsequent cell cycle arrest (Lobrich and Jeggo, 2007). Moreover importantly, we showed that also p97-depleted cells show reduced WEE1 levels, whereas CDC25A is not stabilized in these cells, indicating that p97 functions in multiple pathways to modulate the activity of the G_2/M checkpoint after IR (Figure 2.8 b). Recently, Puumalainen and colleagues showed that the DNA damage sensor proteins DDB2 and XPC are degraded depending on $p97^{Ufd1\text{-}Npl4}$ but not DVC1, further supporting a model in which different p97 co-factors mediate distinct p97 functions in the response to DNA damage.

The majority of studies implicate p97 in the degradation of its substrates, as depletion of p97 mainly leads to the stabilisation and accumulation of its target substrates. However, the work by Ikai and Yanagida demonstrated that cdc48/p97 is essential for the stabilization of cut1/separase in yeast and that depletion of p97 leads loss of cut1 protein (Ikai and Yanagida, 2006). Therefore it might be possible that $p97^{DVC1}$ protects WEE1 from degradation by directly binding to it, which would display an interesting new aspect of p97 function.

Like CDC25A, ubiquitination by $SCF^{\beta TrCP}$ targets WEE1 for proteosomal degradation (Smith et al., 2007). Degradation of Wee1 is initiated by its phosphorylation by the Polo-like kinase 1 (PLK1) prior to ubiquitination by βTrCP and results in the promotion of mitotic entry after DNA damage (van Vugt et al., 2004). Therefore another speculation is that p97 might be involved in the degradation of Plk1 and thus promote G_2/M arrest in response to DNA damage, as Plk1 is ubiquitinated by the APC/C^{Cdh1} complex and subsequently degraded by the proteasome (Bassermann et al., 2008). However, first experiments done by our laboratory did not show a stabilization of PLK1 upon p97 depletion (Grzegorz Dobrynin). But in these experiments, we did not analysed specifically, whether depletion of p97 leads to accumulation of the higher molecular weight form of ubiquitinated PLK1, leaving the possibility that we therefore did not observed an accumulation of PLK1 in p97-

depleted cells. Further experiments might clarify whether indeed depletion of p97 causes the accumulation of PLK1 in the ubiquitinated form.
As p97 has essential roles in many cellular processes, the destabilization of WEE1 upon p97 depletion can also result from pleiotropic effects due to the long term response to reduced p97 function obtained by siRNA-mediated protein knock down. Therefore, further experiments using specific p97 inhibitors, which directly influence p97 function, are useful to analyze the effects of p97 on WEE1 protein levels.

Does the G_2/M checkpoint failure in Ufd1-Npl4 depleted cells depend on p53-deficency?

In response to DNA damage, not only the G_2/M checkpoint but also the G_1/S checkpoint is activated to prevent cell from further cell cycle progression with damaged DNA material and to initiate DNA damage repair. As the above mentioned experiments were carried out in p53-deficient HeLa cells, we suggested that cells with functional p53 would be able to halt cell cycle progression despite the lack of CDC25A inactivation in response to DNA damage in Ufd1- or Npl4-depleted cells. Indeed, we observed that HCT116 p53 proficient cells arrest in their cell cycle progression despite depletion of Ufd1-Npl4 or DVC1, indicating that these cells activated their residual functional DNA damage checkpoints in response to IR. In contrast, we observed that the p53-deficient HCT116 cells behaved similar to HeLa cells upon depletion of Ufd1 and DVC1 and entered mitosis after irradiation (Figure 2.12 a/b), indicating that in 53-deficents cells the $p97^{Ufd1\text{-}Npl4}$ complex is essential to fully activate the G_2/M checkpoint in response to IR. Surprisingly, Npl4-depleted cells did not significantly increase in their mitotic fraction after IR compared to control-depleted cells. This might be due to the generally less pronounced effect of Npl4 depletion on the stabilization of CDC25A also seen in HeLa cells.
A number of human cancer cells lack functional p53 and therefore lost the ability to arrest in the G_1/S checkpoint after DNA damage induction. These cells largely rely on their G_2/M checkpoint to arrest in the cell cycle progression and to repair the DNA damage. Therefore, additional depletion of the G_2/M checkpoint leads to mitotic entry with damaged DNA, which causes genomic instability. As depletion of p97, DVC1 or Ufd1 leads to an impaired G_2/M checkpoint with subsequent mitotic entry after IR, we suggest that these cells undergo mitotic catastrophe with subsequent cell death in or shortly after mitosis. Mitotic catastrophe refers to a mechanism of a delayed mitotic-linked cell death, a sequence of events that results from premature or inappropriate entry of cells into mitosis that was also depicted as the main form of cell death induced by ionizing radiation (Vakifahmetoglu et al., 2008). In this work it was not fully clarified whether depletion of p97, Ufd1 or DVC1 indeed result in a mitotic catastrophe phenotype after IR, also the drastic increase in chromosome segregation

defects and chromosomal aberrations in these cells serves as indication for it (Figure 2.1, Figure 2.2) (Riemer et al., 2014) . Further experiments should be done to clarify whether indeed p97-depleted cells undergo mitotic catastrophe with subsequent cell death after IR.

Taken together our results provide evidence that $p97^{Ufd1\text{-}Npl4}$ ensures proper degradation of CDC25A in response to DNA damage preventing cells to commit to mitosis with damaged DNA material and thus is an important component to maintain genomic stability in p53-deficient cells.

3.2 Part II: The role of p97 in regulation of DNA replication

Depletion of Npl4 leads to a delay in recovery from DNA replication stress

As previously mentioned, p97 has been implicated in different interphase processes, including the regulation of S phase progression. One study showed that depletion of p97 leads to an arrest of *C. elegans* embryos in S phase (Mouysset et al., 2008). Another study by Wójcik and colleagues demonstrated that HeLa cells arrest in S phase and G_2/M phase with a decrease of cells in G_0/G_1 phase upon depletion of p97 (Wojcik et al., 2004). In contrast, yet another study showed that HeLa cells accumulate in G_1 after depletion of p97 (Magnaghi et al., 2013). However in our laboratory, we could not observe changes in the cell cycle profile after p97 depletion in HeLa cells (Figure 2.4 a). The discrepancy in our results and the ones observed by other groups, may result due to different levels of depletion efficiency and also seem to be cell line dependent. Supporting this idea is the recent observation that p97 depletion had no effect on the cell cycle profile in U2OS cells, but led to an accumulation of cells in G_2/M phase in HCT116 cells (Magnaghi et al., 2013). Furthermore, in our experiments depletion of Ufd1 or Npl4 also did not affect the progression through the cell cycle after release from double thymidine-induced S phase arrest. Surprisingly, HeLa cells depleted of Ufd1-Npl4 showed persistent activation of CHK1 after release from the double thymidine block whereas control-depleted cells recovered from replication stress, which might be due to a defect in repair of the DNA damage or due to problems in the recovery from the replication stress (Figure 2.14 a). Using aphidicolin as yet another chemical compound to induce replication stress, we showed that treatment of U2OS cells with low doses of aphidicolin leads to phosphorylation of CHK1 at Ser315, indicating that the DNA damage response is activated upon aphidicolin-induced replication stress (Figure 2.15). Low doses of aphidicolin selectively impair the progression of replication forks and lead to the induction of chromosomal fragile site (CFS) breaks and subsequent activation of CHK1 and CHK2 (Durkin and Glover, 2007). In contrast to HeLa cells, only Npl4-depleted cells but not Ufd1-depleted cells show persistence activation of

CHK1 after release from aphidicolin (Figure 2.15), which provides evidence for a differential relevance of Ufd1 and Npl4 in the regulation of S phase progression in response to DNA damage.

p97 adaptor proteins Npl4, DVC1 and UBXD7 are involved in DNA replication

As mentioned previously, $p97^{Ufd1\text{-}Npl4}$ is involved in the regulation of S phase progression by modulating distinct key proteins during S phase initiation and in response to DNA repair. Our previous results indicate a differential relevance of Ufd1 and Npl4 in the regulation of S phase progression in response to replication stress. Consistently with the previous results, we observed an increase in 53BP1 foci per cell in Npl4-depleted cells, which we did not observe in Ufd1-depleted cells, indicating a higher level of replication stress in the Npl4-depleted population (Figure 2.16). 53BP1 forms foci around DNA lesions in G_1 phase cells that were generated by the mitotic transmission of chromosomes under replication stress (Lukas et al., 2011). The unrepaired replication errors manifest in the following M phase as chromosomal aberrations, which are marked by γH2AX foci (Giunta et al., 2010). Using yet another assay to monitor replication stress, we confirmed that Npl4 depletion leads to an increase in γH2AX foci per cell, which further supports our previous results and indicates a role for Npl4 in DNA replication (Figure 2.17). Interestingly, Ufd1 and not Npl4 was shown to be involved in the regulation of the degradation of the DNA replication-licensing factor Cdt1 in response to DNA damage and under physiological conditions to prevent re-licensing and the replication initiation with damage DNA (Raman et al., 2011). In contrast, another group found also Npl4 involved in this process (Franz et al., 2011), indicating that unravelling the functions of Ufd1 and Npl4 in the single cellular functions is still a challenging task.

In addition to Npl4 depletion, also UBXD7 depletion caused an increase of 53BP1 and γH2AX foci per cell, further supporting a more general role of UBXD7 acting together with $p97^{Npl4}$ (Figure 2.16, Figure 2.17).

However, neither Npl4 nor UBXD7 depleted cells responded to aphidicolin, as none of these cells showed a significant increase in 53BP1 or γH2AX foci number per cell in response to aphidicolin treatment. In contrast, DVC1 depletion caused a significant increase of γH2AX and 53BP1 upon aphidicolin treatment, indicating that DVC1 has an additive effect on the aphidicolin-induced replication stress and might function in the direct repair of aphidicolin-induced DNA damage (Figure 2.16, Figure 2.17). If unrepaired DNA damage is encountered during DNA replication, TLS is activated leading to the bypass of the DNA lesion by specialized translesional DNA polymerases (TLS pol) that are able to read through lesions due to their low replication accuracy (Franz et al., 2014). DVC1 recruits p97 to sites of DNA damage and thus regulates p97 function in the process of translesion DNA synthesis,

confirming its important role the repair of DNA damage during DNA replication (Davis et al., 2012) (Mosbech et al., 2012).

Surprisingly, we did not observe a change in the 53BP1 or γH2AX foci number per cell in p97-depleted cells, which again might be due to pleiotropic effects of p97 depletion. Supporting this idea is the result by Acs and colleagues that $p97^{Ufd1\text{-}Npl4}$ regulates the recruitment of 53BP1 by removing L3MBTL1 from DSB after IR (Acs et al., 2011). Furthermore, they showed that overexpression of a catalytically inactive, dominant-negative version of p97 led to a strong reduction in 53BP1 recruitment after IR. However, overexpression of the p97 inactive version had no influence on the recruitment of γH2AX to the sites of DNA damage.

Taken together our results provide evidence that the p97 cofactors DVC1, UBXD7 and Npl4 are implicated in DNA replication, as their depletion results in an increase of replication errors marked by 53BP1 or γH2AX foci. For further investigation of the relevance of p97 co-factors on DNA replication, additional controls, including the ERAD-related p97-cofactor UBXD8, need to be included into these experiments.

3.3 Part III: Does Npl4 depletion lead to impaired BUBR1 localization on mitotic chromatin?

As mentioned earlier, $p97^{Ufd1\text{-}Npl4}$ is an important component to maintain chromosome stability, as depletion of the complex leads to severe chromosome misalignment and chromosome segregation errors due to persisting Aurora B activity on the kinetochores (Dobrynin et al., 2011). Additionally, our laboratory discovered that depletion of Npl4 in HeLa cells led to a loss of BUBR1 on the chromatin as well as on the protein levels (Sebastian Bremer, data not shown). Upon spindle checkpoint activation by unattached chromosomes, BUBR1 forms a transient complex with BUB3 and Cdc20 leading to the final formation of the mitotic checkpoint complex (MCC), which consist of BUBR1-BUB3-Mad2-Cdc20. The MCC efficiently inhibits APC/C-mediated degradation of downstream key regulators and arrest mitotic progression (Musacchio and Salmon, 2007) (Yu, 2002). Depletion of BUBR1 causes severe chromosome misalignment (Lampson and Kapoor, 2005), similar to the phenotype that we observed upon Npl4-depletion. Interestingly, BUBR1 was only reduced in Npl4-depleted cells but not in Ufd1-depleted cells. This finding could be due to an unspecific off-target effect of the used Npl4 siRNA oligonucleotide or due to a function of Npl4 independent of Ufd1. An Ufd1-independent function of Npl4 was previously reported by Ballar and colleagues in the gp78 mediated ERAD that requires only the Cdc48–Npl4 dimer in yeast, supporting the indication of an Ufd1-independent function in our experiments (Ballar et al., 2011). However, using a stable cell line inducibly expressing a rat Npl4-3myc construct (reNpl4-3myc), which is

resistant against the used Npl4 oligonucleotides, we did not rescue the loss of BUBR1 on the chromatin but we restored the chromosome misalignment and chromosome segregation phenotype in Npl4-depleted cells (Figure 2.20, Figure 2.21). These findings reveal the loss of BUBR1 protein in Npl4-depleted cells as an off-target effect of the used oligonucleotide and do not support a role of Npl4 in BUBR1 protein turnover.

4 Material and Methods

4.1 Cloning

For PCR reactions the PfuUltra Fusion HS DNA polymerase (Agilent Technologies) was used according to manufactures instructions. For enzyme restriction and DNA ligation NEB enzymes were used according to manufactures recommendations. DNA was extracted from agarose gels with help of the QIAquick Gel Extraction Kit (QIAGEN). Plasmid DNA amplification was performed with the Macherey-Nagel NucleoBond® Xtra Maxi Kit. Transformation of plasmid DNA into E.coli XL1-blue cells was performed according to standard procedures.

4.2 Generation of plasmid constructs

3myc-tag

For phosphorylation and annealing of complementary primers (724, 725) 1 µg of each primer was incubated for 1 h at 37 °C with 10 units of T4 PNK. The enzyme was inactivated at 95 °C for 10 min. For annealing, the primers were incubated in T4 Ligase buffer at 74 °C for 90 min. For the generation of a pcDNA5/TO-3myc plasmid vector, the 3myc-tag was cloned into pcDNA5/TO (Invitrogen) vector via BamHI/NotI restriction sites.

reNpl4-3myc

Rat Npl4 was PCR amplified using the oligonucleotides number 704 and 706 out of a pIRES.puro2b.Npl4.3HA DNA vector. The amplified cDNA was cloned into the pcDNA5/TO-3myc vector via HindIII restriction site.

GFP - TrCP

Flag-βTrCP pcDNA3 was obtained from Addgene (plasmid 10865) (Zhou et al., 2000). The flag – βTrCP was cutted out from the vector via BamHI/XhoI restriction sites and was PCR amplified using the oligonucleotides number 1128 and 1129. The amplified cDNA was cloned into a pEGFP_C1 (Clontec) via the BamHI/XhoI restriction sites.

Table 4.1: Nucleotide sequences of oligonucleotides used in this work

Accession number	Oligonucleotide sequence
704	TTGACCTAAGCTTATGGCCGAGAGCATCATAATC
706	AGTTCATAAGCTTTTAGGTCCGGGGAAGGCTGCAC
724	GATCCGCCGCAGAACAAAAACTCATCTCAGAAGAGGAT CTGGCAGAACAAAAACTCATCTCAGAAGAGGATCTGGC AGAACAAAAACTCATCTCAGAAGAGGATCTGTAAGC
725	GGCCGCTTACAGATCCTCTTCTGAGATGAGTTTTTGTT CTGCCAGATCCTCTTCTGAGATGAGTTTTTGTTCTGCC AGATCCTCTTCTGAGATGAGTTTTTGTTCTGCGGCG
1128	TCAGATCTCGAGATGACCCG
1129	TCCGGTGGATCCTTATCTGG

4.3 Cell lines and maintenance

All cells were grown and maintained in a 5 % CO2/air incubator at 37 °C. Parental HeLa Kyoto and U2OS cells were grown in standard D-MEM (Invitrogen) supplemented with 10 % FCS (PAA) and 1 % of penicillin/streptomycin (Gibco). Inducible HEK293 p97WT and EQ cells were generated by Julia Westermeier and grown in D-MEM (Invitrogen) supplemented with 10 % tetracyclin negative FCS (PAA), 1 % penicillin/streptomycin (Gibco), 15 µg/mL Blasticidin (Invitrogen) and 100 µg/ml Hygromycin B (Sigma). Inducible HEK293 HA-CDC25A cells were generated by Grzegorz Dobrynin and grown in D-MEM (Invitrogen) supplemented with 10 % tetracyclin negative FCS (PAA), 1 % penicillin/streptomycin (Gibco), 15 µg/mL Blasticidin (Invitrogen) and 100 µg/ml Hygromycin B (Sigma). HCT116 parental and $p53^{-/-}$ (provided by Prof. Dr. George Illiakis, UK Essen) were grown in Mc Coy´s 5A standard media (c.c.pro) supplemented with 1 % L-Glutamine (Gibco), 10 % FCS (PAA) and 1 % of penicillin/streptomycin (Gibco).

4.4 Transfections

For DNA plasmid transfections, cells were seeded and transfected using Lipofectamine 2000 (Invitrogen) according to the standard protocol.

For siRNAi mediated depletion experiments, cells were grown to about 30 - 40 % density and transfected with siRNA oligonucleotides at final concentration of 10 nM for 48 h using Lipofectamine RNAiMAX (Invitrogen). All siRNAs, if not stated

otherwise, were purchased from Microsynth and diluted to 20 µM stock solutions. Non-coding or luciferase siRNA served as control depletions.

Table 4.2: Oligonucleotide sequences used in RNAi experiments

Target gene	Oligo name	Sequence	Source
Control	siCtrl	UUCUCCGAACGUGUCACGUTT	-
Luciferase	siLuc	CGUACGCGGAAUACUUCGATT	Microsynth
CHK1	siCHK1	AAGGGATAACCTCAAAATCTCTT	Carrassa et al. 2009
Npl4	siNpl4 S1	CGUGGUGGAGGAUGAGAUUTT	-
Npl4	siNpl4 S2	CAGCCUCCUCCAACAAAUCTT	
Npl4	siNpl4 S4	AACAGCCUCCUCCAACAAAUCTT	Porter et al., 2007
DVC1	siDVC1 S2	UCAAGUACCACCUGUAUUATT	Mosbech et al. 2012
Ufd1	siUfd1 S1	GGGCUACAAAGAACCCGAATT	
Ufd1	siUfd1 S2	GUGGCCACCUACUCCAAAUTT	
Ufd1	siUfd1 S4	ACAAAGAACCCGAAAGACATT	
UBXD1	siUBXD1 S	CCAGGUGAGAAAGGAACUUTT	
UBXD6	siUBXD6	GGAUGACGAGAAUUGGGUATT	QIAgen
UBXD7	siUBXD7	CAGCUUGAAAGGAGUGUUUTT	QIAgen
UBXD8	siUBXD8	GAAGUUAUUUCACUAAUAATT	Suzuki et al. 2012
p97	sip97 S2	AACAGCCAUUCUCAAACAGAATT	Qiagen VCP7 -
β- TrCP	siβTrCP 1/2	GUGGAAUUUGUGGAACAUCTT	Busino et al. 2003

4.5 Generation of stable reNpl4-3myc cell line

To generate a cell line expressing rat Npl4, which is resistant against siNpl4 S1 and S2, HeLa Flip-in cells (gift from Prof. Dr. Ulrike Kutay, ETH Zurich) stably expressing HA-tagged Tetracyclin-repressor and H2B-mcherry were co-transfected with pOG44 (Invitrogen) and pcDNA5/TO/reNpl4-3myc in a 9:1 ratio, respectively, with Lipofectamine 2000 (Invitrogen) as described above. 24 h after transfection, cells were cultured in selection media containing 10 % FCS (Tetracyclin free), 1 % Penicillin/Streptomycin, 150 µg/ml Hygromycin and 0,5 µg/ml Pyromycin until single cell colonies were detectable. Single cell clone were picked and cultured in 96- well plates.

4.6 Immunofluorescence staining

HeLa Kyoto or U2OS cells were seeded on sterile coverslips and transfected with siRNA. 48 h after siRNA transfection, coverslips were removed from the cell culture dish, washed once with PBS (Gibco) and fixed for 15 min at room temperature (RT) in 4 % PFA (paraformaldehyde, SIGMA). After fixation, the samples were washed once with PBS and permeabilized with 0.1 % Triton X-100 in PBS for 5 min at RT. Then, the samples were washed trice with PBS for 10 min each and blocked with 3 % BSA (Applichem) in PBS for 30 min. After blocking, the cells were incubated with primary antibodies diluted in blocking solution for 1 h at RT in a wet (humid) chamber. Unbound primary antibodies were removed by washing the samples trice for 10 min with PBS. After washing, samples were incubated with secondary antibodies diluted in blocking solution for 30 – 60 min at RT in a wet (humid) chamber. Unbound secondary antibodies were removed by washing the cells trice for 10 min with PBS. Then, the microscopy slides with cells were shortly immersed in dH2O to remove PBS prior to mounting on glass slides in Mowiol containing 1 µg/mL DAPI.

4.7 Antibodies and other reagents used

Table 4.3: Antibodies used for immunofluorescence and Western blotting experiments.

Antibody	Species	IF	WB	source
53BP1	Rabbit	1:500	-	Santa Cruz Biotech.
BUBR1	mouse	1:1000	1:500	Millipore
CDC25A	Mouse	-	1:500	Neomarker
CHK1	Mouse	-	1:500	Santa Cruz Biotech.
CHK1 phospho Ser317	Rabbit	-	1:500	Cell Signalling
CHK1 phospho Ser345	Rabbit	-	1:500	Cell Signalling
CREST	Human	1:400	-	Antibodies Inc.
Cyclin A1 (6E6)	Mouse	1:500	-	Abcam
GAPDH	Mouse	-	1:20000	Sigma- Aldrich
GFP	Mouse	-	1:2000	Roche
HA	Mouse	-	1:1000	Covance
Histone H3 phospho Ser10	Rabbit	1:1000	-	Millipore
Myc (9E10)	Mouse	1:1000	1:2000	
Npl4 (HME18)	Rabbit	-	1:500	Meyer et al., 2000
p97 (HME08)	Rabbit	-	1:2000	Meyer et al., 2000
UBXD1	rabbit	-	1:10000	Ritz et al, 2013
UBXD7	Sheep	-	1:500	Alexandru et al, 2008
UBXD8	Rabbit	-	1:1000	Novus
Ufd1 (5E2)	Mouse	-	1:500	Meyer et al., 2000
Wee1	Rabbit	-	1:500	Santa Cruz Biotech.
α-tubulin	Mouse	-	1:8000	Sigma Aldrich
γ-H2AX Ser139	Mouse	1:5000	1:500	BioLegend
mouse IgG Alexa 488	Goat	1:500	-	Invitrogen
Rabbit IgG Alexa 488	Goat	1:500	-	Invitrogen
Mouse IgG Alexa 568	Goat	1:500	-	Invitrogen
Rabbit IgG Alexa 568	Goat	1:500	-	Invitrogen
Human IgG Alexa 594		1:500	-	Invitrogen
mouse IgG HRP	Goat	-	1:10000	Bio-Rad
Rabbit IgG HRP	Goat	-	1:10000	Bio-Rad

Sheep IgG HRP				

4.8 Fluorescence imaging

Live cell imaging

HeLa Kyoto cells grown in on µ-Slide 8 well chambers (Ibidi) were transfected with siRNA. For image acquisition cells were cultured in minimal essential medium with Hank's F12 (MEM/F12; Gibco) supplemented with 15 mM HEPES pH 7.4. Images were acquired every 5 min over a 10 hour time period by brightfield microscopy with Nikon Eclipse Ti microscope and Andor DR-328G-C01-SIL camera. During imaging cells were kept at 37 °C and 5 % CO_2. Images were processed using ImageJ software (version 1.43u).

Indirect immunofluorescence

For confocal images a Yokogawa CSU-X1 unit attached to the same microscope was used and images were acquired with an Andor iXon X3 EMCCD camera.

4.9 Flourescence activated cell sorting

HeLa Kyoto or HCT116 cells were seeded and transfected with siRNA. After 48 h cells were exposed to 3 Gy ionizing radiation (IR). 30 min after IR 100 µg/ml nocodazol (Sigma) was added to the cells and 10 h after IR cells were collected and washed once with ice-cold PBS. Cells were pelleted by centrifugation with 1000 x g and fixed in 4 % PFA for 15 min RT. Cells were washed twice in PBS/0,1 %Triton X-100 and incubated in primary antibody against pH3 (S10) for 1 h at RT. Unbound primary antibody was removed by washing cells trice with PBS/0,1 %Triton X-100. Afterwards cells were incubated with secondary antibody for 1h at RT and then resuspended in PBS/0,1 % Triton X-100 with 50 µg/ml RNAse A (Roche) and 25 µg/ml Propidium iodine (Sigma). After 15 min incubation at 37 °C cells were analyzed by fluorescence-activated cell sorting on a BD FACS Calibur machine. The results were quantified by FlowJo software (Version 9.7). Cells were gated for main population of living cells in the forward (FSH) against sideward scatter (SSH). Cell doublets were gated out by FSH-area against FSH-high intensity. Cells were finally gated by pH3 (S10) intensity against propidium iodine (PI) intensity and mitotic index was defined by population with high pH3 and high PI intensity.

4.10 Cell synchronization

To synchronize cells in early S-phase cells were seeded into 6-well plate. When cells were about 30 % confluent 2 mM thymidine (Sigma) was added to the cells for 18 h. Afterwards cells were released into fresh media without thymidine for 9 h. After the

release 2 mM thymidine was added for 17 h. After second block cells were released into fresh media without thymidine and progress synchronously through G2 and M-phase.

4.11 Cell extracts

Collection of cell extracts was done on ice with ice-cold/4 °C cold buffers. Before lysis cells were washed once with PBS and collected by scraping in PBS. Collected cells were centrifuged with 1000 x g for 3 min. The cell pellet was resuspended in extraction buffer containing 150 mM KCl, 25 mM Tris pH 7.4, 5 mM MgCl2, 5 % glycerol, 1 % Triton X-100, 2 mM b-Mercaptoethanol (Sigma), EDTA-free Protease inhibitor cocktail (Roche) and Phosphatase inhibitor (Roche). For lysis cells were incubated in extraction buffer for 20 min on ice and centrifuged with 16.000 x g for 15 min. Supernatant was transferred into fresh tubes, snap frozen in liquid nitrogen and stored at -80 °C for further experiments.

Preparation of cell extracts for immunoprecipitation (IP) experiments.
Cells were collected by scrapping in IP buffer (150 mM KCl, 50 mM Tris pH 7.4, 5 mM MgCl2, 5 % glycerol, 1 % Triton X-100 and 2 mM b-Mercaptoethanol) supplemented with Complete EDTA-free protease inhibitor, PhosphoSTOP phosphatase inhibitor. Cells were incubated for 20 min on ice and pelleted by centrifugation with 16.000 x g at 4 °C for 15 min. Supernatants were transferred into fresh tubes and used for immunoprecipitation experiments.

4.12 Immunoprecipitation

For IP experiments cell extracts were prepared as described above and protein concentration was determined by using BCA assay according to manufactures instructions (VWR). Input samples (IN) were transferred into separate tubes. After addition of antibody (1 µg per 1 mg of protein) samples were incubated for 1 h at 4 °C on a tube rotor. Dynabeads ® Protein G (Life Technologies) were washed trice in PBS and 20 µl beads were added to the IP samples and incubated for 1 h at 4 °C on the tube rotator. After incubation beads were spinned down by centrifugation with 1000 x g for 1 min. From the supernatant flowthrough samples were transferred into separate tubes. IP samples were washed trice with 500 µl IP buffer. After final wash IP samples were resuspended in 10 µl IP buffer and 6 x Laemmli buffer was added. Samples were boiled at 95 °C for 5 min and subjected to SDS PAGE.

4.13 SDS PAGE and Western blotting

Cell extracts were prepared as described above and samples supplemented with 6 x Laemmli buffer and boiled at 95 °C for 5 min. Proteins were separated by standart SDS PAGE protocol using SDS Running Buffer containing 200 mM Glycine, 25 mM Tris-HCl and 0.1 % SDS. Gels were run at a constant current of 20 mA per gel. Western blotting was performed by using a semi-dry Trans-Blot ® SD transfer cell (Bio-Rad). Proteins were blotted for 1 h on a nitrocellulose membrane (Hybond-C super, Amersham Biosciences®) with a constant current of 120 mA per gel using transfer buffer containing 1 x SDS Running Buffer supplemented with 20 % Methanol. After Western blotting membranes were blocked for 1 h at room temperature (RT) with blocking buffer containing 4 % fat free milk powder PBS, 0.05 % Tween® 20 (Fluka) or in 1 xTBS, 0.1 % Tween® 20 (for membranes that were later probed with phospho-specific antibodies).

4.14 Assays used in this study

CDC25A degradation assay

HeLa cells were seeded into 6-well plates and transfected with siRNA. 48 h after transfection cells were mock treated or treated with 6 Gy IR. To block protein synthesis cyclohexamide (CHX) was added to the cells directly after IR. Cell extracts were prepared as described above 15 min and 30 min after IR. Samples were subjected for SDS PAGE and Western blotting. The membranes were stained with CDC25A antibody and the signal density of the CDC25A band on the X-ray film was quantified by ImageJ software tool.

53BP1 foci formation assay

U2OS cells were grown on coverslips and transfected with siRNA for 48 h. Cells were mock or aphidicolin (0,2 µM) treated for 24 h. After treatment cells were fixed in 4 % PFA and stained for cyclin A2 and 53BP1 as described above. For Quantification of 53BP1 foci number in G1 phase cells images were acquired with Nikon Eclipse Ti with a Yokogava CSU10 Spinning Disk Confocal microscope.

γ-H2AX foci formation assay

U2OS cells were grown on coverslips and transfected with siRNA for 48 h. Cells were mock or aphidicolin (0,2 µM) treated for 24 h. After treatment cells were fixed in 4 % PFA and stained for pH3(S10) and γ-H2AX as described above. For quantification of γ-H2AX foci on mitotic chromatin images were acquired with Nikon Eclipse Ti with a Yokogava CSU10 Spinning Disk Confocal microscope.

Statistics

Tests for significance were done using SigmaPlot (version 12.5) software. Results were tested with unpaired t-test.

Literature

Abbas, T., Sivaprasad, U., Terai, K., Amador, V., Pagano, M., and Dutta, A. (2008). PCNA-dependent regulation of p21 ubiquitylation and degradation via the CRL4Cdt2 ubiquitin ligase complex. Genes & development *22*, 2496-2506.

Acs, K., Luijsterburg, M.S., Ackermann, L., Salomons, F.A., Hoppe, T., and Dantuma, N.P. (2011). The AAA-ATPase VCP/p97 promotes 53BP1 recruitment by removing L3MBTL1 from DNA double-strand breaks. Nature structural & molecular biology *18*, 1345-1350.

Alexandru, G., Graumann, J., Smith, G.T., Kolawa, N.J., Fang, R., and Deshaies, R.J. (2008). UBXD7 binds multiple ubiquitin ligases and implicates p97 in HIF1alpha turnover. Cell *134*, 804-816.

Andersen, P.L., Xu, F., and Xiao, W. (2008). Eukaryotic DNA damage tolerance and translesion synthesis through covalent modifications of PCNA. Cell research *18*, 162-173.

Asaithamby, A., Hu, B., and Chen, D.J. (2011). Unrepaired clustered DNA lesions induce chromosome breakage in human cells. Proceedings of the National Academy of Sciences of the United States of America *108*, 8293-8298.

Baboshina, O.V., and Haas, A.L. (1996). Novel multiubiquitin chain linkages catalyzed by the conjugating enzymes E2EPF and RAD6 are recognized by 26 S proteasome subunit 5. The Journal of biological chemistry *271*, 2823-2831.

Bai, C., Sen, P., Hofmann, K., Ma, L., Goebl, M., Harper, J.W., and Elledge, S.J. (1996). SKP1 connects cell cycle regulators to the ubiquitin proteolysis machinery through a novel motif, the F-box. Cell *86*, 263-274.

Ballar, P., Pabuccuoglu, A., and Kose, F.A. (2011). Different p97/VCP complexes function in retrotranslocation step of mammalian ER-associated degradation (ERAD). The international journal of biochemistry & cell biology *43*, 613-621.

Bandau, S., Knebel, A., Gage, Z.O., Wood, N.T., and Alexandru, G. (2012). UBXN7 docks on neddylated cullin complexes using its UIM motif and causes HIF1alpha accumulation. BMC biology *10*, 36.

Bashir, T., Dorrello, N.V., Amador, V., Guardavaccaro, D., and Pagano, M. (2004). Control of the SCF(Skp2-Cks1) ubiquitin ligase by the APC/C(Cdh1) ubiquitin ligase. Nature *428*, 190-193.

Bassermann, F., Eichner, R., and Pagano, M. (2014). The ubiquitin proteasome system - implications for cell cycle control and the targeted treatment of cancer. Biochimica et biophysica acta *1843*, 150-162.

Bassermann, F., Frescas, D., Guardavaccaro, D., Busino, L., Peschiaroli, A., and Pagano, M. (2008). The Cdc14B-Cdh1-Plk1 axis controls the G2 DNA-damage-response checkpoint. Cell *134*, 256-267.

Bebeacua, C., Forster, A., McKeown, C., Meyer, H.H., Zhang, X., and Freemont, P.S. (2012). Distinct conformations of the protein complex p97-Ufd1-Npl4 revealed by electron cryomicroscopy. Proceedings of the National Academy of Sciences of the United States of America *109*, 1098-1103.

Beck, J., Maerki, S., Posch, M., Metzger, T., Persaud, A., Scheel, H., Hofmann, K., Rotin, D., Pedrioli, P., Swedlow, J.R.*, et al.* (2013). Ubiquitylation-dependent localization of PLK1 in mitosis. Nature cell biology *15*, 430-439.

Behrends, C., and Harper, J.W. (2011). Constructing and decoding unconventional ubiquitin chains. Nature structural & molecular biology *18*, 520-528.

Bell, S.P., and Dutta, A. (2002). DNA replication in eukaryotic cells. Annual review of biochemistry *71*, 333-374.
Bergink, S., Ammon, T., Kern, M., Schermelleh, L., Leonhardt, H., and Jentsch, S. (2013). Role of Cdc48/p97 as a SUMO-targeted segregase curbing Rad51-Rad52 interaction. Nature cell biology *15*, 526-532.
Besson, A., Dowdy, S.F., and Roberts, J.M. (2008). CDK inhibitors: cell cycle regulators and beyond. Developmental cell *14*, 159-169.
Bornstein, G., Bloom, J., Sitry-Shevah, D., Nakayama, K., Pagano, M., and Hershko, A. (2003). Role of the SCFSkp2 ubiquitin ligase in the degradation of p21Cip1 in S phase. The Journal of biological chemistry *278*, 25752-25757.
Brandman, O., Stewart-Ornstein, J., Wong, D., Larson, A., Williams, C.C., Li, G.W., Zhou, S., King, D., Shen, P.S., Weibezahn, J.*, et al.* (2012). A ribosome-bound quality control complex triggers degradation of nascent peptides and signals translation stress. Cell *151*, 1042-1054.
Bruderer, R.M., Brasseur, C., and Meyer, H.H. (2004). The AAA ATPase p97/VCP interacts with its alternative co-factors, Ufd1-Npl4 and p47, through a common bipartite binding mechanism. The Journal of biological chemistry *279*, 49609-49616.
Burrell, R.A., McClelland, S.E., Endesfelder, D., Groth, P., Weller, M.C., Shaikh, N., Domingo, E., Kanu, N., Dewhurst, S.M., Gronroos, E.*, et al.* (2013). Replication stress links structural and numerical cancer chromosomal instability. Nature *494*, 492-496.
Busino, L., Donzelli, M., Chiesa, M., Guardavaccaro, D., Ganoth, D., Dorrello, N.V., Hershko, A., Pagano, M., and Draetta, G.F. (2003). Degradation of Cdc25A by beta-TrCP during S phase and in response to DNA damage. Nature *426*, 87-91.
Cao, K., Nakajima, R., Meyer, H.H., and Zheng, Y. (2003). The AAA-ATPase Cdc48/p97 regulates spindle disassembly at the end of mitosis. Cell *115*, 355-367.
Cardozo, T., and Pagano, M. (2004). The SCF ubiquitin ligase: insights into a molecular machine. Nature reviews Molecular cell biology *5*, 739-751.
Carrano, A.C., Eytan, E., Hershko, A., and Pagano, M. (1999). SKP2 is required for ubiquitin-mediated degradation of the CDK inhibitor p27. Nature cell biology *1*, 193-199.
Cenciarelli, C., Chiaur, D.S., Guardavaccaro, D., Parks, W., Vidal, M., and Pagano, M. (1999). Identification of a family of human F-box proteins. Current biology : CB *9*, 1177-1179.
Centore, R.C., Yazinski, S.A., Tse, A., and Zou, L. (2012). Spartan/C1orf124, a reader of PCNA ubiquitylation and a regulator of UV-induced DNA damage response. Molecular cell *46*, 625-635.
Cheng, Y.L., and Chen, R.H. (2010). The AAA-ATPase Cdc48 and cofactor Shp1 promote chromosome bi-orientation by balancing Aurora B activity. Journal of cell science *123*, 2025-2034.
Chien, C.Y., and Chen, R.H. (2013). Cdc48 chaperone and adaptor Ubx4 distribute the proteasome in the nucleus for anaphase proteolysis. The Journal of biological chemistry *288*, 37180-37191.
Crusio, K.M., King, B., Reavie, L.B., and Aifantis, I. (2010). The ubiquitous nature of cancer: the role of the SCF(Fbw7) complex in development and transformation. Oncogene *29*, 4865-4873.
Davis, E.J., Lachaud, C., Appleton, P., Macartney, T.J., Nathke, I., and Rouse, J. (2012). DVC1 (C1orf124) recruits the p97 protein segregase to sites of DNA damage. Nature structural & molecular biology *19*, 1093-1100.

DeHoratius, C., and Silver, P.A. (1996). Nuclear transport defects and nuclear envelope alterations are associated with mutation of the Saccharomyces cerevisiae NPL4 gene. Molecular biology of the cell *7*, 1835-1855.
DeLaBarre, B., and Brunger, A.T. (2005). Nucleotide dependent motion and mechanism of action of p97/VCP. Journal of molecular biology *347*, 437-452.
den Besten, W., Verma, R., Kleiger, G., Oania, R.S., and Deshaies, R.J. (2012). NEDD8 links cullin-RING ubiquitin ligase function to the p97 pathway. Nature structural & molecular biology *19*, 511-516, S511.
Diffley, J.F., Cocker, J.H., Dowell, S.J., and Rowley, A. (1994). Two steps in the assembly of complexes at yeast replication origins in vivo. Cell *78*, 303-316.
Dobrynin, G., Popp, O., Romer, T., Bremer, S., Schmitz, M.H., Gerlich, D.W., and Meyer, H. (2011). Cdc48/p97-Ufd1-Npl4 antagonizes Aurora B during chromosome segregation in HeLa cells. Journal of cell science *124*, 1571-1580.
Donzelli, M., and Draetta, G.F. (2003). Regulating mammalian checkpoints through Cdc25 inactivation. EMBO reports *4*, 671-677.
Donzelli, M., Squatrito, M., Ganoth, D., Hershko, A., Pagano, M., and Draetta, G.F. (2002). Dual mode of degradation of Cdc25 A phosphatase. The EMBO journal *21*, 4875-4884.
Durkin, S.G., and Glover, T.W. (2007). Chromosome fragile sites. Annual review of genetics *41*, 169-192.
Fernandez-Saiz, V., and Buchberger, A. (2010). Imbalances in p97 co-factor interactions in human proteinopathy. EMBO reports *11*, 479-485.
Foe, I., and Toczyski, D. (2011). Structural biology: a new look for the APC. Nature *470*, 182-183.
Fousteri, M., and Mullenders, L.H. (2008). Transcription-coupled nucleotide excision repair in mammalian cells: molecular mechanisms and biological effects. Cell research *18*, 73-84.
Franz, A., Ackermann, L., and Hoppe, T. (2014). Create and preserve: proteostasis in development and aging is governed by Cdc48/p97/VCP. Biochimica et biophysica acta *1843*, 205-215.
Franz, A., Orth, M., Pirson, P.A., Sonneville, R., Blow, J.J., Gartner, A., Stemmann, O., and Hoppe, T. (2011). CDC-48/p97 coordinates CDT-1 degradation with GINS chromatin dissociation to ensure faithful DNA replication. Molecular cell *44*, 85-96.
Frescas, D., and Pagano, M. (2008). Deregulated proteolysis by the F-box proteins SKP2 and beta-TrCP: tipping the scales of cancer. Nature reviews Cancer *8*, 438-449.
Frohlich, K.U., Fries, H.W., Rudiger, M., Erdmann, R., Botstein, D., and Mecke, D. (1991). Yeast cell cycle protein CDC48p shows full-length homology to the mammalian protein VCP and is a member of a protein family involved in secretion, peroxisome formation, and gene expression. The Journal of cell biology *114*, 443-453.
Fu, X., Ng, C., Feng, D., and Liang, C. (2003). Cdc48p is required for the cell cycle commitment point at Start via degradation of the G1-CDK inhibitor Far1p. The Journal of cell biology *163*, 21-26.
Fujii, K., Kitabatake, M., Sakata, T., and Ohno, M. (2012). 40S subunit dissociation and proteasome-dependent RNA degradation in nonfunctional 25S rRNA decay. The EMBO journal *31*, 2579-2589.
Fujita, K., Nakamura, Y., Oka, T., Ito, H., Tamura, T., Tagawa, K., Sasabe, T., Katsuta, A., Motoki, K., Shiwaku, H*., et al.* (2013). A functional deficiency of TERA/VCP/p97 contributes to impaired DNA repair in multiple polyglutamine diseases. Nature communications *4*, 1816.

Ganoth, D., Bornstein, G., Ko, T.K., Larsen, B., Tyers, M., Pagano, M., and Hershko, A. (2001). The cell-cycle regulatory protein Cks1 is required for SCF(Skp2)-mediated ubiquitinylation of p27. Nature cell biology *3*, 321-324.
Geigl, J.B., Obenauf, A.C., Schwarzbraun, T., and Speicher, M.R. (2008). Defining 'chromosomal instability'. Trends in genetics : TIG *24*, 64-69.
Ghosal, G., Leung, J.W., Nair, B.C., Fong, K.W., and Chen, J. (2012). Proliferating cell nuclear antigen (PCNA)-binding protein C1orf124 is a regulator of translesion synthesis. The Journal of biological chemistry *287*, 34225-34233.
Giunta, S., Belotserkovskaya, R., and Jackson, S.P. (2010). DNA damage signaling in response to double-strand breaks during mitosis. The Journal of cell biology *190*, 197-207.
Glinka, T., Alter, J., Braunstein, I., Tzach, L., Wei Sheng, C., Geifman, S., Edelmann, M.J., Kessler, B.M., and Stanhill, A. (2014). Signal-peptide-mediated translocation is regulated by a p97-AIRAPL complex. The Biochemical journal *457*, 253-261.
Guardavaccaro, D., Frescas, D., Dorrello, N.V., Peschiaroli, A., Multani, A.S., Cardozo, T., Lasorella, A., Iavarone, A., Chang, S., Hernando, E.*, et al.* (2008). Control of chromosome stability by the beta-TrCP-REST-Mad2 axis. Nature *452*, 365-369.
Hao, B., Oehlmann, S., Sowa, M.E., Harper, J.W., and Pavletich, N.P. (2007). Structure of a Fbw7-Skp1-cyclin E complex: multisite-phosphorylated substrate recognition by SCF ubiquitin ligases. Molecular cell *26*, 131-143.
Hao, B., Zheng, N., Schulman, B.A., Wu, G., Miller, J.J., Pagano, M., and Pavletich, N.P. (2005). Structural basis of the Cks1-dependent recognition of p27(Kip1) by the SCF(Skp2) ubiquitin ligase. Molecular cell *20*, 9-19.
Harper, J.W., Burton, J.L., and Solomon, M.J. (2002). The anaphase-promoting complex: it's not just for mitosis any more. Genes & development *16*, 2179-2206.
Harrison, J.C., and Haber, J.E. (2006). Surviving the breakup: the DNA damage checkpoint. Annual review of genetics *40*, 209-235.
Hershko, A., and Ciechanover, A. (1998). The ubiquitin system. Annual review of biochemistry *67*, 425-479.
Hoege, C., Pfander, B., Moldovan, G.L., Pyrowolakis, G., and Jentsch, S. (2002). RAD6-dependent DNA repair is linked to modification of PCNA by ubiquitin and SUMO. Nature *419*, 135-141.
Honaker, Y., and Piwnica-Worms, H. (2010). Casein kinase 1 functions as both penultimate and ultimate kinase in regulating Cdc25A destruction. Oncogene *29*, 3324-3334.
Hsieh, M.T., and Chen, R.H. (2011). Cdc48 and cofactors Npl4-Ufd1 are important for G1 progression during heat stress by maintaining cell wall integrity in Saccharomyces cerevisiae. PloS one *6*, e18988.
Hu, J., and Xiong, Y. (2006). An evolutionarily conserved function of proliferating cell nuclear antigen for Cdt1 degradation by the Cul4-Ddb1 ubiquitin ligase in response to DNA damage. The Journal of biological chemistry *281*, 3753-3756.
Huang, J.N., Park, I., Ellingson, E., Littlepage, L.E., and Pellman, D. (2001). Activity of the APC(Cdh1) form of the anaphase-promoting complex persists until S phase and prevents the premature expression of Cdc20p. The Journal of cell biology *154*, 85-94.
Hubbers, C.U., Clemen, C.S., Kesper, K., Boddrich, A., Hofmann, A., Kamarainen, O., Tolksdorf, K., Stumpf, M., Reichelt, J., Roth, U.*, et al.* (2007). Pathological consequences of VCP mutations on human striated muscle. Brain : a journal of neurology *130*, 381-393.
Hurley, J.H., Lee, S., and Prag, G. (2006). Ubiquitin-binding domains. The Biochemical journal *399*, 361-372.

Ikai, N., and Yanagida, M. (2006). Cdc48 is required for the stability of Cut1/separase in mitotic anaphase. Journal of structural biology *156*, 50-61.
Indig, F.E., Partridge, J.J., von Kobbe, C., Aladjem, M.I., Latterich, M., and Bohr, V.A. (2004). Werner syndrome protein directly binds to the AAA ATPase p97/VCP in an ATP-dependent fashion. Journal of structural biology *146*, 251-259.
Irniger, S., and Nasmyth, K. (1997). The anaphase-promoting complex is required in G1 arrested yeast cells to inhibit B-type cyclin accumulation and to prevent uncontrolled entry into S-phase. Journal of cell science *110 (Pt 13)*, 1523-1531.
Isaacson, R.L., Pye, V.E., Simpson, P., Meyer, H.H., Zhang, X., Freemont, P.S., and Matthews, S. (2007). Detailed structural insights into the p97-Npl4-Ufd1 interface. The Journal of biological chemistry *282*, 21361-21369.
Jin, J., Ang, X.L., Ye, X., Livingstone, M., and Harper, J.W. (2008). Differential roles for checkpoint kinases in DNA damage-dependent degradation of the Cdc25A protein phosphatase. The Journal of biological chemistry *283*, 19322-19328.
Jin, J., Cardozo, T., Lovering, R.C., Elledge, S.J., Pagano, M., and Harper, J.W. (2004). Systematic analysis and nomenclature of mammalian F-box proteins. Genes & development *18*, 2573-2580.
Johnson, E.S., Ma, P.C., Ota, I.M., and Varshavsky, A. (1995). A proteolytic pathway that recognizes ubiquitin as a degradation signal. The Journal of biological chemistry *270*, 17442-17456.
Johnson, J.O., Mandrioli, J., Benatar, M., Abramzon, Y., Van Deerlin, V.M., Trojanowski, J.Q., Gibbs, J.R., Brunetti, M., Gronka, S., Wuu, J.*, et al.* (2010). Exome sequencing reveals VCP mutations as a cause of familial ALS. Neuron *68*, 857-864.
Jorgensen, S., Eskildsen, M., Fugger, K., Hansen, L., Larsen, M.S., Kousholt, A.N., Syljuasen, R.G., Trelle, M.B., Jensen, O.N., Helin, K.*, et al.* (2011). SET8 is degraded via PCNA-coupled CRL4(CDT2) ubiquitylation in S phase and after UV irradiation. The Journal of cell biology *192*, 43-54.
Juhasz, S., Balogh, D., Hajdu, I., Burkovics, P., Villamil, M.A., Zhuang, Z., and Haracska, L. (2012). Characterization of human Spartan/C1orf124, an ubiquitin-PCNA interacting regulator of DNA damage tolerance. Nucleic acids research *40*, 10795-10808.
Kanemori, Y., Uto, K., and Sagata, N. (2005). Beta-TrCP recognizes a previously undescribed nonphosphorylated destruction motif in Cdc25A and Cdc25B phosphatases. Proceedings of the National Academy of Sciences of the United States of America *102*, 6279-6284.
Kang, T., Wei, Y., Honaker, Y., Yamaguchi, H., Appella, E., Hung, M.C., and Piwnica-Worms, H. (2008). GSK-3 beta targets Cdc25A for ubiquitin-mediated proteolysis, and GSK-3 beta inactivation correlates with Cdc25A overproduction in human cancers. Cancer cell *13*, 36-47.
Keck, J.M., Summers, M.K., Tedesco, D., Ekholm-Reed, S., Chuang, L.C., Jackson, P.K., and Reed, S.I. (2007). Cyclin E overexpression impairs progression through mitosis by inhibiting APC(Cdh1). The Journal of cell biology *178*, 371-385.
Kim, M.S., Machida, Y., Vashisht, A.A., Wohlschlegel, J.A., Pang, Y.P., and Machida, Y.J. (2013). Regulation of error-prone translesion synthesis by Spartan/C1orf124. Nucleic acids research *41*, 1661-1668.
Kim, Y., Deng, Y., and Philpott, C.C. (2007). GGA2- and ubiquitin-dependent trafficking of Arn1, the ferrichrome transporter of Saccharomyces cerevisiae. Molecular biology of the cell *18*, 1790-1802.
Kirchner, P., Bug, M., and Meyer, H. (2013). Ubiquitination of the N-terminal region of caveolin-1 regulates endosomal sorting by the VCP/p97 AAA-ATPase. The Journal of biological chemistry *288*, 7363-7372.

Koepp, D.M., Schaefer, L.K., Ye, X., Keyomarsi, K., Chu, C., Harper, J.W., and Elledge, S.J. (2001). Phosphorylation-dependent ubiquitination of cyclin E by the SCFFbw7 ubiquitin ligase. Science *294*, 173-177.
Kondo, H., Rabouille, C., Newman, R., Levine, T.P., Pappin, D., Freemont, P., and Warren, G. (1997). p47 is a cofactor for p97-mediated membrane fusion. Nature *388*, 75-78.
Kothe, M., Ye, Y., Wagner, J.S., De Luca, H.E., Kern, E., Rapoport, T.A., and Lencer, W.I. (2005). Role of p97 AAA-ATPase in the retrotranslocation of the cholera toxin A1 chain, a non-ubiquitinated substrate. The Journal of biological chemistry *280*, 28127-28132.
Kraft, C., Herzog, F., Gieffers, C., Mechtler, K., Hagting, A., Pines, J., and Peters, J.M. (2003). Mitotic regulation of the human anaphase-promoting complex by phosphorylation. The EMBO journal *22*, 6598-6609.
Kramer, E.R., Scheuringer, N., Podtelejnikov, A.V., Mann, M., and Peters, J.M. (2000). Mitotic regulation of the APC activator proteins CDC20 and CDH1. Molecular biology of the cell *11*, 1555-1569.
Kress, E., Schwager, F., Holtackers, R., Seiler, J., Prodon, F., Zanin, E., Eiteneuer, A., Toya, M., Sugimoto, A., Meyer, H.*, et al.* (2013). The UBXN-2/p37/p47 adaptors of CDC-48/p97 regulate mitosis by limiting the centrosomal recruitment of Aurora A. The Journal of cell biology *201*, 559-575.
Lamothe, B., Besse, A., Campos, A.D., Webster, W.K., Wu, H., and Darnay, B.G. (2007). Site-specific Lys-63-linked tumor necrosis factor receptor-associated factor 6 auto-ubiquitination is a critical determinant of I kappa B kinase activation. The Journal of biological chemistry *282*, 4102-4112.
Lampson, M.A., and Kapoor, T.M. (2005). The human mitotic checkpoint protein BubR1 regulates chromosome-spindle attachments. Nature cell biology *7*, 93-98.
Lapenna, S., and Giordano, A. (2009). Cell cycle kinases as therapeutic targets for cancer. Nature reviews Drug discovery *8*, 547-566.
Lavoie, C., Chevet, E., Roy, L., Tonks, N.K., Fazel, A., Posner, B.I., Paiement, J., and Bergeron, J.J. (2000). Tyrosine phosphorylation of p97 regulates transitional endoplasmic reticulum assembly in vitro. Proceedings of the National Academy of Sciences of the United States of America *97*, 13637-13642.
Lee, J.H., and Paull, T.T. (2005). ATM activation by DNA double-strand breaks through the Mre11-Rad50-Nbs1 complex. Science *308*, 551-554.
Lehmann, A.R. (2011). DNA polymerases and repair synthesis in NER in human cells. DNA repair *10*, 730-733.
Lehmann, A.R., Niimi, A., Ogi, T., Brown, S., Sabbioneda, S., Wing, J.F., Kannouche, P.L., and Green, C.M. (2007). Translesion synthesis: Y-family polymerases and the polymerase switch. DNA repair *6*, 891-899.
Li, J., and Baker, M.D. (2000). Formation and repair of heteroduplex DNA on both sides of the double-strand break during mammalian gene targeting. Journal of molecular biology *295*, 505-516.
Li, J.M., Wu, H., Zhang, W., Blackburn, M.R., and Jin, J. (2014). The p97-UFD1L-NPL4 protein complex mediates cytokine-induced IkappaBalpha proteolysis. Molecular and cellular biology *34*, 335-347.
Li, L., and Zou, L. (2005). Sensing, signaling, and responding to DNA damage: organization of the checkpoint pathways in mammalian cells. Journal of cellular biochemistry *94*, 298-306.
Li, W., Bengtson, M.H., Ulbrich, A., Matsuda, A., Reddy, V.A., Orth, A., Chanda, S.K., Batalov, S., and Joazeiro, C.A. (2008). Genome-wide and functional annotation of human E3 ubiquitin ligases identifies MULAN, a mitochondrial E3 that regulates the organelle's dynamics and signaling. PloS one *3*, e1487.

Li, X., Zhao, Q., Liao, R., Sun, P., and Wu, X. (2003). The SCF(Skp2) ubiquitin ligase complex interacts with the human replication licensing factor Cdt1 and regulates Cdt1 degradation. The Journal of biological chemistry *278*, 30854-30858.
Lindon, C., and Pines, J. (2004). Ordered proteolysis in anaphase inactivates Plk1 to contribute to proper mitotic exit in human cells. The Journal of cell biology *164*, 233-241.
Littlepage, L.E., and Ruderman, J.V. (2002). Identification of a new APC/C recognition domain, the A box, which is required for the Cdh1-dependent destruction of the kinase Aurora-A during mitotic exit. Genes & development *16*, 2274-2285.
Lobrich, M., and Jeggo, P.A. (2007). The impact of a negligent G2/M checkpoint on genomic instability and cancer induction. Nature reviews Cancer *7*, 861-869.
Lukas, C., Savic, V., Bekker-Jensen, S., Doil, C., Neumann, B., Pedersen, R.S., Grofte, M., Chan, K.L., Hickson, I.D., Bartek, J.*, et al.* (2011). 53BP1 nuclear bodies form around DNA lesions generated by mitotic transmission of chromosomes under replication stress. Nature cell biology *13*, 243-253.
Lukas, C., Sorensen, C.S., Kramer, E., Santoni-Rugiu, E., Lindeneg, C., Peters, J.M., Bartek, J., and Lukas, J. (1999). Accumulation of cyclin B1 requires E2F and cyclin-A-dependent rearrangement of the anaphase-promoting complex. Nature *401*, 815-818.
Macurek, L., Lindqvist, A., Lim, D., Lampson, M.A., Klompmaker, R., Freire, R., Clouin, C., Taylor, S.S., Yaffe, M.B., and Medema, R.H. (2008). Polo-like kinase-1 is activated by aurora A to promote checkpoint recovery. Nature *455*, 119-123.
Madeo, F., Schlauer, J., Zischka, H., Mecke, D., and Frohlich, K.U. (1998). Tyrosine phosphorylation regulates cell cycle-dependent nuclear localization of Cdc48p. Molecular biology of the cell *9*, 131-141.
Madsen, L., Kriegenburg, F., Vala, A., Best, D., Prag, S., Hofmann, K., Seeger, M., Adams, I.R., and Hartmann-Petersen, R. (2011). The tissue-specific Rep8/UBXD6 tethers p97 to the endoplasmic reticulum membrane for degradation of misfolded proteins. PloS one *6*, e25061.
Madsen, L., Seeger, M., Semple, C.A., and Hartmann-Petersen, R. (2009). New ATPase regulators--p97 goes to the PUB. The international journal of biochemistry & cell biology *41*, 2380-2388.
Magnaghi, P., D'Alessio, R., Valsasina, B., Avanzi, N., Rizzi, S., Asa, D., Gasparri, F., Cozzi, L., Cucchi, U., Orrenius, C.*, et al.* (2013). Covalent and allosteric inhibitors of the ATPase VCP/p97 induce cancer cell death. Nature chemical biology *9*, 548-556.
Maia, A.R., Garcia, Z., Kabeche, L., Barisic, M., Maffini, S., Macedo-Ribeiro, S., Cheeseman, I.M., Compton, D.A., Kaverina, I., and Maiato, H. (2012). Cdk1 and Plk1 mediate a CLASP2 phospho-switch that stabilizes kinetochore-microtubule attachments. The Journal of cell biology *199*, 285-301.
Mailand, N., Bekker-Jensen, S., Bartek, J., and Lukas, J. (2006). Destruction of Claspin by SCFbetaTrCP restrains Chk1 activation and facilitates recovery from genotoxic stress. Molecular cell *23*, 307-318.
Mamely, I., van Vugt, M.A., Smits, V.A., Semple, J.I., Lemmens, B., Perrakis, A., Medema, R.H., and Freire, R. (2006). Polo-like kinase-1 controls proteasome-dependent degradation of Claspin during checkpoint recovery. Current biology : CB *16*, 1950-1955.
Margottin-Goguet, F., Hsu, J.Y., Loktev, A., Hsieh, H.M., Reimann, J.D., and Jackson, P.K. (2003). Prophase destruction of Emi1 by the SCF(betaTrCP/Slimb) ubiquitin ligase activates the anaphase promoting complex to allow progression beyond prometaphase. Developmental cell *4*, 813-826.
McGarry, T.J., and Kirschner, M.W. (1998). Geminin, an inhibitor of DNA replication, is degraded during mitosis. Cell *93*, 1043-1053.

Meerang, M., Ritz, D., Paliwal, S., Garajova, Z., Bosshard, M., Mailand, N., Janscak, P., Hubscher, U., Meyer, H., and Ramadan, K. (2011). The ubiquitin-selective segregase VCP/p97 orchestrates the response to DNA double-strand breaks. Nature cell biology *13*, 1376-1382.
Melixetian, M., Klein, D.K., Sorensen, C.S., and Helin, K. (2009). NEK11 regulates CDC25A degradation and the IR-induced G2/M checkpoint. Nature cell biology *11*, 1247-1253.
Mendez, J., Zou-Yang, X.H., Kim, S.Y., Hidaka, M., Tansey, W.P., and Stillman, B. (2002). Human origin recognition complex large subunit is degraded by ubiquitin-mediated proteolysis after initiation of DNA replication. Molecular cell *9*, 481-491.
Metzger, M.B., Hristova, V.A., and Weissman, A.M. (2012). HECT and RING finger families of E3 ubiquitin ligases at a glance. Journal of cell science *125*, 531-537.
Meyer, H., Bug, M., and Bremer, S. (2012). Emerging functions of the VCP/p97 AAA-ATPase in the ubiquitin system. Nature cell biology *14*, 117-123.
Meyer, H.H., Shorter, J.G., Seemann, J., Pappin, D., and Warren, G. (2000). A complex of mammalian ufd1 and npl4 links the AAA-ATPase, p97, to ubiquitin and nuclear transport pathways. The EMBO journal *19*, 2181-2192.
Meyer, H.H., Wang, Y., and Warren, G. (2002). Direct binding of ubiquitin conjugates by the mammalian p97 adaptor complexes, p47 and Ufd1-Npl4. The EMBO journal *21*, 5645-5652.
Michaelis, C., Ciosk, R., and Nasmyth, K. (1997). Cohesins: chromosomal proteins that prevent premature separation of sister chromatids. Cell *91*, 35-45.
Moore, J.K., and Haber, J.E. (1996). Cell cycle and genetic requirements of two pathways of nonhomologous end-joining repair of double-strand breaks in Saccharomyces cerevisiae. Molecular and cellular biology *16*, 2164-2173.
Mosbech, A., Gibbs-Seymour, I., Kagias, K., Thorslund, T., Beli, P., Povlsen, L., Nielsen, S.V., Smedegaard, S., Sedgwick, G., Lukas, C.*, et al.* (2012). DVC1 (C1orf124) is a DNA damage-targeting p97 adaptor that promotes ubiquitin-dependent responses to replication blocks. Nature structural & molecular biology *19*, 1084-1092.
Mouysset, J., Deichsel, A., Moser, S., Hoege, C., Hyman, A.A., Gartner, A., and Hoppe, T. (2008). Cell cycle progression requires the CDC-48UFD-1/NPL-4 complex for efficient DNA replication. Proceedings of the National Academy of Sciences of the United States of America *105*, 12879-12884.
Musacchio, A., and Salmon, E.D. (2007). The spindle-assembly checkpoint in space and time. Nature reviews Molecular cell biology *8*, 379-393.
Nakayama, K.I., and Nakayama, K. (2006). Ubiquitin ligases: cell-cycle control and cancer. Nature reviews Cancer *6*, 369-381.
Nasmyth, K., Peters, J.M., and Uhlmann, F. (2001). Splitting the chromosome: cutting the ties that bind sister chromatids. Novartis Foundation symposium *237*, 113-133; discussion 133-118, 158-163.
Neuwald, A.F., Aravind, L., Spouge, J.L., and Koonin, E.V. (1999). AAA+: A class of chaperone-like ATPases associated with the assembly, operation, and disassembly of protein complexes. Genome research *9*, 27-43.
Nie, M., Aslanian, A., Prudden, J., Heideker, J., Vashisht, A.A., Wohlschlegel, J.A., Yates, J.R., 3rd, and Boddy, M.N. (2012). Dual recruitment of Cdc48 (p97)-Ufd1-Npl4 ubiquitin-selective segregase by small ubiquitin-like modifier protein (SUMO) and ubiquitin in SUMO-targeted ubiquitin ligase-mediated genome stability functions. The Journal of biological chemistry *287*, 29610-29619.
Niwa, H., Ewens, C.A., Tsang, C., Yeung, H.O., Zhang, X., and Freemont, P.S. (2012). The role of the N-domain in the ATPase activity of the mammalian AAA ATPase p97/VCP. The Journal of biological chemistry *287*, 8561-8570.

Ogi, T., Shinkai, Y., Tanaka, K., and Ohmori, H. (2002). Polkappa protects mammalian cells against the lethal and mutagenic effects of benzo[a]pyrene. Proceedings of the National Academy of Sciences of the United States of America *99*, 15548-15553.
Ogura, T., and Wilkinson, A.J. (2001). AAA+ superfamily ATPases: common structure--diverse function. Genes to cells : devoted to molecular & cellular mechanisms *6*, 575-597.
Ozkan, E., Yu, H., and Deisenhofer, J. (2005). Mechanistic insight into the allosteric activation of a ubiquitin-conjugating enzyme by RING-type ubiquitin ligases. Proceedings of the National Academy of Sciences of the United States of America *102*, 18890-18895.
Papouli, E., Chen, S., Davies, A.A., Huttner, D., Krejci, L., Sung, P., and Ulrich, H.D. (2005). Crosstalk between SUMO and ubiquitin on PCNA is mediated by recruitment of the helicase Srs2p. Molecular cell *19*, 123-133.
Park, S., Isaacson, R., Kim, H.T., Silver, P.A., and Wagner, G. (2005). Ufd1 exhibits the AAA-ATPase fold with two distinct ubiquitin interaction sites. Structure (London, England : 1993) *13*, 995-1005.
Peng, J., Schwartz, D., Elias, J.E., Thoreen, C.C., Cheng, D., Marsischky, G., Roelofs, J., Finley, D., and Gygi, S.P. (2003). A proteomics approach to understanding protein ubiquitination. Nature biotechnology *21*, 921-926.
Peschiaroli, A., Dorrello, N.V., Guardavaccaro, D., Venere, M., Halazonetis, T., Sherman, N.E., and Pagano, M. (2006). SCFbetaTrCP-mediated degradation of Claspin regulates recovery from the DNA replication checkpoint response. Molecular cell *23*, 319-329.
Petersen, B.O., Wagener, C., Marinoni, F., Kramer, E.R., Melixetian, M., Lazzerini Denchi, E., Gieffers, C., Matteucci, C., Peters, J.M., and Helin, K. (2000). Cell cycle- and cell growth-regulated proteolysis of mammalian CDC6 is dependent on APC-CDH1. Genes & development *14*, 2330-2343.
Petroski, M.D., and Deshaies, R.J. (2005). Function and regulation of cullin-RING ubiquitin ligases. Nature reviews Molecular cell biology *6*, 9-20.
Pines, J. (1999). Four-dimensional control of the cell cycle. Nature cell biology *1*, E73-79.
Puumalainen, M.R., Lessel, D., Ruthemann, P., Kaczmarek, N., Bachmann, K., Ramadan, K., and Naegeli, H. (2014). Chromatin retention of DNA damage sensors DDB2 and XPC through loss of p97 segregase causes genotoxicity. Nature communications *5*, 3695.
Pye, V.E., Dreveny, I., Briggs, L.C., Sands, C., Beuron, F., Zhang, X., and Freemont, P.S. (2006). Going through the motions: the ATPase cycle of p97. Journal of structural biology *156*, 12-28.
Ramadan, K., Bruderer, R., Spiga, F.M., Popp, O., Baur, T., Gotta, M., and Meyer, H.H. (2007). Cdc48/p97 promotes reformation of the nucleus by extracting the kinase Aurora B from chromatin. Nature *450*, 1258-1262.
Raman, M., Havens, C.G., Walter, J.C., and Harper, J.W. (2011). A genome-wide screen identifies p97 as an essential regulator of DNA damage-dependent CDT1 destruction. Molecular cell *44*, 72-84.
Rape, M., Hoppe, T., Gorr, I., Kalocay, M., Richly, H., and Jentsch, S. (2001). Mobilization of processed, membrane-tethered SPT23 transcription factor by CDC48(UFD1/NPL4), a ubiquitin-selective chaperone. Cell *107*, 667-677.
Rape, M., and Kirschner, M.W. (2004). Autonomous regulation of the anaphase-promoting complex couples mitosis to S-phase entry. Nature *432*, 588-595.
Reinhardt, H.C., and Yaffe, M.B. (2013). Phospho-Ser/Thr-binding domains: navigating the cell cycle and DNA damage response. Nature reviews Molecular cell biology *14*, 563-580.

Reyes-Turcu, F.E., Ventii, K.H., and Wilkinson, K.D. (2009). Regulation and cellular roles of ubiquitin-specific deubiquitinating enzymes. Annual review of biochemistry *78*, 363-397.
Ribar, B., Prakash, L., and Prakash, S. (2007). ELA1 and CUL3 are required along with ELC1 for RNA polymerase II polyubiquitylation and degradation in DNA-damaged yeast cells. Molecular and cellular biology *27*, 3211-3216.
Riemer, A., Dobrynin, G., Dressler, A., Bremer, S., Soni, A., Iliakis, G., and Meyer, H. (2014). The p97-Ufd1-Npl4 ATPase complex ensures robustness of the G2/M checkpoint by facilitating CDC25A degradation. Cell cycle *13*, 919-927.
Ritz, D., Vuk, M., Kirchner, P., Bug, M., Schutz, S., Hayer, A., Bremer, S., Lusk, C., Baloh, R.H., Lee, H.*, et al.* (2011). Endolysosomal sorting of ubiquitylated caveolin-1 is regulated by VCP and UBXD1 and impaired by VCP disease mutations. Nature cell biology *13*, 1116-1123.
Rossi, M., Duan, S., Jeong, Y.T., Horn, M., Saraf, A., Florens, L., Washburn, M.P., Antebi, A., and Pagano, M. (2013). Regulation of the CRL4(Cdt2) ubiquitin ligase and cell-cycle exit by the SCF(Fbxo11) ubiquitin ligase. Molecular cell *49*, 1159-1166.
Rotin, D., and Kumar, S. (2009). Physiological functions of the HECT family of ubiquitin ligases. Nature reviews Molecular cell biology *10*, 398-409.
Rudolph, J. (2007). Cdc25 phosphatases: structure, specificity, and mechanism. Biochemistry *46*, 3595-3604.
Rumpf, S., and Jentsch, S. (2006). Functional division of substrate processing cofactors of the ubiquitin-selective Cdc48 chaperone. Molecular cell *21*, 261-269.
Saifee, N.H., and Zheng, N. (2008). A ubiquitin-like protein unleashes ubiquitin ligases. Cell *135*, 209-211.
Sasagawa, Y., Higashitani, A., Urano, T., Ogura, T., and Yamanaka, K. (2012). CDC-48/p97 is required for proper meiotic chromosome segregation via controlling AIR-2/Aurora B kinase localization in Caenorhabditis elegans. Journal of structural biology *179*, 104-111.
Saxena, S., Yuan, P., Dhar, S.K., Senga, T., Takeda, D., Robinson, H., Kornbluth, S., Swaminathan, K., and Dutta, A. (2004). A dimerized coiled-coil domain and an adjoining part of geminin interact with two sites on Cdt1 for replication inhibition. Molecular cell *15*, 245-258.
Schreiber, A., Stengel, F., Zhang, Z., Enchev, R.I., Kong, E.H., Morris, E.P., Robinson, C.V., da Fonseca, P.C., and Barford, D. (2011). Structural basis for the subunit assembly of the anaphase-promoting complex. Nature *470*, 227-232.
Schuberth, C., and Buchberger, A. (2008). UBX domain proteins: major regulators of the AAA ATPase Cdc48/p97. Cellular and molecular life sciences : CMLS *65*, 2360-2371.
Seki, A., Coppinger, J.A., Du, H., Jang, C.Y., Yates, J.R., 3rd, and Fang, G. (2008a). Plk1- and beta-TrCP-dependent degradation of Bora controls mitotic progression. The Journal of cell biology *181*, 65-78.
Seki, A., Coppinger, J.A., Jang, C.Y., Yates, J.R., and Fang, G. (2008b). Bora and the kinase Aurora a cooperatively activate the kinase Plk1 and control mitotic entry. Science *320*, 1655-1658.
Sherr, C.J., and Roberts, J.M. (1999). CDK inhibitors: positive and negative regulators of G1-phase progression. Genes & development *13*, 1501-1512.
Shibata, E., Abbas, T., Huang, X., Wohlschlegel, J.A., and Dutta, A. (2011). Selective ubiquitylation of p21 and Cdt1 by UBCH8 and UBE2G ubiquitin-conjugating enzymes via the CRL4Cdt2 ubiquitin ligase complex. Molecular and cellular biology *31*, 3136-3145.
Smith, A., Simanski, S., Fallahi, M., and Ayad, N.G. (2007). Redundant ubiquitin ligase activities regulate wee1 degradation and mitotic entry. Cell cycle *6*, 2795-2799.

Sobhian, B., Shao, G., Lilli, D.R., Culhane, A.C., Moreau, L.A., Xia, B., Livingston, D.M., and Greenberg, R.A. (2007). RAP80 targets BRCA1 to specific ubiquitin structures at DNA damage sites. Science *316*, 1198-1202.
Spruck, C., Strohmaier, H., Watson, M., Smith, A.P., Ryan, A., Krek, T.W., and Reed, S.I. (2001). A CDK-independent function of mammalian Cks1: targeting of SCF(Skp2) to the CDK inhibitor p27Kip1. Molecular cell *7*, 639-650.
Stewart, S., and Fang, G. (2005). Destruction box-dependent degradation of aurora B is mediated by the anaphase-promoting complex/cyclosome and Cdh1. Cancer research *65*, 8730-8735.
Strohmaier, H., Spruck, C.H., Kaiser, P., Won, K.A., Sangfelt, O., and Reed, S.I. (2001). Human F-box protein hCdc4 targets cyclin E for proteolysis and is mutated in a breast cancer cell line. Nature *413*, 316-322.
Sumara, I., Maerki, S., and Peter, M. (2008). E3 ubiquitin ligases and mitosis: embracing the complexity. Trends in cell biology *18*, 84-94.
Sumara, I., Quadroni, M., Frei, C., Olma, M.H., Sumara, G., Ricci, R., and Peter, M. (2007). A Cul3-based E3 ligase removes Aurora B from mitotic chromosomes, regulating mitotic progression and completion of cytokinesis in human cells. Developmental cell *12*, 887-900.
Tanaka, A., Cleland, M.M., Xu, S., Narendra, D.P., Suen, D.F., Karbowski, M., and Youle, R.J. (2010). Proteasome and p97 mediate mitophagy and degradation of mitofusins induced by Parkin. The Journal of cell biology *191*, 1367-1380.
Tanaka, S., and Araki, H. (2013). Helicase activation and establishment of replication forks at chromosomal origins of replication. Cold Spring Harbor perspectives in biology *5*, a010371.
Tedesco, D., Lukas, J., and Reed, S.I. (2002). The pRb-related protein p130 is regulated by phosphorylation-dependent proteolysis via the protein-ubiquitin ligase SCF(Skp2). Genes & development *16*, 2946-2957.
Teixeira, L.K., and Reed, S.I. (2013). Ubiquitin ligases and cell cycle control. Annual review of biochemistry *82*, 387-414.
Timofeev, O., Cizmecioglu, O., Settele, F., Kempf, T., and Hoffmann, I. (2010). Cdc25 phosphatases are required for timely assembly of CDK1-cyclin B at the G2/M transition. The Journal of biological chemistry *285*, 16978-16990.
Tresse, E., Salomons, F.A., Vesa, J., Bott, L.C., Kimonis, V., Yao, T.P., Dantuma, N.P., and Taylor, J.P. (2010). VCP/p97 is essential for maturation of ubiquitin-containing autophagosomes and this function is impaired by mutations that cause IBMPFD. Autophagy *6*, 217-227.
Tron, A.E., Arai, T., Duda, D.M., Kuwabara, H., Olszewski, J.L., Fujiwara, Y., Bahamon, B.N., Signoretti, S., Schulman, B.A., and DeCaprio, J.A. (2012). The glomuvenous malformation protein Glomulin binds Rbx1 and regulates cullin RING ligase-mediated turnover of Fbw7. Molecular cell *46*, 67-78.
Uchida, S., Yoshioka, K., Kizu, R., Nakagama, H., Matsunaga, T., Ishizaka, Y., Poon, R.Y., and Yamashita, K. (2009). Stress-activated mitogen-activated protein kinases c-Jun NH2-terminal kinase and p38 target Cdc25B for degradation. Cancer research *69*, 6438-6444.
Vakifahmetoglu, H., Olsson, M., and Zhivotovsky, B. (2008). Death through a tragedy: mitotic catastrophe. Cell death and differentiation *15*, 1153-1162.
van Vugt, M.A., Bras, A., and Medema, R.H. (2004). Polo-like kinase-1 controls recovery from a G2 DNA damage-induced arrest in mammalian cells. Molecular cell *15*, 799-811.
Vaz, B., Halder, S., and Ramadan, K. (2013). Role of p97/VCP (Cdc48) in genome stability. Frontiers in genetics *4*, 60.

Verma, R., Oania, R., Fang, R., Smith, G.T., and Deshaies, R.J. (2011). Cdc48/p97 mediates UV-dependent turnover of RNA Pol II. Molecular cell *41*, 82-92.
Vodermaier, H.C. (2004). APC/C and SCF: controlling each other and the cell cycle. Current biology : CB *14*, R787-796.
Wang, Q., Song, C., and Li, C.C. (2003a). Hexamerization of p97-VCP is promoted by ATP binding to the D1 domain and required for ATPase and biological activities. Biochemical and biophysical research communications *300*, 253-260.
Wang, Q., Song, C., Yang, X., and Li, C.C. (2003b). D1 ring is stable and nucleotide-independent, whereas D2 ring undergoes major conformational changes during the ATPase cycle of p97-VCP. The Journal of biological chemistry *278*, 32784-32793.
Watanabe, N., Arai, H., Nishihara, Y., Taniguchi, M., Watanabe, N., Hunter, T., and Osada, H. (2004). M-phase kinases induce phospho-dependent ubiquitination of somatic Wee1 by SCFbeta-TrCP. Proceedings of the National Academy of Sciences of the United States of America *101*, 4419-4424.
Watts, G.D., Wymer, J., Kovach, M.J., Mehta, S.G., Mumm, S., Darvish, D., Pestronk, A., Whyte, M.P., and Kimonis, V.E. (2004). Inclusion body myopathy associated with Paget disease of bone and frontotemporal dementia is caused by mutant valosin-containing protein. Nature genetics *36*, 377-381.
Welcker, M., and Clurman, B.E. (2008). FBW7 ubiquitin ligase: a tumour suppressor at the crossroads of cell division, growth and differentiation. Nature reviews Cancer *8*, 83-93.
Wojcik, C., Yano, M., and DeMartino, G.N. (2004). RNA interference of valosin-containing protein (VCP/p97) reveals multiple cellular roles linked to ubiquitin/proteasome-dependent proteolysis. Journal of cell science *117*, 281-292.
Wolf, D.H., and Stolz, A. (2012). The Cdc48 machine in endoplasmic reticulum associated protein degradation. Biochimica et biophysica acta *1823*, 117-124.
Xia, Y., Padre, R.C., De Mendoza, T.H., Bottero, V., Tergaonkar, V.B., and Verma, I.M. (2009). Phosphorylation of p53 by IkappaB kinase 2 promotes its degradation by beta-TrCP. Proceedings of the National Academy of Sciences of the United States of America *106*, 2629-2634.
Yamada, T., Okuhara, K., Iwamatsu, A., Seo, H., Ohta, K., Shibata, T., and Murofushi, H. (2000). p97 ATPase, an ATPase involved in membrane fusion, interacts with DNA unwinding factor (DUF) that functions in DNA replication. FEBS letters *466*, 287-291.
Yamanaka, K., Sasagawa, Y., and Ogura, T. (2012). Recent advances in p97/VCP/Cdc48 cellular functions. Biochimica et biophysica acta *1823*, 130-137.
Yang, W., and Woodgate, R. (2007). What a difference a decade makes: insights into translesion DNA synthesis. Proceedings of the National Academy of Sciences of the United States of America *104*, 15591-15598.
Yeung, H.O., Forster, A., Bebeacua, C., Niwa, H., Ewens, C., McKeown, C., Zhang, X., and Freemont, P.S. (2014). Inter-ring rotations of AAA ATPase p97 revealed by electron cryomicroscopy. Open biology *4*, 130142.
Yu, H. (2002). Regulation of APC-Cdc20 by the spindle checkpoint. Current opinion in cell biology *14*, 706-714.
Zhang, J., Wan, L., Dai, X., Sun, Y., and Wei, W. (2014). Functional characterization of Anaphase Promoting Complex/Cyclosome (APC/C) E3 ubiquitin ligases in tumorigenesis. Biochimica et biophysica acta *1845*, 277-293.
Zhang, Y., Yuan, F., Wu, X., and Wang, Z. (2000). Preferential incorporation of G opposite template T by the low-fidelity human DNA polymerase iota. Molecular and cellular biology *20*, 7099-7108.

Zhang, Z., Lv, X., Yin, W.C., Zhang, X., Feng, J., Wu, W., Hui, C.C., Zhang, L., and Zhao, Y. (2013). Ter94 ATPase complex targets k11-linked ubiquitinated ci to proteasomes for partial degradation. Developmental cell *25*, 636-644.
Zheng, J., Yang, X., Harrell, J.M., Ryzhikov, S., Shim, E.H., Lykke-Andersen, K., Wei, N., Sun, H., Kobayashi, R., and Zhang, H. (2002). CAND1 binds to unneddylated CUL1 and regulates the formation of SCF ubiquitin E3 ligase complex. Molecular cell *10*, 1519-1526.
Zhou, P., Bogacki, R., McReynolds, L., and Howley, P.M. (2000). Harnessing the ubiquitination machinery to target the degradation of specific cellular proteins. Molecular cell *6*, 751-756.
Zou, L., and Elledge, S.J. (2003). Sensing DNA damage through ATRIP recognition of RPA-ssDNA complexes. Science *300*, 1542-1548.

List of figures

List of tables

Abbreviations

53BP1	tumor protein p53 binding protein 1
AAA	ATPase associated with various cellular activities
ADP	adenosine 5’-diphosphate
APC/C	anaphase promoting complex/cyclosome
ATM	ataxia telangiectasia mutated
ATP	adenosine 5’-triphosphate
ATPase	adenosine 5’-triphosphatase
ATR	ataxia telangiectasia and Rad3 related
BRCA1	breast cancer 1
Bub3	budding uninhibited by benzimidazoles 3
Cdc20	cell division cycle 20
Cdc25	cell division cycle 25
Cdc48	cell division cycle protein 48
Cdh1	cadherin 1
CDK	cyclin dependent kinase
Cdt1	chromatin licensing factor 1
CHK1/2	checkpoint kinase ½
CHX	cyclohexamide
Cip/Kip	CDK interacting protein/kinase inhibitory proteins
CKI	CDK inhibitor
CPC	chromosomal passenger complex
CRL	cullin- RING- ligase
DAPI	4’,6’-diamidino-2-phenylindole; DNA stain
DDB2	DNA damage binding protein
DDK	Dbf4 – and Drf1 – dependent kinase
DDT	DNA damage tolerance
DDR	DNA damage response
DMSO	dimethyl sulfoxide
Dox	doxycycline
DSB	double strand breaks
DUB	deubiquitylating enzyme
DVC1	C1orf124, Spartan
E1	ubiquitin activating enzyme
E2	ubiquitin conjugating enzyme
E3	ubiquitin ligase

E4	ubiquitin E4 ligase
EQ	p97 E578Q mutation
ER	endoplasmatic reticulum
ERAD	ER associated degradation
FACS	fluorescence activated cell sorting
FCS	fetal calf serum
GINS	go-Ichi-Ni-San
H2AX	H2A histone member X
HECT	homologous to the E6-AP carboxyl-terminus
HIF1α	hypoxia-inducible factor 1 alpha
IR	ionizing radiation
L3MBTL1	L(3)mbt-like 1
Lys	lysine
Mad2	mitotic arrest-deficient 2
MCC	mitotic checkpoint component
MCM2-7	minichromosome maintainance complex 2-7
MRN	Mre11, Rad50 and Nbs1 complex
Nek11	NIMA (never in mitosis gene a) –related kinase 11
Npl4	nuclear protein localization homolog 4
ORC	origin-recognition complex
PAGE	polyacrylamide gel electrophoresis
PBS	phosphate-buffered saline
PCNA	proliferating nuclear antigen
PCR	polymerase chain reaction
PFA	paraformaldehyde
Plk1	polo-like kinase 1
Pol	polymerase
RING	really interesting new gene
RNA	ribonucleid acid
RNAi	RNA-interference
RNF8	ring finger protein 8 E3 ubiquitin ligase
RNF168	ring finger protein 168 E3 ubiquitin ligase
ROI	region of interest
SAC	spindle assembly checkpoint
SCF	Skp1-Cul1-F-Box
SDS	sodium dodecyl sulfate
Ser	serine
siRNA	small interfereing RNA
Skp1	S phase kinase associated protein 1

SHR	seconf region of homology
Thr	threonine
TLS	translesion synthesis
TrCP	beta-transducin repeat containing protein
Tyr	tyrosine
Ub	ubiquitin
UBA	ubiquitin-associated domain
UBX-L	ubiquitin-like domain
UBX	ubiquitin-regulatory X
UBXD	UBX domain-containing protein
UBZ	ubiquitin binding zinc finger
Ufd1	ubiquitin fusion degradation protein 1
UPS	ubiquitin- proteasome system
VBM	VCP binding motif
VIM	VCP interaction motif
WT	wild type

Acknowledgments

In the first place, I want to thank Hemmo for giving me the opportunity to start and successfully finish my PhD in his laboratory, for his scientific and moral support and the always fruitful discussions to define the project. Also, I want to thank him for letting me peruse my work in a guided but independent way, which has helped to shape my scientific abilities.

I also want to thank Prof. Dr. Illiakis for taking part of my thesis committee and support of my project through inspiring and helpful discussions.

Special thanks goes to Greg for his patience to improve my writing skills as well as for successful, inspiring and always good-humoured sub-group working together with Alina.

I want to thank Sebastian Bremer for giving me a good start into my PhD and for reminding to first prove and then trash things. Special thanks goes also to Monika for being my “post-doc of the hearths” and for a lot of support and scientific input. I thank all the people from the Meyer-lab for a great and fun time, which gave me a lot of energy and motivation and during my PhD.

I like to say thanks to all the girls from the GRK1431 for inspiring discussions, good friendship and spreading motivation during the seminars, retreats and meetings

Special thanks go to Julia and Jara for a great friendship and reading between the lines.

And of course I want to thank Gregor and my family for always being there for me and for always supporting me.

Curriculum vitiae

Personal information

Anne Riemer, M. Sc.
Born on May 12th 1985 in Dresden, Germany
Nationality: German

Contact information

Adress: Elisabethstrasse 18a, 45139 Essen, Germany
E - mail: anne.riemer@uni-due.de, riemer_anne@yahoo.de

Education and research experience

Since 10/10	PhD candidate in the laboratory of Prof. Dr. Hemmo Meyer , Center of Medical Biotechnology, Faculty of Biology, University of Duisburg - Essen, Essen, Germany
10/08 - 9/10	M. Sc. in Medical Biology, University of Duisburg - Essen, Essen, Germany
10/05 - 6/08	B. Sc. in Molecular Biology, University of Rostock, Rostock, Germany
10/04 – 6/05	Work and travel, Ireland
6/04	Abitur (Matura), Gotthold-Ephraim-Lessing Gymnasium, Neubrandenburg, Germany

Courses and meetings

04/11 - 03/14	Graduate research program 1431 of DFG, University of Duisburg-Essen, Essen 1/13 - 12/13 speaker of the GRK1431
10/13	EMBO conference “Ubiquitin and Ubiquitin-like proteins: from structure to function”, Riva del Garda, Italy
8/13	Workshop Adobe Illustrator basics, GRK1431, Essen

4/13	Organization of the annual retreat of the GRK 1431, Ostbevern
3/13	Workshop “Personalführung” (human resources management), GRK1431, Essen
9/12	43rd annual conference of the german genetics society “Chromatin and Epigenentics”, Essen
5/12	Annual retreat of the GRK1431, Dormagen/Zons
5/12	Workshop Scientific Writing, GRK1431, Essen
3/11	Workshop SciencePlus: Communication and presentation in the academic context: How to be confident and persuasive, GRK 1431, Essen

Publications

Anne Riemer, Grzegorz Dobrynin, Alina Dressler, Sebastian Bremer, Aashish Soni, George Iliakis, Hemmo Meyer (2014)
„The p97-Ufd1-Npl4 ATPase complex ensures robustness of the G_2/M checkpoint by facilitating CDC25A degradation“
Cell cycle **13**(6): 919-927

Languages

German – native, English – proficient, Latin – basics

Erklärungen

Erklärung:
Hiermit erkläre ich, gem. § 6 Abs. (2) f) der Promotionsordnung der Fakultäten für Biologie, Chemie und Mathematik zur Erlangung der Dr. rer. nat., dass ich das Arbeitgebiet, dem das Thema „Studien zu Cecropin P1 – einem antimikrobiellen Peptid“ zuzuordnen ist, in Forschung und Lehre vertrete und den Antrag von Julia Herfurth befürworte und die Betreuung auch im Falle eines Weggangs, wenn nicht wichtige Gründe dem entgegenstehen, weiterführen werde.

Essen, den _____ _____

Unterschrift eines Mitglieds der Universität Duisburg-Essen

Erklärung:
Hiermit erkläre ich, gem. § 7 Abs. (2) c) + e) der Promotionsordnung Fakultäten für Biologie, Chemie und Mathematik zur Erlangung des Dr. rer. nat., dass ich die vorliegende Dissertation selbständig verfasst und mich keiner anderen als der angegebenen Hilfsmittel bedient habe.

Essen, den _____ _____

Unterschrift des/r Doktoranden/in

Erklärung:
Hiermit erkläre ich, gem. § 7 Abs. (2) d) + f) der Promotionsordnung der Fakultäten für Biologie, Chemie und Mathematik zur Erlangung des Dr. rer. nat., dass ich keine anderen Promotionen bzw. Promotionsversuche in der Vergangenheit durchgeführt habe und dass diese Arbeit von keiner anderen Fakultät/Fachbereich abgelehnt worden ist.

Essen, den _____ _____

Unterschrift des Doktoranden